Development of a rapid fluorescent assay to detect cationic antimicrobial tolerance based on Gram-negative bacterial membrane integrity

By

Branden Steven John Gregorchuk

Thesis submitted to the Faculty of Graduate Studies of the University of Manitoba in partial fulfilment of the requirement of the degree of:

Master of Science

Department of Medical Microbiology and Infectious Diseases
University of Manitoba
Winnipeg
Manitoba
Canada

Copyright © 2020 by Branden Gregorchuk

Abstract

Bacterial cationic antimicrobials (CA) encompass a wide spectrum of molecules that can be separated into two main CA categories: antibiotics which can be used parenterally and biocides which are administered topically to inhibit cell growth. CAs possess a mechanism of action that disrupts bacterial cell membrane integrity. Previous studies have shown that bacteria with increased tolerance to biocide CAs can provide these organisms cross-tolerance/resistance to other antimicrobials. CA biocide tolerance is not routinely tested due to a lack of recognized international standards. When biocide CA tolerance is tested, measurements are based on minimal inhibitory concentration values collected using methods which are laborious and time-consuming, highlighting the need for a rapid assay. In this thesis, I describe the development of a rapid fluorescent dye membrane integrity assay (RFDMIA), which is able to distinguish between biocide CA susceptibility and tolerance within 30 minutes utilizing a fluorescent 96-well microplate assay format. To validate this assay, we examined various Gram-negative Enterobacterial species (*Escherichia, Klebsiella* and *Shigella* spp.) as well as *Pseudomonas* and *Acinetobacter* species exposed to two major biocide CAs classes (quaternary ammonium compounds (QACs) and bisbiguanides) and two CA antibiotic classes (polymyxins and aminoglycosides). The RFDMIA assay was validated using QACs and confirmed that QAC tolerance and susceptibility could be distinguished in *E. coli* when exposed to increasing concentrations of biocide. RFDMIA was also able to predict QAC and bisbiguanide tolerance in all tested isolates except for *P. aeruginosa,* likely due to its inherent fluorescent properties. Scanning electron microscopy was used to visualize the membrane disruptive capacities of both biocide CA classes, revealing that QAC-adapted replicates had a novel biocide “dependant” phenotype and that all biocide CA adapted isolates displayed altered morphology after a 30 minutes of biocide exposure. Lastly, we examined if the RFDMIA assay could predict antibiotic CA resistance to colistin, tobramycin, and gentamicin with similar bacterial species. RFDMIA could not predict antibiotic CA susceptibilities, potentially due to the slower and diverse mechanisms of action of these antibiotics. Together, this project has developed a new assay to rapidly and accurately detect of biocide CA tolerance in a high throughput assay.

Acknowledgements

First and foremost, I would like to thank my Dad (Perry) for being my rock through this all, being the person, I could talk to at any time and for giving me my work ethic and determination; without him, I wouldn't have gotten this far. Next, I would like to thank Dr. Denice Bay for giving me a chance and taking on the risk of someone with a lacklustre GPA. I hope to have proved to her and others that GPA isn't everything and that it can be outworked. Denice provided me every opportunity possible, helped me out even if it was just someone to talk to, and became someone I have in my corner. I hope that one day I can provide the type of opportunity she gave me to another person. I would also like to acknowledge my committee members (Dr. George Zhanel, Dr. Mazdak Khajehpour, Dr. Michael Mulvey, and Dr. Grant McClarty) for all their advice and fantastic suggestions during my Master's process. Of course, I would like to thank all the Bay lab members: Carmine Slipski for helping me get established in the lab and teaching me the ropes, Nikki Cartwright for being someone I could go to for help and a good laugh, Kieran Milner for being someone to step up when needed most despite my constant jokes, Kari Green for working her like crazy helping fill in the gaps. I would like to especially like to thank Shelby Reimer for having my back and being my go-to person for questions, suggestions, debates, and laughs, no matter how long it took. I would also like to thank the other students that worked with me on the many projects: Andy Seo, Michelle Wuzinski, Brielle Funk, and Vanessa Leung-Shing, for helping me out along the way and helping me how to work with others and being critical parts of this project. I of course want to recognize the members of the Baychuks (Brayden Schindell, Andrew Webb, Michaela Nickol) and the WannaBays (Dominica De Luca and Derek Tan) for being a source of good times, great laughs, and even better beers. I would to thank Jude Zieske and Angela Nelson for their incredible knowledge and their help navigating the system. I want to thank my four best friends: Adam Grabowiecki, Daniel Hewak, North Eagles Calling Smith, and Zack Swain, who have watched me go through so many different moments and emotions and helped me through all of them, despite me not wanting to or not able to pick myself back up; you four held me together. I want to thank Irene Davies for shaking me up and setting me on the correct path, making me realize what I want, and showing me that there is more to life than school. I need to thank Dr. Anne-Marie Bernier who was the reason why I continued higher education at Université de St. Boniface and is someone that I owe so much of my education to. I

also want to thank Mr. Montgomery for inspiring me in high school with his love of Science and by showing me that it doesn't have to be a purely serious subject. I also need to thank Linda Churchill and Dr. Chittal who saved me in my worst moments of despair and doubt during my educational career.

Finally, I want to thank myself. It has taken far too long for me to realize that I am worth something and I want this thesis to stand in the place of all the negative emotions and memories that have a habit of popping back up. Over the years, I have been torn apart by others and myself, stating that I can't make it and that I will end up just like everyone else, a disappointment. I have fought for my whole life and now I get a moment of solace, to breath and take it all in; I made something, I did it, I succeeded despite every single object in my way.

Table of Contents

Abstract.....ii

Acknowledgements.....iii

Table of Contents.....v

List of Tables.....x

List of Figures.....xi

Abbreviations.....xiii

Chapter 1: Introduction..... 1

1.1 Antimicrobials and their classifications..... 1

1.2 Cationic antimicrobials..... 3

1.2.1 Biocide CAs..... 6

1.2.1.1 Quaternary ammonium compounds..... 6

1.2.1.2 Bisbiguanides..... 6

1.2.2 Antibiotic cationic antimicrobials..... 7

1.2.2.1 Aminoglycosides..... 7

1.2.2.2 Polymyxins..... 7

1.3 The problem of antimicrobial resistance..... 8

1.3.1 Critical priority AMR Gram-negative pathogens..... 10

1.3.1.1 *Pseudomonas aeruginosa*..... 10

1.3.1.2 *Acinetobacter baumannii*..... 11

1.3.1.3 *Escherichia coli*..... 11

1.3.1.4 *Klebsiella pneumoniae*..... 12

1.3.1.5 *Shigella sonnei*..... 13

1.4 CAs and their impact on AMR in Gram-negative bacteria 13
1.4.1 Biocide CA tolerance in Gram-negative species 14
1.4.2 Mechanisms of Antibiotic CA resistance and biocide CA tolerance 15
1.4.3 Biocide and antibiotic cross-resistance/cross-tolerance 16
1.5 AMR detection methods 20
1.5.1 Detection of antibiotic CA resistance phenotypes by Gram-negative bacteria 20
1.5.2 Detection of biocide CA tolerance for Gram-negative bacteria 22
1.6 Thesis Aims and Hypotheses 23
Chapter 2: Materials and Methods 26
2.1 Bacterial species and chemicals used within the study 26
2.1.1 Cryopreservation and growth conditions 26
2.1.2 Gene cloning/transformation methods 27
2.2 RFDMIA fluorescent spectroscopy 28
2.2.1 RFDMIA optimal fluorescent dye and cell concentration determination. 28
2.2.2. RFDMIA cell culture preparations. 28
2.2.3 RFDMIA protocol. 30
2.2.4 RFDMIA with alternative dyes 30
2.2.5 RFDMIA EM RFU calculations. 30
2.3 Antimicrobial susceptibility testing (AST) 31
2.3.1 Broth microdilution AST for MIC calculations. 31
2.3.2 30-minute MBC (30MBC) determination 32
2.4 Scanning Electron Microscopy 32
2.5 Statistical analyses 32

Chapter 3. Rapid fluorescent dye-based membrane integrity assay to detect QAC susceptibility among adapted Gram-negative reveals quaternary ammonium compound dependant phenotype 34

3.1 Aims, Hypotheses, and Approaches 34

3.2 Results and discussions 35

3.2.1 AST of tested strains and isolates 35

3.2.2 RFDMIA can discriminate QAC susceptible from QAC tolerant *E. coli* isolates 37

3.2.2.1 Discussion of *E. coli* QAC RFDMIA results 41

3.2.3 Stationary phase cultures were optimal for RFDMIA QAC susceptibility prediction with *E. coli* 42

3.2.3.1 Discussion of RFDMIA *E. coli* growth phase results 44

3.2.4 RFDMIA can discriminate QAC-tolerant and QAC-susceptible *E. coli* cells for DDAB, CPC, and CDAB 44

3.2.5 RFDMIA can predict QAC susceptibility for *A. baumannii*, *K. pneumoniae*, and *S. sonnei*, but not *P. aeruginosa*. 47

3.2.5.1 *A. baumannii* (BZK, CET) RFDMIA 47

3.2.5.2 *K. pneumoniae* (BZK) RFDMIA 47

3.2.5.3 *S. sonnei* (BZK) RFDMIA 49

3.2.5.4 *P. aeruginosa* (BZK, CET) 49

3.2.6 Sytox^{TM} Blue RFDMIA can predict CET and BZK susceptibility in *E. coli* but not *P. aeruginosa* 52

3.2.6.1 Discussion of Sytox^{TM} Blue RFDMIA results 52

3.2.7 QAC-adapted *E. coli* demonstrate morphological changes and a type of QAC dependence to maintain membrane morphology 53

3.2.7.1 Discussion of SEM 57

Chapter 4: Examination of chlorhexidine adapted *Escherichia coli* membrane permeance and morphology using a rapid fluorescent dye-based membrane impermeant assay and scanning electron microscopy 62

4.1 Aims and Hypotheses of Chapter 4 62

4.2 Results and Discussion 63

4.2.1 AST of tested isolates 63

4.2.2 RFDMIA can detect CHX susceptibility 63

4.2.3 SEM imaging of CHX adapted *E. coli* reveals that have longer cell lengths but variable width morphologies 66

4.2.3.1 Discussion of SEM results 71

Chapter 5. Antibiotic CAs cause minimal membrane disruption as revealed by indirect measurement of a membrane impermeant dye 75

5.1 Chapter 5 Aims, hypotheses, and approaches 75

5.2 Results and discussions 76

5.2.1 AST of various *E. coli* isolates verifies MIC and 30MBC values for colistin and aminoglycosides. 76

5.2.2 RFDMIA cannot reliably discriminate antibiotic CA susceptibility or resistance in *E. coli* 78

5.2.2.1 Colistin 78

5.2.2.1.1 Discussion of COL RFDMIA 81

5.2.2.2 Gentamicin and tobramycin RFDMIA of clinical *E. coli* isolates 81

5.2.2.2.1 Discussion of GNT and TOB resistant *E. coli* isolates' RFDMIA 82

5.2.3 COL adaptation causes a reduction in length and width in *E. coli* but no COL dependence. 84

5.2.3.1 Discussion of COL SEM images 84

Chapter 6 Final Discussion and Summary 89

6.1 RFDMIA's benefits and limitations 89

6.2 RFDMIA insights into CA mechanisms of action 90

6.3 Dependence phenotype seen in SEM images..... 91

References 96

Appendix I..... 118

Appendix II..... 119

List of Tables

Table 1.1. A summary of proteobacterial biocide CA tolerance and antimicrobial cross-resistance AST findings (as fold change values) determined from previously published MIC data.

Table 3.1. A summary of mean MIC and 30MBC values of all bacterial strains tested Chapter 3 for a 2-fold dilution series.

Table 3.2. Mean length and width values of *E. coli* EC and ECBZKT after 30-minute exposure to BZK at indicated concentrations based off of five 5000X magnification SEM images.

Table 3.3. Mean length and width values of *E. coli* EC and ECCETT after 30-minute exposure to CET at indicated concentrations based off of five 5000X magnification SEM images.

Table 4.1. Summary of mean MIC and 30MBC values of CHX for strains in Chapter 4.

Table 4.2. Mean length and width measurements of EC and ECCHXT after 30-minute exposure to CHX based on individual cells visualized from five SEM images collected at 5000X magnification.

Table 5.1 A summary of mean MIC and 30MBC values for COL and aminoglycoside susceptibility for strains used in Chapter 5.

Table 5.2. Mean length and width values of *E. coli* EC, MCR1, and ECCOLR after 30-minute exposure to COL at indicated concentrations based off of five 5000X magnification SEM images.

List of Figures

Figure 1.1 Examples of cationic antimicrobials (CAs) studied in this thesis.

Figure 1.2. A cartoon summary of biocide and antibiotic CA mechanisms of action.

Figure 1.3. Traditional MIC AST methods used for determining susceptibility of antibiotics.

Figure 2.1. RFDMIA data from increasing concentrations of PI and cells.

Figure 3.1. PI RFU_{30min} EM 620nm of *E. coli* K12 BW25113 after 30-minute exposure to increasing concentrations of QAC.

Figure 3.2. RFDMIA of stationary phase *E. coli* K-12 BW25113 strains with increasing concentrations of BZK or CET.

Figure 3.3. RFDMIA results of *E. coli* EC, ECBZKT and ECCETT strains prepared by multiple growth conditions presence of increasing concentrations of BZK or CET.

Figure 3.4 RFDMIA results of EC, ECBZKT, and ECCETT with alternative QACs.

Figure 3.5. RFDMIA results of multiple bacterial samples exposed to increasing concentrations of BZK or CET.

Figure 3.6. RFDMIA results for the comparison between PI and Sytox^{TM} Blue in the presence of increasing concentrations of BZK with EC and PA.

Figure 3.7. RFDMIA results for the comparison between PI and Sytox^{TM} Blue in the presence of increasing concentrations of CET with EC and PA.

Figure 3.8. SEM images of *E. coli* K-12 BW25113 (EC, ECBZKT) exposed to increasing concentrations of BZK for 30 minutes.

Figure 3.9. A summary of measured *E. coli* K-12 strains' cell length and width measurements at various QAC concentrations from SEM images.

Figure 3.10. SEM images of *E. coli* K-12 BW25113 (EC, ECCETT) strains exposed to increasing concentrations of CET for 30 minutes.

Figure 3.11. A summary of measured *E. coli* K-12 strains' cell length and width measurements at various QAC concentrations from SEM images.

Figure 4.1. RFDMIA of *E. coli* K-12 BW25113 (EC, ECCHXT) strains incubated with increasing concentrations of CHX

Figure 4.2. 10,000X magnified SEM images of *E. coli* K-12 BW25113 (EC, ECCHXT) strains exposed to increasing concentrations of CHX for 30 minutes.

Figure 4.3. 5000X magnified SEM images of *E. coli* K-12 BW25113 (EC, ECCHXT) strains exposed to increasing concentrations of CHX for 30 minutes.

Figure 4.4. A summary of measured EC and ECCHXT cell length and width measurements at various CHX concentrations from SEM images.

Figure 4.5. SEM images of EC and PBS controls after heat-treatment.

Figure 5.1. RFDMIA results of *E. coli* K-12 BW25113 strains adapted to COL (ECCOLR) or transformed with *mcr-1* containing plasmid (MCR1).

Figure 5.2. RFDMIA results of *E. coli* K12 BW25113 TOB resistant clinical isolates and GNT resistant clinical isolates after 30-minute exposure to increasing concentrations of aminoglycosides.

Figure 5.3. SEM images of *E. coli* K-12 BW25113 (EC, MCR1, ECCOLR) strains exposed to increasing concentrations of COL for 30 minutes.

Figure 5.4. A summary of measured EC, MCR1, and ECCOLR cell length and width measurements at indicated COL concentrations from SEM images.

Figure 6.1. Comparison of traditional MIC AST assays to RFDMIA.

Abbreviations

30MBC	30-minute minimum biocidal concentration
60MBC	60-minute minimum biocidal concentration
AB	*A. baumannii*
AMP	Ampicillin
AMR	Antimicrobial resistance
AST	Antimicrobial susceptibility testing
BZK	Benzalkonium Chloride
CA	Cationic antimicrobial
CANWARD	Canadian hospital ward study
CARA	Canadian Antimicrobial Resistance Alliance
CDAB	Cetyldimethylammonium bromide
CET	Cetrimide bromide
CHX	Chlorhexidine hydrochloride
CLSI	Clinical Laboratory Standards Institute
COL	Colistin
CPC	Cetylpyridinium chloride
DDAB	Didodecyldimethylammonium bromide
DMSO	Dimethyl sulfoxide
EC	*E. coli* K12 BW25113
EC93	*E. coli* clinical isolate 93
EC96	*E. coli* clinical isolate 96
EC97	*E. coli* clinical isolate 97
EC102	*E. coli* clinical isolate 102
ECBZKT	*E. coli* K12 BW25113 derived BZK-adapted isolate
ECCETT	*E. coli* K12 BW25113 derived CET-adapted isolate
ECCHXT	*E. coli* K12 BW25113 derived CHX-adapted isolate
ECCOLR	*E. coli* K12 BW25113 derived COL-adapted isolate
EM	Emission
EUCAST	European Union Committee on Antimicrobial Susceptibility Testing
EX	Excitation
GNT	Gentamicin
ICU	Intensive care unit
KP	*K. pneumoniae*
KPBZKT	*K. pneumoniae* BZK-adapted
LB	Luria-Bertani
LPS	Lipopolysaccharide
MBC	Minimum biocidal concentration
MDR	Multidrug resistance/resistant
MIC	Minimum inhibitory concentration
PA	*P. aeruginosa*
PBS	Phosphate buffered saline
PI	Propidium iodide

QAC	Quaternary ammonium compound
RFDMIA	Rapid Fluorescent Dye Membrane Integrity Assay
RFU	Relative fluorescent unit
SS	*S. sonnei*
SSBZKT	*S. sonnei* BZK-adapted
TOB	Tobramycin
v/v	Volume by volume
WHO	World Health Organization

Chapter 1: Introduction

This section introduces background information pertaining to all antimicrobials, biocides and compounds used in this project, and their classifications. It overviews the problem of antimicrobial resistance in Gram-negative bacteria, its importance to antiseptic and disinfectant tolerance, and summarizes the current methods used to detect biocide antimicrobial resistance. Together, it justifies why a new rapid fluorescent assay (RFDMIA) developed and tested in the following chapters is necessary.

1.1 Antimicrobials and their classifications

Antimicrobials are defined as "drugs that treat infections by killing or slowing the growth of microbes causing infection" (1). We rely on antimicrobials to inhibit or eliminate bacteria and fungi from a variety environments, such as agricultural processing plants, to the fields where cattle are raised, to the hospitals and clinics where we go when we are sick, and, of course, within our own bodies as antimicrobial peptides protect us from microbial invasion (2–5). For the purposes of this thesis and broadly speaking, antimicrobials can be classified into two main categories: antibiotics and biocides.

'Antibiotics' described in this thesis can be broadly defined as a molecule that inhibits and/or kills microbes by specific interactions with bacterial targets (6). Antibiotics can be given orally, parenterally, or applied to the skin, which are used to treat bacterial infections in animals and humans (7, 8). Often, antibiotics take time (hours-days) to exert a bacteriostatic (preventing bacteria growth) and/or bactericidal activities (killing bacteria) (7–9). In contrast, "biocide"' is a term to define any chemical agent that inactivates microorganisms and encompasses a wide variety of chemicals that are used as either disinfectants (*i.e.* biocide used on inanimate objects/surfaces (10)), antiseptics (*i.e.* biocide used on living tissue (10)), and/or preservatives (*i.e.* biocide that prevents multiplication of microorganisms in formulated products (10)). Consequently, a biocide's destructive abilities activity and actions on a microorganism(s) are often exerted rapidly, in seconds to minutes in concentration dependent manners (11).

There have been serious concerns from public health agencies in Canada (12) and internationally (13) regarding antimicrobial over usage and the emergence of bacterial

antimicrobial resistance (AMR), which has been continually highlighted as one of the most concerning issues for public health in recent years and in the foreseeable future (7, 14). The World Health Organization (WHO) recently stated that antibiotic resistance is one of the biggest threats to global health today and prioritized bacteria according to their "Critical", "High", and "Medium" threat level to categorize AMR species for study (15). For antibiotics, the Clinical Laboratory Standards Institute (CLSI) and European Union Committee on Antimicrobial Susceptibility Testing (EUCAST) have definitions as to what would be considered antimicrobial "resistant" (16, 17). These organizations collect a wide variety of antimicrobial susceptibility data based on antimicrobial susceptibility tests (ASTs) such as the minimum inhibitory concentration (MIC) determination and the minimum biocidal concentration (MBC) determination. From these data, these institutes decide on individual antimicrobial breakpoints as to what would be considered antibiotic "Susceptible", "Intermediate", or "Resistant" (16, 17). Breakpoints corresponding to biocides have not yet been established (18) preventing a "resistance" determination/definition for biocides. As a result, the term "tolerance" is recommended for biocides and is based on a relative measurement of the tolerant isolate's susceptibility as compared to a control (18). This approach can add some bias and variations between studies, as the methods used to test biocide susceptibility are not established and lack reference AMR bacterial strains for precise biocide chemical compounds (18, 19).

Biocides are widely used compounds and used extensively in hospitals, clinics, and food processing industries (11, 20–22). Many of these compounds serve as the disinfectants as they rapidly (seconds-minutes) destroy bacteria in a concentration dependant fashion (19), leading them to being used more often than antibiotics (5, 11, 23). Biocide over-usage has led researchers to propose the idea of "biocide tolerance" and has led to research investigating its influence on overall antimicrobial resistance (19, 24, 25). There has also been some debate as to what role biocides play in exasperating the wide-spread emergence of antibiotic resistance with some studies highlighting the lack of *in situ* evidence for the emergence of biocide tolerant AMR pathogens (10, 11, 19, 25, 26). It is important to note here that most studies examining bacterial biocide tolerance involve the use of laboratory exposed clinical isolates (27, 28) or reference strains (28–30) that are gradually adapted to biocides though successive subculturing. These

biocide “adapted” (also known as “exposed”) species have been useful for investigating how biocide tolerance due to the lack of acceptable approved biocide susceptibility testing standards (18). Based on these biocide adaptation studies, there appears to be some discordance between a biocide adapted species’ ability to provide increased susceptibility to antibiotics or to other classes of biocides. Some studies indicate that biocide adaptation does not always confer antibiotic resistance (5, 11, 19, 20, 22, 25, 31, 32), making it more difficult to ascertain the impact biocides have on overall AMR mechanisms. Before discussing this issue in more depth, a discussion on biocide classes, their mechanisms of action, and their biocide tolerance is summarized in the following sections below with respect to all cationic biocide and therapeutic antimicrobials examined in this project.

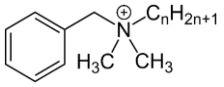
1.2 Cationic antimicrobials

Cationic antimicrobials (CAs) are broadly defined as any molecule with a net positive charge at neutral pH that exerts an antimicrobial activity (11). As a result, CAs can encompass both antibiotics such as polymyxins (colistin/polymyxin E, polymyxin B) and high concentrations of aminoglycosides (gentamicin, tobramycin), as well as biocides classes such as quaternary ammonium compounds (QACs) (benzalkonium, cetrimide) and bisbiguanides (chlorhexidine, alexidine) (11, 33–36) (Figure 1.1). Most antibiotic CAs and biocide CAs share a common mechanism of action involving bacterial cell membrane disruption (11, 34, 37). This mechanism initially involves the electrostatic attraction of the positively charged the CA to the net negative charge of the bacterial membrane (11, 34). Once adsorbed, the CA displaces divalent cations (Mg^{2+}, Ca^{2+}) destabilizing the bacterial membrane (11, 34). Ultimately, each CA penetrates one or more bacterial membranes disrupting cell integrity, leading to cell cytoplasmic leakage and eventual cell death (11, 19). The specific way by which various CA molecule classes achieve membrane disruption can be quite different and is highlighted in Figure 1.2 (11, 32, 34, 38). In this thesis I will focus on specific examples of the most widely used biocide CAs: benzalkonium, cetrimide, chlorhexidine, as well as important antibiotic CAs: colistin, tobramycin, and gentamicin.

Cationic antimicrobials

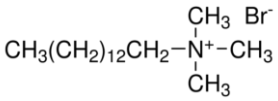
Biocides

Quaternary ammonium compounds (QACs)

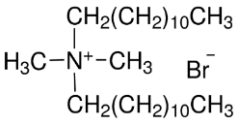


n=8, 10, 12, 14, 16, 18

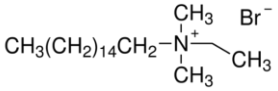
Benzalkonium (BZK)



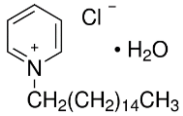
Cetrimide (CET)



Didodecyldimethylammonium bromide (DDAB)

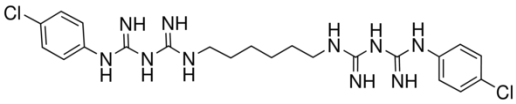


Cetyldimethylethylammonium bromide (CDAB)



Cetylpyridinium chloride (CPC)

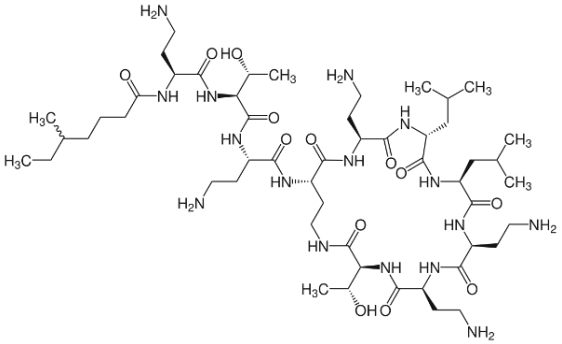
Bisbiguanides



Chlorhexidine (CHX)

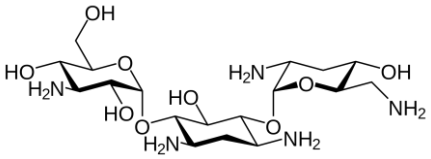
Antibiotics

Polymyxins

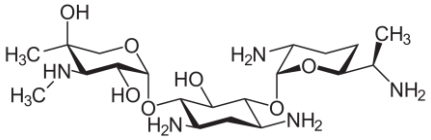


Colistin (COL)

Aminoglycosides



Tobramycin (TOB)



Gentamicin (GNT)

Figure 1.1 Examples of cationic antimicrobials (CAs) studied in this thesis. Panels are separated into biocide CAs (left) and antibiotic CAs (right).

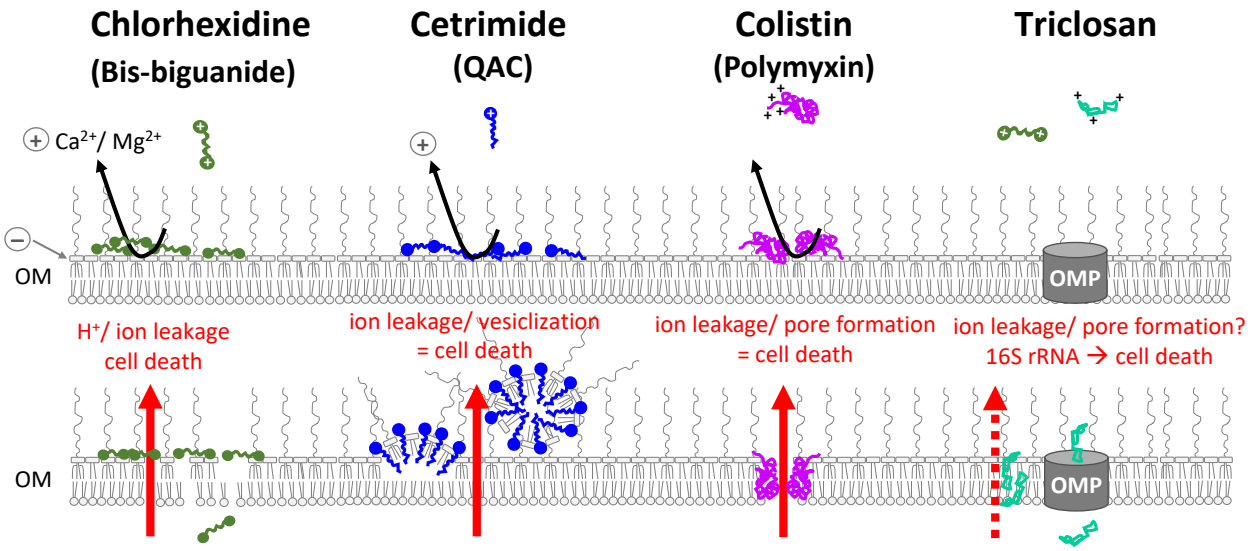


Figure 1.2. A cartoon summary of biocide and antibiotic CA mechanisms of action from the perspective of a Gram-negative bacterial outer membrane (OM) (11, 39, 40).

1.2.1 Biocide CAs

1.2.1.1 Quaternary ammonium compounds

Quaternary ammonium compound (QAC) is a term used to describe a collection of organic compounds that contain four functional groups attached one or more permanently charged amine atom (41, 42) (Figure 1.1.). This category of biocide CA includes many disinfectants and antiseptics (11). QACs are manufactured or imported at a rate of more than 45,000 kilograms per year in the United States alone (41). QACs can be synthesized with relative ease, and can be synthesized to generate a library of unique structures, ultimately allowing industries to use QACs with a wide variety of structures and compounds (43). Clinically and industrially important antimicrobial QACs include: benzalkonium (BZK), cetrimide (CET), didodecyldimethylammonium bromide (DDAB), cetylpyridinium chloride (CPC), and cetyldimethylammonium bromide (CDAB) (Figure 1.1). QACs can be found in a wide variety of products including: disinfectants, cosmetics, industrial cleaners, ointments and eye drops, as well as many other household cleaning products (44–49). As with all CAs, QACs exert their antimicrobial action by cation displacement and membrane disruption as shown in Figure 1.2 (11, 50). Initially, the positively charged quaternary nitrogen adsorbs to the acidic phospholipids of the bacterial membrane (11, 37, 51). Next, the divalent cations are displaced, and the hydrophobic tail of the QAC inserts itself into the hydrophobic membrane core (11, 37, 51). This causes a decrease in membrane fluidity resulting in hydrophilic voids (11, 37, 51). Consequently, the membrane transitions from a fluid to a more crystalline state, losing many of its osmoregulatory and physiological functions (11, 37, 51). As the concentration of QAC increases, the solubilization of phospholipids and proteins into QAC/phospholipid micelles also increases, leading to cell death (11, 37, 51).

1.2.1.2 Bisbiguanides

Bisbiguanides are another prominent biocide CAs with its most representative member chlorhexidine (CHX) being classified as an essential medicine by the WHO (38) (Figure 1.1). These widely used antiseptics are primarily found in a variety of oral hygiene products (11), in personal care wipes (52, 53), and surgical handwashes and are occasional additives in household products (11, 54). CHX has a similar mechanism of action to QACs, where the biguanide groupings strongly

associates with the exposed anionic sites of the bacterial membrane, particularly phospholipids and proteins (11). Unlike QACs, CHX does not become solubilized in the hydrophobic core of the membrane (11). Instead, due its shorter carbon length (CHX: C6; QACs: C8-16 (11)) and its relatively inflexible hydrophobic regions, CHX is suggested to bridge the gaps between pairs of phospholipid head groups (11, 38, 55). The subsequent displacement of divalent cations and interaction of CHX with the membrane phospholipid head groups and proteins disrupts membrane fluidity and osmoregulatory actions (11, 38) (Figure 1.2). This causes a loss of structural integrity and lethal cellular ion/content leakage (11, 38).

1.2.2 Antibiotic cationic antimicrobials

1.2.2.1 Aminoglycosides

Aminoglycosides such as tobramycin (TOB) and gentamicin (GNT) (Figure 1.1) are important broad-spectrum bactericidal antibiotics that strongly bind to the A-site of the 16S ribosomal RNA of the 30S ribosome (33, 56, 57). In so doing, they promote error prone protein synthesis, resulting in an abundance of incorrectly formed polypeptides and misfolded proteins to over-accumulate within the bacterial cell (33, 56, 57). However, some studies have proposed that aminoglycosides may increase membrane permeability, similar in mechanism of action to other CAs classes (33, 56, 57). As shown in Figure 1.2, entry of aminoglycosides into bacterial cells has three distinct stages. Initially, there is an electrostatic binding of the positively charged aminoglycoside to the net negative charge of the bacterial membrane to displace divalent cations (33, 56, 57). This results in the disruption of the bacterial membrane thereby increasing the overall permeability of the membrane and the uptake of aminoglycoside into the bacterium (11, 33, 56, 57). Once inside the bacterium, an aminoglycoside exerts its protein translation disruptive abilities, resulting in the accumulation of mistranslated proteins in the cell and membrane, causing further uptake of aminoglycosides resulting in cell growth arrest and death (33, 56, 57).

1.2.2.2 Polymyxins

Polymyxins are antibiotic CA peptides with significant *in vitro* activity against a variety of Gram-negative bacterial species due to the presence of lipopolysaccharides (LPS) in their membrane (58, 59). For clinical use, there are two main polymyxins: polymyxin B and polymyxin

E (also known as colistin; COL); both are considered drugs of last resort, as they are usually employed when other therapeutic antimicrobials (β-lactams, aminoglycosides, or quinolones) are ineffective (39, 58, 60). Despite their conservative therapeutic allocations, COL usage has increased substantially in veterinary medicine (34, 61) and is a common additive in animal feed with it being the 5th most commonly used antimicrobial on European union farms in 2011 (62). As with other CAs, polymyxins have a similar membrane disruptive mechanism of action, however, its exact mechanism is currently unclear and remains debated with several models proposed (60, 63, 64). The long-accepted model of polymyxin, specifically COL, mechanism of action involves a two-step mechanism (Figure 1.2) (34, 39), where, at physiological pH, there is a protonation of the polymyxin, allowing for it to electrostatically binds to the cell envelope between the polycationic ring of polymyxin and the outer membrane (LPS) lipids (39, 58). This displaces Ca^{2+} and Mg^{2+} ions in a competitive fashion (39, 58). Subsequently, the polymyxin inserts itself into the membrane, weakens the packing of the membrane, causing the membrane to expand further, eventually causing a fusion between the outer and the inner membranes resulting in an osmotic imbalance and subsequently, cell death (39, 58).

1.3 The problem of antimicrobial resistance

The concept of AMR was acknowledged shortly after the introduction of penicillin, the "first" antibiotic discovered during the 1940's (7, 65, 66). Since then, there has been a constant expansion of AMR bacteria (14). This has caused AMR to become a global health concern with many national and international organizations, from the Public Health Agency of Canada (12) to the WHO (13), to create their own resources and plans on how to best deal with this emerging health crisis. This concern is fuelled by the importance of antimicrobial usage within society, especially in the healthcare, chemical, and agricultural industries (7, 67, 68). Antimicrobial usage has increased for a number of reasons beyond their application as a treatment of infections, and include growth promotion in livestock to their uses as surface antiseptics/disinfectants for surface sterilization (69–72). This has placed greater selective pressure on bacteria to withstand and adapt to their bactericidal and/or bacteriostatic actions.

Bacterial AMR selection pressure has intensified due to the overuse and inappropriate use of antimicrobials (73, 74). AMR mechanisms that emerge within bacteria can be categorized into two main groups, “intrinsic” and “acquired” AMR (25, 41, 75, 76). Intrinsic or naturally occurring AMR describes a bacterium’s ability to resist the actions of an antimicrobial due to its inherent structural or functional properties (23, 51, 77). Generally, intrinsic AMR are due to traits shared within a species that is independent of horizontal gene transfer (78). A simple example of intrinsic AMR differences is seen when comparing AMR of Gram-positive to Gram-negative bacteria; Gram-positive bacteria with only a cytoplasmic membrane are often susceptible to more classes of antibiotics when compared to the dual membrane (outer membrane and cytoplasmic membrane) architecture of Gram-negative bacteria (66, 79–81).

Acquired AMR occurs when a bacterium acquires exogenous genetic material, usually from horizontal gene transfer that provides an increase in resistance/tolerance towards one or more antimicrobial molecules (78, 81). An example of acquired resistance is the transmission of mobile genetic elements between various strains/species containing plasmids which frequently encode AMR genes (14, 41, 66, 77, 82, 83). For CA resistance/tolerance, mobile genetic elements play a critical role by spreading of genes associated with AMR. There have been multiple studies that have found biocide CA tolerance genes (*qacA* (35, 84–87)*, mdfa* (21, 88)*, aceI* (21), *qacH* (84, 87), Etc.) in plasmids or transposons containing additional antibiotic resistance genes within clinical isolates (21, 84–86, 89, 90). This is alarming as acquisition of biocide CA tolerance would provide bacteria with an ability to persist on a surface even after it had been “disinfected”. Furthermore, for COL, the mobilization of COL resistance genes for the phosphoethanolamine transferase gene known as mobilized colistin resistance gene *mcr (e.g*. *mcr-1*, *mcr-2*) that had been discovered in 2015, has caused world-wide concern as COL is considered a drug of last resort (91–93). Additionally, there have been multiple studies that have found COL resistance genes in addition to carbapenemase genes (*e.g*. bla_{NDM} (94)) on the same plasmids (92, 94, 95). Together, this sets up a frightening future where AMR is rampant and efforts to disinfect surfaces could prove fruitless.

1.3.1 Critical priority AMR Gram-negative pathogens

In 2017, the WHO released its first ever list of AMR priority pathogens where 12 bacterial groups were compiled in consultation with various industries and professions using a variety of parameters, that included mortality, healthcare burden, prevalence, specific important antibiotics, and trend of resistance, to help prioritize the study of the most important AMR pathogens (15). From this listing, the WHO designated three groups of Gram-negative bacteria as critical AMR priorities, these groups represent the species focused on in this thesis. Critical AMR priority species were carbapenem resistant Enterobacterales (formally know as Enterobacteriaceae) species (including *Escherichia coli*, *Klebsiella pneumoniae*, and *Shigella sonnei*) as well as two Pseudomonadales species (*Pseudomonas aeruginosa* and *Acinetobacter baumannii*) (15). A discussion of each species is briefly provided in the subsections below.

1.3.1.1 *Pseudomonas aeruginosa*

P. aeruginosa is a motile, Gram-negative, non-fermentative aerobe, that is an important opportunistic pathogen (96). This bacterium can be found in a variety of settings including soil (97), aqueous environments such as hospital sinks (98), and a variety of abiotic surfaces, where it generally grows as a surface attached, drug-resistant biofilm (96, 99–101). *P. aeruginosa* is a ubiquitous aerobic species affecting plants and animals (102). As a pathogen, *P. aeruginosa* is often found colonizing the lungs of individuals with cystic fibrosis as well as on many patients during hospitalization (101). It is considered a major healthcare threat and is one of the leading causes of nosocomial lung infections worldwide (97, 103, 104). Importantly, *P. aeruginosa* is notoriously difficult to treat with most available antibiotics justifying its placement on the WHO's list of critical AMR pathogens (Section 1.3.1) (15, 105). With a relatively large genome (5-7 Megabase pairs), *P. aeruginosa* possesses many previously identified and characterized AMR gene mutations and enzymatic mechanisms of AMR in addition to an impressive collection of genes that allow it to metabolize toxic compounds and persist in harsh aerobic environments (100, 106). Additionally, *P. aeruginosa* is intrinsically tolerant towards CET as well as other biocides due to the presence of many efflux pump systems and its preference for biofilm (106, 107). *P. aeruginosa* was the second most common organism isolated from Canadian ICUs

between 2007 and 2016, with 15% of the isolates being multidrug resistant (MDR) (108); where MDR is defined as non-susceptible to at least 1 agent in 3 or more antimicrobial categories (109).

1.3.1.2 *Acinetobacter baumannii*

A. baumannii is a Gram-negative, strict aerobe, non-fermentative, non-motile pathogen. In contrast to *P. aeruginosa*, *A. baumannii* lacks a well-defined habitat outside of clinical/nosocomial environments (110, 111). This bacterium was previously considered to be a low-priority AMR pathogen until recently (past 10 years), where it has been emerging as a leading cause of nosocomial and community acquired infections (110, 111). Similar to *P. aeruginosa*, *A. baumannii* has the ability to resist a wide variety of antimicrobials due to its intrinsic resistance mechanisms that include efflux pumps (112, 113), its ability to easily incorporate foreign DNA (110, 113), and its low membrane permeability (110, 112). In Canadian ICUs, *A. baumannii* is not listed among the top 10 most common isolates from Canadian ICU patients from 2007-2016 as there were only 90 carbapenem-resistant isolates collected from the past 7 years of the 2019 Canadian hospital ward (CANWARD) study; the majority of *A. baumannii* species in Canada were susceptible to most antimicrobial testing panels (114, 115). However, of these carbapenem resistant isolates identified, 74 would be classified as extensively drug resistant (XDR) (114); XDR being defined as non-susceptible to more than one antimicrobial agent in all but two categories (109). A study by Fernández-Cuenca *et al.* 2015 proposed that the success of *A. baumannii* to persist primarily in hospitals and clinics may be due to the co-association of biocide tolerance genes, especially efflux and porins, with known antibiotic resistance genes (116).

1.3.1.3 *Escherichia coli*

Enterobacterales member *E. coli* is Gram-negative, motile, fermentative, facultative anaerobe that is considered to be one of the most well-studied Gram-negative organisms (117, 118). Depending on the *E. coli* strain or serotype antigen, it can be considered as either a pathogen or a commensal organism (117, 119). In Canadian ICUs, *E. coli* is the most commonly isolated pathogen in patient reparatory, blood, wound, and urine specimen sites (68, 115), which reflects similar global trends with *E. coli* continuing to be the most frequently identified Gram-negative bacterium that causes bloodstream and urinary tract infections worldwide (117). *E. coli*

is often characterized as having a flexible genome allowing them to acquire genes or intrinsically mutate to rapidly adapt to a wide variety of conditions (66, 117). *E. coli* also has a propensity to carry and transfer various mobile genetic elements that confer resistance/tolerance to antimicrobial agents (117). A recent CANWARD study from 2019, indicated that there was an important rise in extended spectrum β-lactamase producing *E. coli* isolates from 2007-2016 (120). Well established CA resistance/tolerance mechanisms of *E. coli* are similar to many other Gram-negative bacteria and involve efflux pump activity, membrane modifications, and porin downregulation (this will be detailed in section 1.4.2) (24). AMR gene surveillance studies often detect various biocide CA resistance genes in *E. coli* AMR clinical isolates (21, 121), suggesting a co-association between biocide CA tolerant genes and antibiotic resistance.

1.3.1.4 *Klebsiella pneumoniae*

Enterobacterales species *K. pneumoniae* is a Gram-negative, non-motile, fermentative, facultative anaerobe (122). This bacterium can be found in the soil, in surface waters, medical devices, and human mucosal surfaces (123). *K. pneumoniae* had gaining notoriety as an AMR pathogen due to its increasing identification in infections as well as by being capable of being both antimicrobial resistant as well as hypervirulent (122, 123). In Canada, *K. pneumoniae* is the 5th most common bacterial AMR pathogen isolated from Canadian hospital laboratories between 2007-2016 (115). This pathogen is considered to be an opportunistic pathogen but, impressively, many hypervirulent *K. pneumoniae* serotypes has been able to infect healthy patients causing bacteremia, pneumonia, necrotizing fasciitis among other serious infections (123, 124). *K. pneumoniae* can modify lipopolysaccharides (LPS) and capsule formation, allowing it to become more virulent and enhance its transmission from person to person with relative ease (122, 123). Additionally, the ease of LPS and capsule formation modifications by this species has enabled it to become more intrinsically tolerant/resistant towards CAs (125). In a study by Wand *et al.* (2016) the researchers found that CHX tolerance provided cross-resistance towards COL and that these factors were driven by lipid modifications (55).

1.3.1.5 *Shigella sonnei*

Enterobacterales species *S. sonnei* is a Gram-negative, non-motile, fermentative, facultative anaerobe that is a highly infectious organism capable of cause shigellosis disease, also known as dysentery (126–128). This species causes serious infections in young children aged 2-5 years with shigellosis being responsible for approximately 53,000 deaths per year worldwide (127). Normally, shigellosis is a self-limiting disease, but complications can arise where treatment with antimicrobials is necessary (127). Unfortunately, no antimicrobial agent emerges as the superior treatment (127). One of the best ways to prevent the spread of *S. sonnei* is by proper hygiene practices, where disinfectants play an important role (126, 127, 129). Fortunately, in Canada *S. sonnei* has not appeared in the top 20 most frequently isolated Canadian hospital AMR pathogens from the CANWARD initiative from 2008-2016 (115). Similar to *E. coli*, AMR among *Shigella* spp. is driven, in part, by lower outer membrane permeability and increased efflux pump activity (130). By reducing permeability *Shigella* spp. have the capacity to become CA tolerant/resistant though, this area is still underdeveloped as there are few publications investigating *Shigella* spp. CA resistance/tolerance (130). This is reflected in Table 1.1 which will be discussed later.

1.4 CAs and their impact on AMR in Gram-negative bacteria

Gram-negative infections are some of the most serious and the most common types of AMR infections (131). In an international study from 2009, examined the prevalence of bacterial infections within ICUs found that, of the infected individuals, 62% were infected with a Gram-negative pathogen (131). In a separate study from 2007 found that infection with an AMR Gram-negative pathogen was predictive of increased hospital cost as compared to an antimicrobial susceptible Gram-negative pathogen (132). The increase in median cost for an antibiotic sensitive Gram-negative bacterial infections was $29,604 USD while AMR Gram-negative infection was $80,500 USD (132). Further, it is projected that by 2050, if the current usage and resistance trends continue, AMR will be responsible for 10 million deaths worldwide(133).

CAs play a dual role within the issue of AMR and represent an excellent example of AMR as a “One Health” problem (134). One Heath is defined as a collaborative effort of multiple health

science professions to attain optimal health for people, domestic animals, wildlife, plants, and our environment, and with respect to AMR (134). It seeks to regulate/steward more appropriate usage of antimicrobials for agriculture, industrial usage to preserve them for therapeutic treatment (134). Using COL as an antibiotic CA specific example which is depended on more frequently to treat a variety MDR Gram-negative bacterial infections (60, 135). While the rate of COL resistance remains low in Canada (115), COL-resistant isolate rates from hospital infections have been increasing internationally and correlate to regions that overuse COL often for agricultural applications (74). With respect to biocide CAs, QAC represent another One Health AMR example, since they are often overused in a multitude of products some only to extend the shelf-life of commercial products. Biocide CAs such as QACs are used for disinfectant (11), antiseptic (11), industrial surfactants (41, 46), and preservatives purposes (70). As a result of their widespread usage, these compounds magnify and increase in concentration in soil and water systems (46, 136), placing greater selective pressure on species that live in wastewaters allowing them the opportunity to adapt and tolerate these biocide CAs (41, 46). QAC tolerance has been associated with antibiotic resistant bacterial outbreaks (31, 44, 137–139), and as result may reduce our ability to adequately disinfect surfaces with QACs. Together, biocide CAs and antibiotic CAs plays key roles in AMR to both treat multidrug resistant infections as well as to reduce the transmission of bacteria.

1.4.1 Biocide CA tolerance in Gram-negative species

Biocide CA tolerance is field of AMR research that has a critical problem, it lacks defined drug concentration breakpoint definitions (16). The lack of defined resistance breakpoints often result in biocide studies that must define how they measure CA tolerance, making it harder to compare different studies of the same drugs together since “tolerance” is a relative measurement (18). Furthermore, there is considerable controversy with respect to whether or not biocide CA tolerance is a real AMR threat (22). This debate is fueled by the fact there has been no noted increases in biocide CA tolerance within industrial or healthcare settings (11, 19, 25, 70), particularly if CAs are used at their recommended working concentrations (67). It is important to note that even when proper biocide CA usage is abided by, these compounds ultimately dilute and become a wastewater or environmental contaminant, and act as a potential

selective pressure driver (46, 140). Additionally, other studies suggest that the bactericidal membrane disruptive mechanism of action of most biocide CAs may be another explanation for low rates of biocide CA tolerance among clinical isolates (70, 141). Ironically, the same statement has been made as to why there has been little COL resistance and this notion was recently proven incorrect by the identification of COL resistant bacteria worldwide (39, 93). In contrast to COL resistance, biocide CA tolerance is not tested for due to the lack of accepted standards, which creates the right conditions for a sudden emergence of widespread biocide tolerance if we begin to test for it. In an effort to understand biocide CA tolerance and antibiotic CA resistance it is important to review their mechanisms as described in the next sections.

1.4.2 Mechanisms of Antibiotic CA resistance and biocide CA tolerance

In general, there is far more knowledge about the mechanism of action of antibiotics when compared to biocide CAs. Antibiotics typically target a specific, essential function or system in a bacterium; for example, its ability to synthesize peptidoglycan, DNA replication, protein translation. Antibiotics can be separated into classes based on their function and chemistry (β-lactams, quinolones, aminoglycosides, etc.). Resistance to an antibiotic can be generally attributed to a single gene, such as *mcr-1* which provides COL resistance by adding an ethanolamine to LPS, which will modify the targeted system (39, 142). These genes can be genetically tested for, allowing for the determination of resistance. Though, it is noted that detection of the specific gene does not necessarily indicate resistant phenotype (143). In contrast to antibiotics, biocide CAs generally do not target a single essential system due to their mechanism of action; bisbiguanides and QACs can denature hydrophobic or negatively charged proteins, can generate reactive oxygen and nitrogen species affecting multiple essential systems in a concentration dependent manner (4, 11, 144). Hence, the detection of individual genes specifically associated to biocide CA tolerance has been more difficult when compared to antibiotic CAs.

There are three well known mechanisms associated with Gram-negative bacterial species that exhibit antibiotic CA resistance or biocide CA tolerance: i) Lipid A content alterations (Mcr-1, KdtA) that reduce the net negative charge of the bacterial membrane, thereby, reducing the

electrostatic attraction between the CA and the negatively charged membrane (34, 145–147), ii) altered porin expression (OmpC and OmpF) to prevent CA diffusion across the outer membrane (51, 81, 105, 148), and iii) increased efflux pump activity (AcrAB, MdfA) to allow any CA that has entered a cell to be expelled out of the cell periplasm or cytoplasm preventing the CA from further antimicrobial action (21, 31, 39, 57, 149, 150). It is important to note that bacteria may use one of the mechanisms listed above on their own or in combinations to achieve a CA resistant/tolerant phenotype. This complicates antimicrobial susceptibility testing to determine biocide CA tolerance, as these bacteria can employ one or all of the currently know mechanisms of CA resistance/tolerance. Further, efflux pump activity (81, 151) and porin regulation (81) are key components of proper metabolic and osmoregulatory functions within a bacterium; CA tolerance/resistance plays a secondary role to these metabolic functions. As a result, the detection of a specific efflux pump gene, such as the AcrAB-TolC complex of *E. coli*, does not necessarily imply CA resistance/tolerance. Additionally, many CA resistant/tolerant Gram-negative species have demonstrated increased cross-resistance to a variety of antibiotic classes as well as cross-tolerance to other biocide classes, likely due to the overlap of these CA resistant/tolerant mechanisms which will be discussed below.

1.4.3 Biocide and antibiotic cross-resistance/cross-tolerance

Previous studies have shown that many AMR proteobacteria considered to be critical priority AMR pathogens (e.g. Enterobacteriales, *Acinetobacter* spp. and *Pseudomonas* spp.) are intrinsically tolerant to higher concentrations of biocide CAs than Gram-positive species (15, 23). Critical priority AMR species have demonstrated an ability to adapt to biocide CAs after prolonged or repeated exposures at sub-lethal CA concentrations, that can consequently increase antimicrobial cross-resistance/tolerance (65, 152, 153) (Table 1.1). Enhanced CA tolerance caused by low level CA exposure is concerning if we consider biocide CAs are common soil and wastewater environmental contaminants (44, 46, 154, 155). For example, our global QAC usage is estimated to be 100 times greater than the total amount of therapeutic antibiotics used annually (41, 156). Previous studies show evidence of antimicrobial cross-resistance/cross-tolerance phenotypes in *E. coli* (27, 30, 157), *P. aeruginosa* (28, 152), *A. baumannii* (32), and

Table 1.1. A summary of proteobacterial biocide CA tolerance and antimicrobial cross-resistance AST findings (as fold change values) determined from previously published MIC data.

Species tested	Clinical (C) or adaptation	CA	MIC baseline (mg/L)	MIC of tolerant/resistant isolate(s)	Mean fold-increase in resistance/tolerance	Cross-resistance (Antibiotics)	Fold-change	Cross-tolerance (Biocides)	Fold-change	Reference
A. baumannii Clinical isolate	C	N/A	N/A	N/A	N/A	TET	128.0	CHX	2.0	(32)
						GNT	16.0	BZK	0.0	
						CIP	64.0	BZT	2.0	
						CAZ	0.0	ADH	2.0	
A. baumannii Clinical isolate	C	N/A	N/A	N/A	N/A	TET	-2.0	CHX	4.0	(32)
						GNT	-2.0	BZK	0.0	
						CIP	-4.0	BZT	2.0	
						CAZ	0.0	ADH	0.0	
A. baumannii ATCC 17978	A	COL	1	>64	64	AMK	-4.0	CHX	0.0	(29)
						CIP	0.0	Quat	-3.9	
						CEF	0.0			
						GNT	-2.0			
A. baumannii NCTC 13424	A	COL	1	>64	64	AMK	0.0	CHX	-4.0	(29)
						CIP	0.0	Quat	-3.9	
						CEF	-16.0			
						GNT	0.0			
E. coli ATCC 11775	A	BZK	25	150	6	AMP	5.0	N/A		(30)
						TET	4.0			
						GNT	2.0			
						CHL	24.0			
E. coli DSM 682	A	BZK	25	150	6	AMP	4.0	N/A		(30)
						TET	1.5			
						GNT	2.0			
						CHL	12.0			
E. coli	A	CTAB	5.47		3.3	AMP	>200.0	BZK	3.5	(157)

OW6				18.88		CHL	7.9	CPC	4.0	
						TET	2.7	Paraquat	12.0	
						KAN	3.0			
E. coli Clinical isolate	A	BZK	32	83.2	2.6	AMP	5.0	BZK	2.6	(27)
						GNT	1.2	DDAC	2.9	
						CHL	6.2	OCDAC	1.8	
						TET	4.2			
E. coli Clinical isolate	A	DDAC	3	10.5	3.5	AMP	3.0	BZK	2.6	(27)
						GNT	1.2	DDAC	3.5	
						CHL	9.0	OCDAC	3.4	
						TET	4.0			
K. pneumoniae NCTC 13443	A	CHX	16	512	32	COL	>64.0	BZK 0.0		(55)
						CEF	0.0	CPC	0.0	
						CHL	-8.0			
						AMK	0.0			
K. pneumoniae NCTC 13368	A	CHX	32	256	8	COL	>64.0	BZK	-2.0	(55)
						CEF	0.0	CPC	-4.0	
						CHL	-8.0			
						AMK	0.0			
K. pneumoniae Clinical isolate	A	BZK	*	*	*	AMP	4.0	N/A		(158)
						CHL	0.0			
						TET	4.0			
						GNT	2.8			
P. aeruginosa ATCC 15692	A	BZK	30	500	16.7	PMB	11.1	CET	3.6	(28)
						TOB	-0.1	CPC	4.2	
						CIP	2.1	CHX	0.0	
						CHL	2.0			
P. aeruginosa Clinical isolate	A	BZK	150	500	3.3	PMB	0.0	CET	-1.7	(28)
						TOB	-6.7	CPC	0.0	
						CIP	-1.6	CHX	0.3	
						CHL	1.1			
P. aeruginosa NCIMB 10421	A	BZK	25	350	14	TOB	-1.5	N/A		(160)
						PMB	-2.0			
						AMK	-1.3			
						MIN	-8.0			

All fold changes are compared to respective baselines in each study

Negative values show an increase in susceptibility; positive values indicate decreased susceptibility
N/A: Not applicable
*: Study did not give values, simply that they were adapted.
NB: This is not an exhaustive list, simply examples of the discordant results within the literature.
ADH: Alkyldiaminoethylglycine hydrochloride, AMK: Amikacin, BZK: Benzalkonium chloride BZT: Benzethonium, CAZ: Ceftazidime , CEF: Cefepime, CHL: Chloramphenicol, CHX: Chlorhexidine, CIP: Ciprofloxacin, COL: Colistin, DDAC: Didecyl dimethyl ammonium chloride, GNT: Gentamicin, MIN: Minocycline, OCDAC: dioctyldimethylammonium chloride, Quat: Quaternary ammonium disinfectant, TET: Tetracycline.

K. pneumoniae (55, 158) and was recently reviewed by Kampf, 2018 (159) (Table 1.1). To date, biocide CA tolerance mechanisms are rarely identified or examined in most CA phenotypic studies listed in Table 1.1, and few identify biocide CA tolerance genes. Among the studies listed in Table 1.1, are a few conflicts with respect to how biocide CA adaptation alters antibiotic cross-resistance and vice versa. Hence, bacterial adaptation to biocide CAs does not consistently provide significant cross-resistance/tolerance to other antimicrobials (23, 25, 28, 29, 160), suggesting other as yet unidentified factors play a role.

1.5 AMR detection methods

1.5.1 Detection of antibiotic CA resistance phenotypes by Gram-negative bacteria

Current clinically recognized and standardized antimicrobial susceptibility testing methods used to detect AMR in Gram-negative bacterial species permit the calculation of an MIC value as well as an MBC value when any strain/species is exposed to a range of antimicrobial drug concentrations (16–18). MIC AST approaches to measure tolerance values involves traditional AST methods that frequently involve agar plate Etest® strips (bioMérieux), agar plate disk diffusion, broth microdilution methods (Figure 1.3). Many clinical diagnostic labs and facilities have moved to the use of automated systems such as the VITEK® 2 system (bioMérieux) to determine MIC values. For MBC approaches, they are based on broth media exposures at predefined concentrations of antibiotic with pre-set time intervals (161). At each timepoint, the exposed culture and a growth control are spread plated and loss of viability is calculated after 24-hour incubation (161). In all cases, AST methods examine defined identical suspensions of a pure cultured bacterial isolate grown at increasing antimicrobial drug concentrations, often $\log_2$ dilution series or pre-defined concentrations at resistant, susceptible, or intermediate breakpoints. The MIC value is based on the lowest concentration at which cell growth is inhibited (16), while MBC is defined as where there has been a reduction (at least 90% reduction after 6

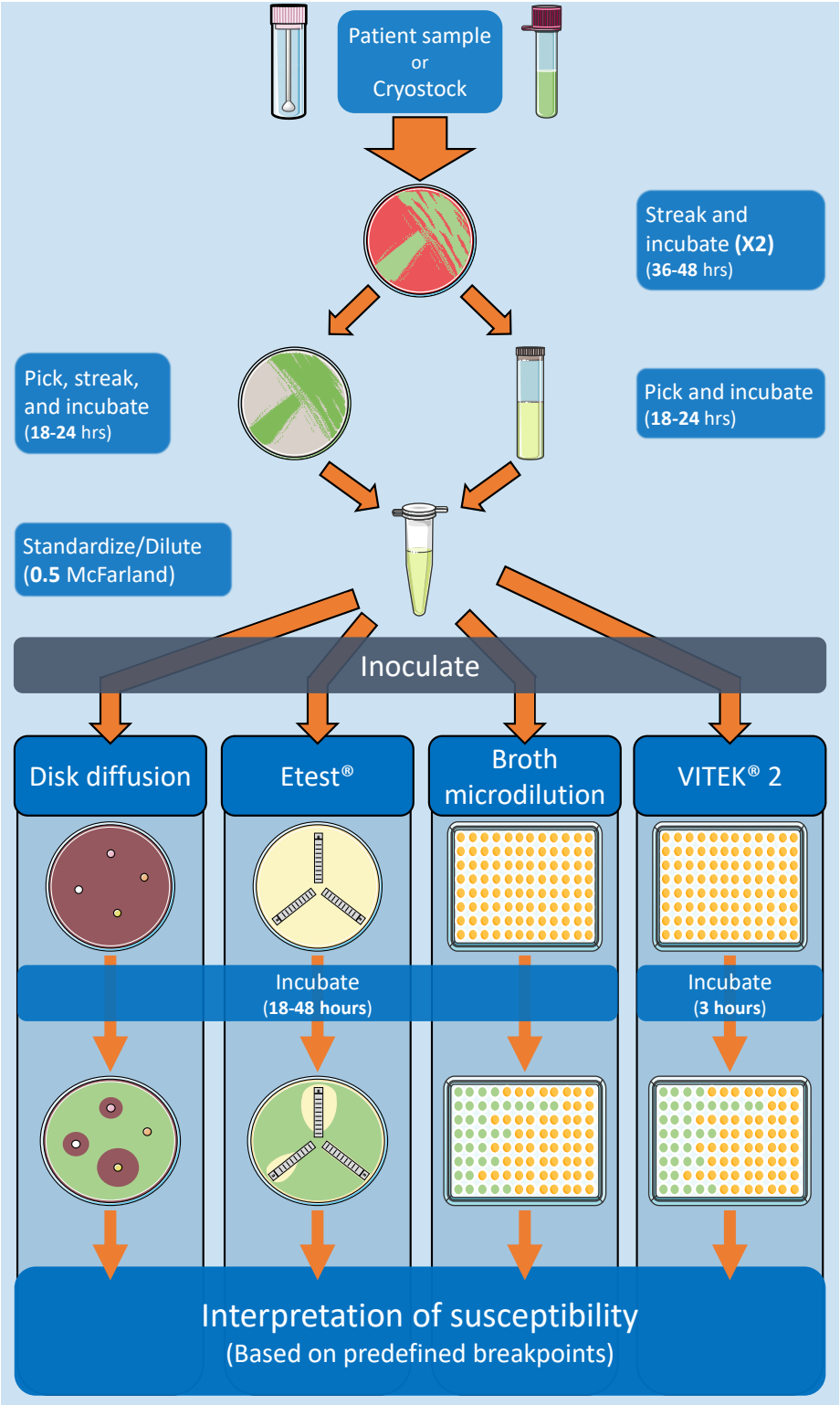


Figure 1.3. Currently used AST methods used for determining MIC values of antimicrobials. Clip art images supplied by Servier Medical Art and used under creative commons licence. hours of exposure) in the number of living cells as compared to a growth control (161).

Once known, MIC and MBC can be compared to various reference strains of known drug susceptibility (10, 18, 26, 162). For antibiotics, these methods have been rigorously tested by CLSI and EUCAST to develop regulated clinical international standards and testing procedures that ensure reproducible identification of MIC values (Figure 1.3) and MBC values between labs. With these rigorous standards and testing procedures it allows for standard interpretations of "susceptible", "intermediate", and "resistant" isolates that a lab would be examining. As seen in Figure 1.3 many of the traditional MIC AST methods are laborious and time-consuming requiring days to complete (16–18). Even the expensive automated VITEK® 2 system, requires at least 3 hours to determine antimicrobial susceptibility towards premade panels of antibiotics. However, MIC values determined using CLSI and EUCAST AST methods represent the most reliable and reproducible techniques for measuring AMR at the current time.

1.5.2 Detection of biocide CA tolerance for Gram-negative bacteria

One of the major knowledge gaps in bacterial QAC susceptibility studies is the lack of routine, standardized, clinical antimicrobial susceptibility tests to measure biocide CA tolerance. Additionally, biocide CAs are not regulated by European Committee on Antimicrobial Susceptibility Testing (EUCAST) or Clinical and Laboratory Standards Institute (CLSI); biocide CAs lack defined breakpoint concentrations that can be used for antimicrobial susceptibility testing (AST) (25, 63). Consequently, QAC "resistance" values are not standardized, and should be referred to as "tolerance" values herein (18). Current approaches to measure QAC tolerance values involves the aforementioned AST methods (Figure 1.3) (10, 18, 26, 162) but are not included in automated AST drug testing panels. These laborious methods are the only established techniques to reliably measure MIC and MBC values; biocide CA AST methods are time consuming (requiring 24-48 hrs) and frequently do not involve the use of a bacterial reference strain control, as few have been reliably determined or agreed upon. Hence, there is considerable need for a rapid and sensitive assay to determine biocide CA susceptibility and overcome these current knowledge gaps and more in-depth study of biocide CA tolerance mechanisms.

1.6 Thesis Aims and Hypotheses

In contrast to antibiotic susceptibility determination methods, there are no standardized methods to detect biocide CA tolerance. When biocide CA susceptibility testing is performed, most methods are based on the MIC and MBC assays. This causes an increased workload for technicians and researchers when investigating biocide CA tolerance. Since biocide CAs lack defined clinical break points, distinction between tolerant from susceptible phenotypes are rarely measured clinically or industrially, making it harder to determine what the actual rates of CA tolerance are among infectious AMR pathogens. These factors highlight the need to develop an assay that is rapid, reproducible, standardizable, and capable of differentiating between CA tolerant/resistant bacteria and CA susceptible species.

The aim of this thesis was to develop an assay to detect CA tolerant/resistant phenotypes and predict proteobacterial CA susceptibility or tolerance in a rapid 30-minute fluorescent impermeant dye-based assay with the use of live and heat-treated bacteria; this assay is referred to as the Rapid Fluorescent Dye Membrane Integrity Assay (RFDMIA). RFDMIA was designed to detect CA susceptibility among critical AMR priority Gram-negative species. This assay monitors the uptake of a membrane impermeant dye by bacteria disrupted by exposure to increasing CA concentrations, where the dye fluorescence increase is an indirect proxy to measure overall cell membrane integrity.

We **hypothesize** that cells incubated with increasing concentrations of CAs in the presence of a membrane impermeant dye, propidium iodide (PI), can be fluorescently monitored to detect bacterial CA susceptibility. Based on this hypothesis, we expected that a CA resistant/tolerant bacterial isolate will exhibit a lower level of relative fluorescent units (RFUs) from the excited dye when compared to a CA susceptible isolate exposed to the same CA concentration. To test this hypothesis and confirm applicability of this RFDMIA assay, the following questions related to project aim were addressed in Chapters 3 to 5 of this thesis:

1. What growth phase (mid-log, stationary phase broth cultures or agar colony) is most efficiently used to accurately discriminate CA susceptibility in *E. coli*? (Addressed in Chapter 3)

2. Can RFDMIA differentiate CA susceptible from CA tolerant *E. coli* BW25113 adapted to various biocide CAs when compared to MIC or MBC values? (Addressed in Chapter 3-4)
3. Does RFDMIA predicted *E. coli* cell/membrane disruption at increasing biocide or antibiotic CA concentrations agree with bacterial cells imaged by scanning electron microscopy? (Addressed in Chapters 3-5).
4. Can RFDMIA differentiate CA susceptibilities of critical priority Gram-negative species *E. coli, K. pneumoniae, S. sonnei, A. baumannii, and P. aeruginosa* exposed to biocide CAs? (Addressed in Chapters 3-4)
5. Can RFDMIA predict antibiotic CA resistance in colistin-adapted, colistin resistant, tobramycin-resistant, and gentamicin-resistant *E. coli* isolates? (Examined in Chapter 5)

In this project, we address the main hypothesis and each question with this assay using a collection of biocide CAs and antibiotic CAs against Gram-negative isolates adapted to or possessing acquired resistance to CAs generated in the Bay lab. To compare RFDMIA measurements, we performed a modified broth microdilution AST testing to measure the MIC and 30-minute spot plate MBC (30MBC) values of all RFDMIA tested isolates to compare with the RFDMIA results. With these CA tolerance/resistance profiles for all isolates examined using RFDMIA, we could address each question above. RFDMIA involved a 96-well fluorescent microplate assays, with propidium iodide (PI) or Sytox^{TM} Blue as a membrane impermeant fluorescent dye and CA resistant/tolerant bacteria incubated for 30 minutes in the presence of increasing CA in each microplate well. Fluorescent emission (EM) from dye was measured at 620nm (PI) or 480nm (Sytox^{TM} Blue) and changes in the RFUs were calculated to determine final change in RFUs for each sample over time ($\Delta RFU_{\Delta 30min}$) and at each CA concentration.

To address **question 1**, we confirmed that RFDMIA could accurately predict biocide CA tolerance using stationary phase and mid-log phase bacteria but not with agar plated colony resuspensions. For **question 2**, we used heat-treated and live bacterial cultures exposed to the same RFDMIA conditions to confirm that RFDMIA $\Delta RFU_{\Delta 30min}$ was able to predict the susceptibility of CA-adapted *E. coli* replicates to all biocide CAs tested (CET, BZK, and CHX) except for antibiotic CAs (COL or aminoglycosides) when compared to their MIC and 30MBC values. To answer **question 3**, we confirmed that *E. coli* cell integrity was lost at expected MIC and 30MBC value CA

concentrations (of BZK, CET, CHX, and COL) after 30-minute exposures as predicted by RFDMIA experiments using scanning electron microscopy (SEM). By answering this question, we also observed that based on the collected RFDMIA and SEM analyses, biocide CA-adapted *E. coli* isolates have a "dependence" on their CA to maintain cell integrity. This result represents a novel finding for biocide CA tolerance studies, as there have been no studies to date that have reported a biocide CA-dependant phenotype. **Question 4** was answered by investigating the robustness of the RFDMIA using CET and BZK-adapted *E. coli* isolates exposed to increasing concentrations of other QACs (DDAB, CPC, and CDAB) and by examining other critical priority species' (*A. baumannii*, *K. pneumoniae*, *P. aeruginosa*, and *S. sonnei*) susceptibilities towards QACs. The RFDMIA was able do discern the varied susceptibilities of CET and BZK-adapted *E. coli*. Additionally, I determined that RFDMIA could predict QAC susceptibility in *A. baumannii*, *K. pneumoniae*, and *S. sonnei* but not *P. aeruginosa.* Even using the alternative membrane impermeant dye (Sytox^{TM} Blue), the RFDMIA was unable to predict QAC tolerance in *P. aeruginosa*. Lastly, to address **question 5** we performed RFDMIA on a COL-adapted *E. coli*, a COL resistant *E. coli*, as well as GNT or TOB resistant clinical *E. coli* isolates and identified that this assay was not able to predict antibiotic resistance in these isolates within 30 minutes. However, after 1-hour COL exposure, we were able to discriminate between the adapted, resistant, and susceptible *E. coli* isolates. Together, my thesis results show that RFDMIA can rapidly discriminate biocide CA susceptibilities for various drugs in a variety of Gram-negative bacteria. This technology represents a more rapid way to discern biocide CA susceptibilities than current methods available.

Chapter 2: Materials and Methods

2.1 Bacterial species and chemicals used within the study

CAs and chemicals used in this study were purchased from Millipore Sigma (Massachusetts, USA), Fisher Scientific (New Hampshire, USA), or Invitrogen (California, USA); a full detailed list can be found in Appendix I. *E. coli* BW25113 (163) was purchased from the Coli Genetic Stock Centre (https://cgsc.biology.yale.edu/). CA-adapted *E. coli* BW25113 were generated by Dr. Nicola Cartwright. BZK-adapted *K. pneumoniae* replicates were generated by Shelby Reimer, Kieran Milner, and I. BZK-adapted *S. sonnei* was generated by Brielle Funk. All CA-adapted bacteria were generated utilizing the same method by the repeated sub-culturing method described by Bore *et al* (164). Gentamicin and tobramycin resistant isolates were generously donated by Dr. David Alexander from Cadham provincial labs. *P. aeruginosa* PA01 (DSM6974) and *A. baumannii* (DSM22644) were given as a gift by Dr. Ayush Kumar.

2.1.1 Cryopreservation and growth conditions

All strains and isolates, except the CA-adapted, were cryopreserved in lysogeny broth (LB), made in accordance with the Cold Harbour Springs protocol (165), containing 16% v/v dimethyl sulfoxide and stored at -80°C. CA-adapted bacteria were cryopreserved in LB+16% v/v glycerol. All bacteria were grown overnight in LB with selection when necessary (refer to Appendix II for more details) at 37°C at 170 revolutions per minute (RPM) in a shaking incubator. For plate growth, 75 µL of standardized OD_{600nm} of 1.0 was spread plated on LB agar (1.25% agar) that contained selection when necessary (Appendix II). A total of 16 bacterial strains/isolates were selected to validate the RFDMIA and are listed in Appendix II. A parental BW25113 (EC) strain, and 4 laboratory adapted isolates derived from EC that were repeatedly sub-cultured with either BZK (ECBZKT), CET (ECCETT), CHX (ECCHXT), or COL (ECCOLR) to obtain isolates with $\geq$2-fold increased CA MIC's as compared to EC. Analysis of the QAC-adapted *E. coli* replicates used in our study was described in the thesis of Dr. Nicola Cartwright (166). The same method used to gradually adapt *E. coli* isolates was used to adapt *S. sonnei* (SSBZKT) and *K. pneumoniae* (KPBZKT) to BZK as listed in appendix ii. Aminoglycoside resistant clinical *E. coli* isolates (EC93, EC96, EC97, EC97) were donated by Dr. David Alexander of CADHAM provincial labs. *A. baumannii* (AB) and

P. aeruginosa (PA) were donated by Dr. Ayush Kumar from the Department of Microbiology of the University of Manitoba.

2.1.2 Gene cloning/transformation methods

As many genes providing CA resistance can be found on mobile genetic elements (88, 93), we cloned and subsequently transformed our *E. coli* BW25113 control strain with the *mcr-1* gene on our pMS119EH plasmid (167) (Chapter 5). Initially, *E. coli* DH5α carrying pUC57-*mcr-1* was grown overnight in LB with 100 µg/mL ampicillin (AMP). The next day, the pUC57-*mcr-1* plasmid was extracted with the EZ-10 Spin Column Plasmid DNA Minipreps Kit (BS614-250, Biobasic, Canada) from 5 mL of overnight culture. Once the plasmid had been isolated, it was confirmed by a 1% agarose gel. Next, the plasmid was digested with Eco*RI* and Xba*I* from the ANZA restriction enzyme collection (IVGN0116 and IVGN0126, Thermo-Fisher, USA) following their protocol with no changes. After, the digested plasmid was run on a 1% agarose gel to purify the *mcr-1* fragment. The fragment was then isolated with a gel extraction kit (9K-006-007, Biobasic Inc., Canada) following the manufacturers instructions. Once the purified *mcr-1* fragment had been extracted, it, along with our pMS119EH vector, was digested with Eco*RI* and XbaI (Thermo-Fisher, USA) following the manufacturers instructions. Next, the digested purified fragment was ligated with increasing ratios of fragment to vector purified and digested (3:1-9:1) for 16 hours at 16°C. The following day, the ligation mixture was transformed into competent *E. coli* DH5α and spread onto LB+100 µg/mL AMP agar plates and incubated overnight. After 18 hours, 3 isolated colonies were aseptically picked and grown overnight in LB with 100 µg/mL AMP. The following day, the transformed plasmid was isolated by mini-prep kit (BS614-250, Biobasic, Canada) and confirmed by a 1% gel electrophoresis. Once confirmed, the pMS119EH-*MCR1* plasmid was transformed into $CaCl_2$ competent (168) *E. coli* K12 BW25113 . Once confirmed by gel electrophoresis and plasmid insert was confirmed by Sanger sequencing provided by Biobasic Inc. (Canada).

2.2 RFDMIA fluorescent spectroscopy

2.2.1 RFDMIA optimal fluorescent dye and cell concentration determination.

To determine the appropriate concentration of PI impermeant fluorescent dyes for RFDMIAs, an initial fluorescent emission checkerboard assay was performed to optimize dye and cell concentrations. To this end, checkerboard assays were performed in polystyrene optical bottom black-walled fluorescent 96-well microplates (265301, Thermo Scientific, USA), at increasing concentrations of PI dye (0-10 μg/mL). For PI, we used 10 flashes every five minutes for 30 minutes at an excitation (EX) wavelength (λ) of 544nm and detected emission (EM) λ at 620nm +/-10nm in a POLARstar OPTIMA fluorescent microplate spectrophotometer (BMG Labtech, Germany) (Figure 2.1). Checkerboard assays measured increasing dye concentrations incubated with increasing concentrations of genomic DNA extracted from EC cultures grown to 0, 0.05, 0.1, 0.2, 0.4 OD_{600nm} units, or live EC cell suspensions at OD_{600nm} values 0, 0.05, 0.1, 0.2, 0.4 units, or heat-treated EC cells at OD_{600nm} values of 0, 0.05, 0.1, 0.2, 0.4 units. All cells used for fluorescent analyses were resuspended in 0.2 μm filtered (CA28145-501, VWR, Canada) phosphate buffered saline (PBS). Based on results of the checkerboard assay, we selected live cell suspensions of OD_{600nm} = 0.2 units and 2.0 μg/mL PI. dye, as this concentration was optimal to detect a reasonable amount of dye emission from the dye, as this concentration was optimal to detect a reasonable amount of dye emission from the lowest number of cells added (Figure 2.1; black arrow). For assays involving SYTOX^{TM} Blue (S11348, Fisher, USA), we followed recommend manufacturer concentrations of 1 μM final concentration with an EX λ of 436nm+/-20nm and an EM λ of 482nm+/-25nm in a Synergy Neo2 hybrid multi-mode reader (BioTek, USA).

2.2.2. RFDMIA cell culture preparations.

Prior to RFDMIA experiments, cell culture preparation was performed to standardize cells using the following protocol. Cryo-preserved stocks of each strain/isolate were grown in 10 mL LB as three biological replicates overnight (~18 hrs). OD_{600nm} values of each culture were measured by spectrophotometer (DU530, Beckman and Coulter, USA) and standardized to a final OD_{600nm} value of 2.0 units. Standardized stationary phase cultures were divided into samples used for “live” (or intact cell) measurements and “heat-treated” control sample preparations. Divided

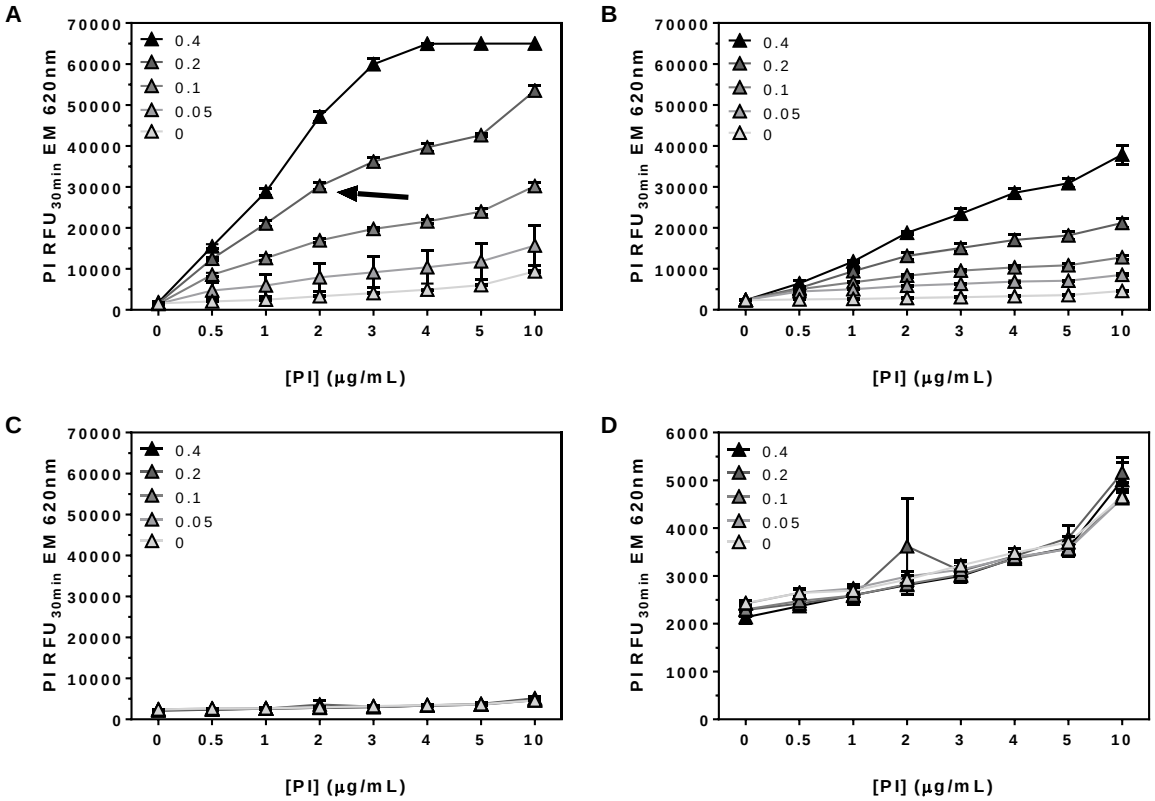


Figure 2.1. RFDMIA data from increasing concentrations of PI (EX: 540nm; EM: 620nm+/-10nm) and cell or extracted DNA preparations. **A)** RFU of Heat-treated cells at increasing OD_{600nm}. **B)** RFU of DNA extracted from bacteria at increasing OD_{600nm}. **C)** RFU of live cells at increasing OD_{600nm}. **D)** RFU of live cells at increasing OD_{600nm} with a smaller EM range. Data represents 3 biological and 3 technical replicates with error bars indicating variation among the samples. The solid black arrow is indicating the concentration of PI as well as bacterial cells to be utilized for the assay. Range of OD_{600nm} is colored by grayscale gradient with OD_{600nm} 0 (Light grey), 0.05,0.1,0.2,0.4 (Black).

cell samples were centrifuged for 2 mins at 14,000 RPM, washed twice with filtered PBS, resuspended in filtered PBS and stored on ice until aliquoted for the RFDMIA. Heat-treated samples were placed in a heating block at 121°C for 30 mins. Suspensions of live and heat-treated samples were diluted with filtered PBS to achieve a final bacterial suspension with OD_{600nm} = 0.2 units. For mid-log samples, overnight cultures were diluted 1:50 into 10 mL of fresh LB with selection if needed and left to grow to mid-log in a shaking incubator. Once mid-log (OD_{600nm} = 0.5 units) was achieved, the cells were treated in the exact same manner as the stationary phase preparation. For colony samples, 50 µl of overnight culture was spread plated onto agar containing selection if necessary and left to grow overnight. After, the bacteria were scraped into filtered PBS and standardized to OD_{600nm} of 2.0 units then were treated the same way as stationary and mid-log cells.

2.2.3 RFDMIA protocol.

Optical bottom black fluorescent 96-well microplates (265301, Thermo Scientific, USA) were used for RFDMIA. Each plate well contained PI at a final concentration of 2 µg/mL and each column contained increasing concentrations of CA. 100 µL of either filtered PBS (blank) or standardized bacterial resuspension (heat-treated or sample) was added to each well. The plates were placed into a fluorescent microplate-reader (Polarstar Optima, BMG labtech, Germany) and were measured in the same manner as in section 2.2.1 for each well. After the assay was complete, a 30-minute spot-plate viability was performed using the 30-minute MBC AST procedure detailed in section 2.3.2.

2.2.4 RFDMIA with alternative dyes

To investigate the use of an alternative membrane-impermeant dye would function with the RFDMIA, we used Sytox^{TM} Blue as detailed in section 2.2.1.

2.2.5 RFDMIA EM RFU calculations.

This analysis involved three stepwise calculations (equations 1-3) to measure the change in RFUs after 30 min ($\Delta RFU_{\Delta 30min}$) at a given "X" CA concentration (µg/mL). Note that for the COL RFDMIA in section 5.2.1, instead of using 30 minutes, 60 minutes was used. The formulas were adjusted as to calculate RFU_{60min} and $\Delta RFU_{\Delta 60min}$ by swapping out the 30-minute calculations with the 60-minute equivalents.

EQ1: $T_{0min} = RFU_{Sample} - RFU_{Blank} = RFU_{0min\ [X\ \mu g/mL\ CA]}$

$T_{30min} = RFU_{Sample} - RFU_{Blank} = RFU_{30min\ [X\ \mu g/mL\ CA]}$

Equation 1 (EQ) calculates the sample RFU values at a given EM wavelength at the start (T_{0min}) and the end (T_{30min}) of the assay incubation (RFU_{0min} and RFU_{30min}), by subtracted the "blank" RFU values from wells containing only dye at each X µg/mL CA (RFU_{Blank}) from the live cell suspension samples at the same X µg/mL CA concentration (RFU_{Sample}); where "X" designates a defined concentration of CA (µg/mL).

EQ2: $RFU_{30min} - RFU_{0min} = RFU_{\Delta 30min\ [X\ \mu g/mL\ CA]}$

Equation 2 (EQ2) measures the difference in RFU values for an isolate at the same CA concentration over 30 minutes ($RFU_{\Delta 30min\ [X\ \mu g/mL\ CA]}$), by subtracting the $RFU_{30min\ [X\ \mu g/mL\ CA]}$ from the $RFU_{0min\ [X\ \mu g/mL\ CA]}$.

EQ3: $RFU_{\Delta 30min\ [X\ \mu g/mL\ CA]} - RFU_{\Delta 30min\ [0\ \mu g/mL\ CA]} = \Delta RFU_{\Delta 30min}$

Lastly, equation 3 (EQ3) is used to control for any fluorescent dye uptake by the replicate without CA exposure 0 µg/mL CA ($RFU_{\Delta 30min\ [0\ \mu g/mL\ CA]}$). For this, we subtracted $RFU_{\Delta 30min\ [0\ \mu g/mL\ CA]}$ from $RFU_{\Delta 30min\ [X\ \mu g/mL\ CA]}$.

2.3 Antimicrobial susceptibility testing (AST)

2.3.1 Broth microdilution AST for MIC calculations.

Broth microdilution AST as described by Balouiri *et al.* (161) was used to determine MIC values for all strains/isolates against their respective CAs. Briefly, cryopreserved stocks of each bacterial strain/isolate were grown overnight (18 hrs.) and the next day, the OD_{600nm} of the cultures were measured using a spectrophotometer (DU530, Beckman and Coulter, USA) and adjusted to 1.0 units with LB broth. Standardized cultures were diluted to $0.2x10^{-4}$ units into 96-well microplates (167008, Thermo Scientific, USA) containing LB and increasing concentrations of CA. After inoculation, the 96-well microplates were incubated at 37°C with shaking at 170 RPM. After 18 hours incubation, OD_{600nm} were measured with an Ultraviolet/Visible wavelength plate spectrophotometer (Multiskan™ spectrum, Fisher Scientific, USA). The MIC value was defined by the lowest concentration of antimicrobial where there is no discernable growth (OD_{600nm}) from the "blank" well. MIC values were based on 3 biological replicates and at least 3 technical replicates.

2.3.2 30-minute MBC (30MBC) determination.

A "30-minute MBC" (30MBC) for each isolate tested using the RFDMIA was measured using a LB agar spot plating method to determine each isolates' viability after CA exposure. This method involved LB agar spotting approximately 1-2 µL of each bacterial suspension per well of a RFDMIA microplate after 30-minute incubation using a sterilized 48-pin replicator (05-450-10, Boekel Scientific, USA). CA-adapted isolates (ECCETT, ECBZKT, SSBZKT, KPBZKT, ECCOLR) were spotted onto LB agar with CA selection when necessary (Appendix II). Spotting was performed at a minimum of technical triplicate and the spotted plates were incubated at 37°C overnight. We defined the 30MBC value as the lowest CA concentration at which no bacterial growth occurred on the agar spot plate based on at least three spotted replicates of the 3 technical and 3 biological replicates. For 60-minute MBC (60MBC) calculation, the same above-mentioned procedure was followed and adjusted to 60 minutes (Section 5.2.1)

2.4 Scanning Electron Microscopy

We utilized scanning electron microscopy (SEM) (JCM-5700, JEOL USA, USA) to visualize bacterial cell morphology and to verify alterations to bacterial membrane integrity at CA concentrations. Bacterial samples were prepared and processed using the same protocol as described in 2.3.2 for the RFDMIA. SEM imaging of bacterial PBS suspensions followed the gold sputtering protocol described by Golding *et al.*(169), with a modification that we diluted bacteria 1:1000. Five different areas of each filter were examined at 5000X magnification. Brightness and contrast standardized SEM images at each concentration of QAC were examined to measure cell lengths and widths were performed using ImageJ V1.52a (170). With this software, 20 lengths and 20 widths were measured (in µm) per image from each of the five 5000X magnification images for each isolate (n= 100/isolate) to assess differences in morphology. Additionally, we did image five different areas of each filter for our CHX isolates (Chapter 4) at 10,000X magnification to better observe morphological changes using the abovementioned process.

2.5 Statistical analyses

All statistical analyses were performed using GraphPad Prism V6 (GraphPad Software, USA) or Excel365 (Microsoft, USA). For RFDMIA analysis, we utilized a two-tailed Student's t-tests were used to analyze all increased or decreased RFDMIA $\Delta RFU_{\Delta 30min}$ data values, where *P*-values of <0.01 were considered significant. All RFDMIA values shown in figures represent the mean $\Delta RFU_{\Delta 30min}$ of PI dye at EX 540nm EM 620nm +/-10nm values (unless otherwise stated) and the standard deviations were determined from 3 technical and 3 biological replicates of a replicate unless otherwise indicated.

Chapter 3. Rapid fluorescent dye-based membrane integrity assay to detect QAC susceptibility among adapted Gram-negative reveals quaternary ammonium compound dependant phenotype

This chapter will be submitted to Scientific Reports with the exception of DDAB, CPC, and CDAB (Section 3.2.4) as these may be included in a publication with Chapter 4. MIC AST for all isolates was performed employing the broth microdilution method (Section 2.3.1). EC, ECBZKT, and ECCETT was initially performed by Dr. Nicola Cartwright and Kari Green which was repeated by Branden Gregorchuk later. SS and SSBZKT MIC AST was performed by Brielle Funk which was repeated by Branden Gregorchuk. KP and KPBZKT MIC AST was done by Branden Gregorchuk. 30MBC testing (Section 2.3.2) was done by Branden Gregorchuk, Michelle Wuzinski, or Andy Seo at the time when the RFDMIA was performed. RFDMIA (Section 2.2) was performed by either Branden Gregorchuk (SS, SSBZKT, KP, KPBZKT, EC, ECBZKT, ECCETT, AB, PA), Michelle Wuzinski (EC, ECBZKT, ECCETT, AB, PA), or Andy Seo (EC, ECBZKT, ECCETT, AB, PA). SEM imaging (Section 2.4) was performed by Branden Gregorchuk and Shelby Reimer with assistance from Dr. Dan Beniac and Shannon Heibert. SEM length and width measurements with ImageJ were performed by Branden Gregorchuk, Shelby Reimer, and Brielle Funk. Editing of this paper/section was done by Branden Gregorchuk, Shelby Reimer, and Dr. Denice Bay.

3.1 Aims, Hypotheses, and Approaches

I hypothesize that bacterial cells incubated with increasing concentrations of QACs in the presence of a membrane impermeant dye, PI, can be fluorescently monitored to detect bacterial QAC susceptibility. I would expect that a QAC-tolerant bacterial replicates will exhibit a lower level of $\Delta RFU_{\Delta 30min}$ EM 620 nm values when compared to a QAC-susceptible isolate (EC, SS, KP) exposed to the same QAC concentration. Additionally, we propose that QAC adaptation and exposure will cause profound changes in bacterial cell morphology in terms of length, width, and membrane integrity. To test our hypotheses, we have compared BZK and CET MIC values using broth microdilution AST methodology to $\Delta RFU_{\Delta 30min}$ collected from 30-minute RFDMIA fluorescent experiments for *Escherichia coli* K-12 BW25113 isolates adapted to BZK or CET (Section 3.2.2). To confirm that 30 minutes of QAC exposure time were sufficient to inhibit kill cells, a 30-minute MBC (30MBC) value was measured by spot plating bacterial cells directly from

each RFDMIA assay plate (Section 3.2.3). The outcome from this analysis demonstrated that the assay was able to discriminate QAC tolerant from susceptible *E. coli* and identified a membrane integrity phenotype that we describe as a "QAC dependent phenotype" when we visualized these cells using scanning electron microscopy (SEM) (Section 3.2.2 and Section 3.2.8). To determine the ideal cell cultivation method, we examined *E. coli* cell resuspensions from overnight cultures, mid-log growth, as well as agar plate colonies (Section 3.2.3). We found that the ideal condition was stationary phase resuspensions due to its ease of preparation and speed, though, mid-log phase cells also worked well but not colony cell resuspensions. Next, we examined if the RFDMIA was able to detect difference in susceptibility of additional QACs (DDAB, CPC, and CDAB) by QAC adapted *E. coli* (Section 3.2.4). We found that the assay was able to discriminate between the susceptible controls and the tolerant isolates. To determine assay robustness in estimating QAC tolerance in other proteobacterial species, we also performed RFDMIA with *Acinetobacter baumannii*, *Pseudomonas aeruginosa, Shigella sonnei*, and *Klebsiella pneumoniae* strains/isolates (Section 3.6). Comparison of other species revealed that RFDMIA could successfully predict their QAC susceptibility and discriminate between tolerant species and susceptible controls except for intrinsically fluorescent *Pseudomonas aeruginosa.* We also compared the use of another impermeant fluorescent dye as a replacement for PI, SYTOX^{TM} Blue, and revealed that both were sufficiently sensitive for QAC susceptibility prediction by RFDMIA with PI being less susceptible to signal loss (Section 3.7). Overall, this section described the validation of a new, rapid, sensitive fluorescent assay capable of detecting QAC susceptible phenotypes and cell membrane perturbations.

3.2 Results and discussions

3.2.1 AST of tested strains and isolates

MIC AST was performed utilizing the broth microdilution method against increasing concentrations of all QACs tested as described in section 2.3.1. 30MBC AST of tested isolates/strains was performed as described in section 2.3.2. Results for all AST is summarized in Table 3.1. The QAC-adapted isolates (ECBZKT, ECCETT, SSBZKT, KPBZKT) showed significant (≥2-fold) increased tolerance towards their respective QACs for their MIC and 30MBC AST values as

Table 3.1. A summary of mean MIC and 30MBC values of all bacterial strains/isolates tested Chapter 3 for a 2-fold dilution series (n=9).

Bacterial strains/isolates tested in this study; strain/isolate abbreviation	MIC (µg/mL) (n=9)*					30MBC (µg/mL) (n=9)*				
	BZK	CET	CPC	CDAB	DDAB	BZK	CET	CPC	CDAB	DDAB
Escherichia coli K-12 BW25113; **EC**[a]	18.8	37.5	8	32	8	75	75	256	64	16
Escherichia coli K-12 BW25113; **ECBZKT**[b]	150	150	128	128	16	150	150	265	128	64
Escherichia coli K-12 BW25113; **ECCETT**[c]	75	300	128	128	16	150	300	256	128	64
Acinetobacter baumannii DSM 6974; **AB**[d]	18.8	37.5	-	-	-	75	75	-	-	-
Pseudomonas aeruginosa PA01 DSM 22644; **PA**[d]	75	150	-	-	-	150	300	-	-	-
Klebsiella pneumoniae DSM 6135; **KP**[e]	18.8	-	-	-	-	37.5	-	-	-	-
Klebsiella pneumoniae DSM 6135; **KPBZKT**[f]	75	-	-	-	-	150	-	-	-	-
Shigella sonnei DSM 5570; **SS**[e]	9.4	-	-	-	-	37.5	-	-	-	-
Shigella sonnei DSM 5570; **SSBZKT**[g]	37.5	-	-	-	-	75	-	-	-	-

* n=9 refers to 3 biological replicate cultures and 3 technical replicate dilutions used for AST.

a. Strain sourced from the Yale Coli Genetic Stock Centre; CGSC (https://cgsc.biology.yale.edu/)
b. BZK-adapted BW25113 isolate, tolerant to 75 µg/mL BZK (166).
c. CET-adapted BW25113 isolate, tolerant to 150 µg/mL CET(166).
d. Strain donated by Dr. Ayush Kumar.
e. Strain sourced from the Leibniz Institute DSMZ-German Collection of Microorganisms and Cell Cultures GmbH; DSMZ (https://www.dsmz.de/).
f. BZK adapted DSM 6135 isolate, tolerant to 75 µg/mL BZK.
g. BZK adapted DSM 5570 isolate, tolerant to 37.5 µg/mL BZK

compared to their respective with unadapted controls (EC, SS, KP). AB demonstrated similar susceptibility to BZK and CET as compared to EC while PA was generally more tolerant towards BZK and CET than EC and AB. Additionally, ECBZKT and ECCETT had increased tolerance towards the other QACs tested (≥2-fold increase) as compared to EC.

3.2.2 RFDMIA can discriminate QAC susceptible from QAC tolerant *E. coli* isolates

To determine the accuracy of the RFDMIA as a technique to rapidly predict and detect QAC susceptibility based on PI $\Delta RFU_{\Delta 30min}$ at EM 620nm, we focused our initial analyses on *E. coli* K12 BW25113 replicates adapted to BZK (ECBZKT) or CET (ECCETT) and compared them to their parental BW25113 (EC) strain. Both QAC-adapted isolates demonstrated >2-fold higher tolerance to their respective QAC and their corresponding AST data is summarized in Table 3.1. Our initial RFDMIA analyses sought to distinguish significant differences in PI emission signal a fixed dye concentration (2.0 µg/mL PI) when incubated with stationary phase culture cell preparations exposed to increasing concentrations of BZK or CET over a 30-minute timeframe. The RFDMIA was used to compare QAC susceptible (EC) to BZK tolerant (ECBZKT) or CET tolerant (ECCETT) *E. coli* (Table 3.1). In the same assays, RFUs corresponding to identical cell preparations that were heat-treated with PI and QACs served as membrane disrupted controls to help establish total PI RFU_{30min} EM 620nm values for each QAC concentration tested (Figure 3.1). Although differences could be seen in uncorrected PI RFU_{30min} values at EM 620nm and when compared to their identical heat-treated controls, live cell samples unexposed to QACs (0 µg/mL QAC) often had some background RFU_{30min} emission signal between assays which required adjustment in the final $\Delta RFU_{\Delta 30min}$ values to observe increases due to QAC addition (Figure 3.1).

To distinguish QAC susceptible from tolerant phenotypes among stationary phase *E. coli* isolates using RFDMIA, we wanted to compare if the lowest significantly increased PI $\Delta RFU_{\Delta 30min}$ EM values for a particular replicate exposed to increasing QAC concentrations coincided with its respective MIC or 30MBC value determined by AST (Table 3.1). Figure 3.2A shows RFDMIA results of *E. coli* EC and ECBZKT isolates and confirmed that the first significantly increased PI $\Delta RFU_{\Delta 30min}$ value at the lowest BZK concentration for both the EC (18.75 µg/mL BZK) and ECBZKT (75.0 µg/mL BZK) occurred at their respective MIC values measured by AST. A similar outcome for RFDMIA PI $\Delta RFU_{\Delta 30min}$ values of EC exposed to CET was demonstrated, where the both the MIC value and EC

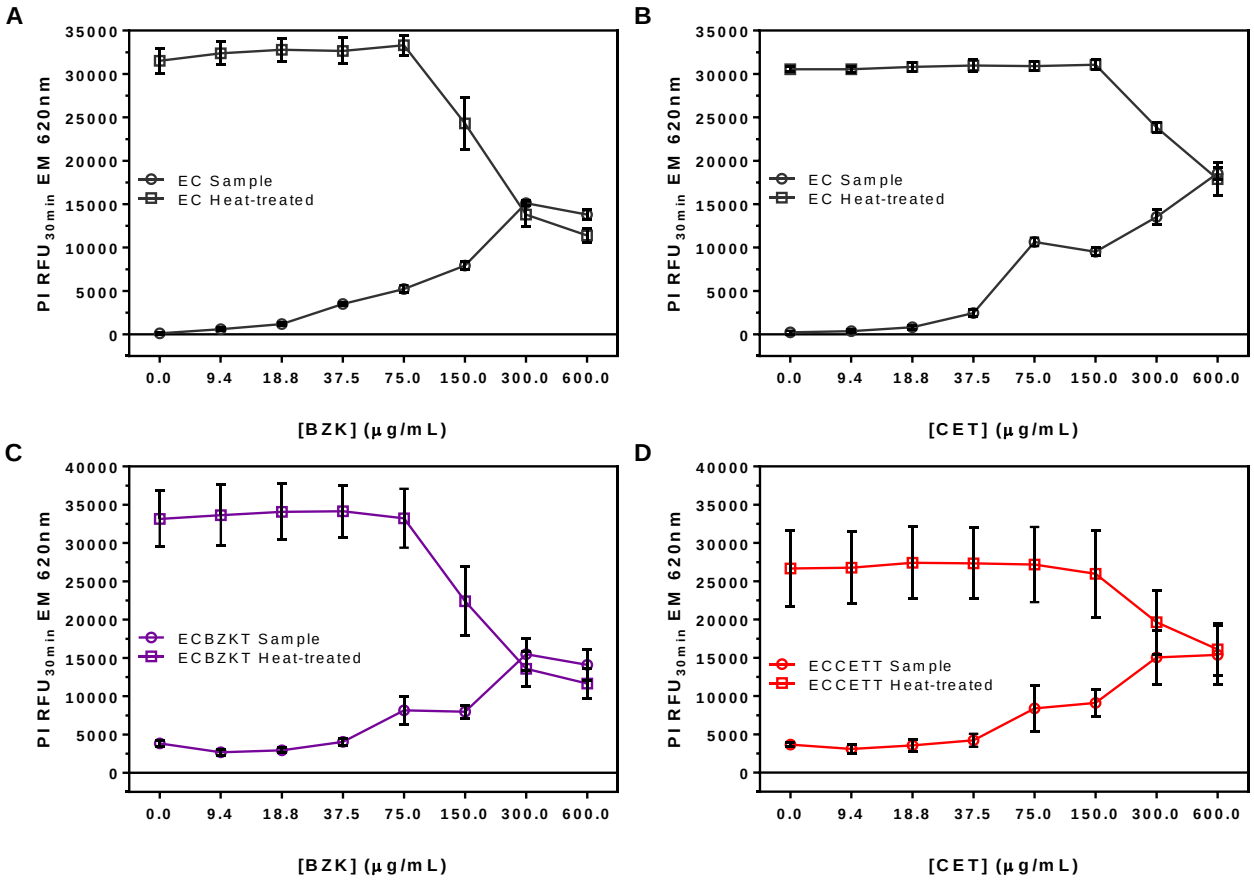


Figure 3.1. PI RFU_{30min} EM 620nm of *E. coli* K12 BW25113 after 30-minute exposure to increasing concentrations of QAC. A) EC live (Circle) and heat-treated cells (Square) after 30-minute BZK exposure. B) EC live and heat-treated cells after 30-minute CET exposure. C) ECBZKT live (Circle) and heat-treated (Square) cells after 30-minute exposure to BZK. BZKT live cells at 0 µg/mL of BZK shows high PI RFU_{30min} EM 620nm values that diminish until 37.5 µg/mL BZK. D) ECCETT live (Circle) and heat-treated (Square) cells after 30-minute exposure to increasing concentrations of CET. ECCETT live cells at 0 µg/mL CET reveals high PI RFU_{30min} EM 620nm values that diminish until 37.5 µg/mL CET. PI RFU_{30min} EM 620nm values are representative of 3 biological and 3 technical replicates. Error bars represent standard deviation within the samples.

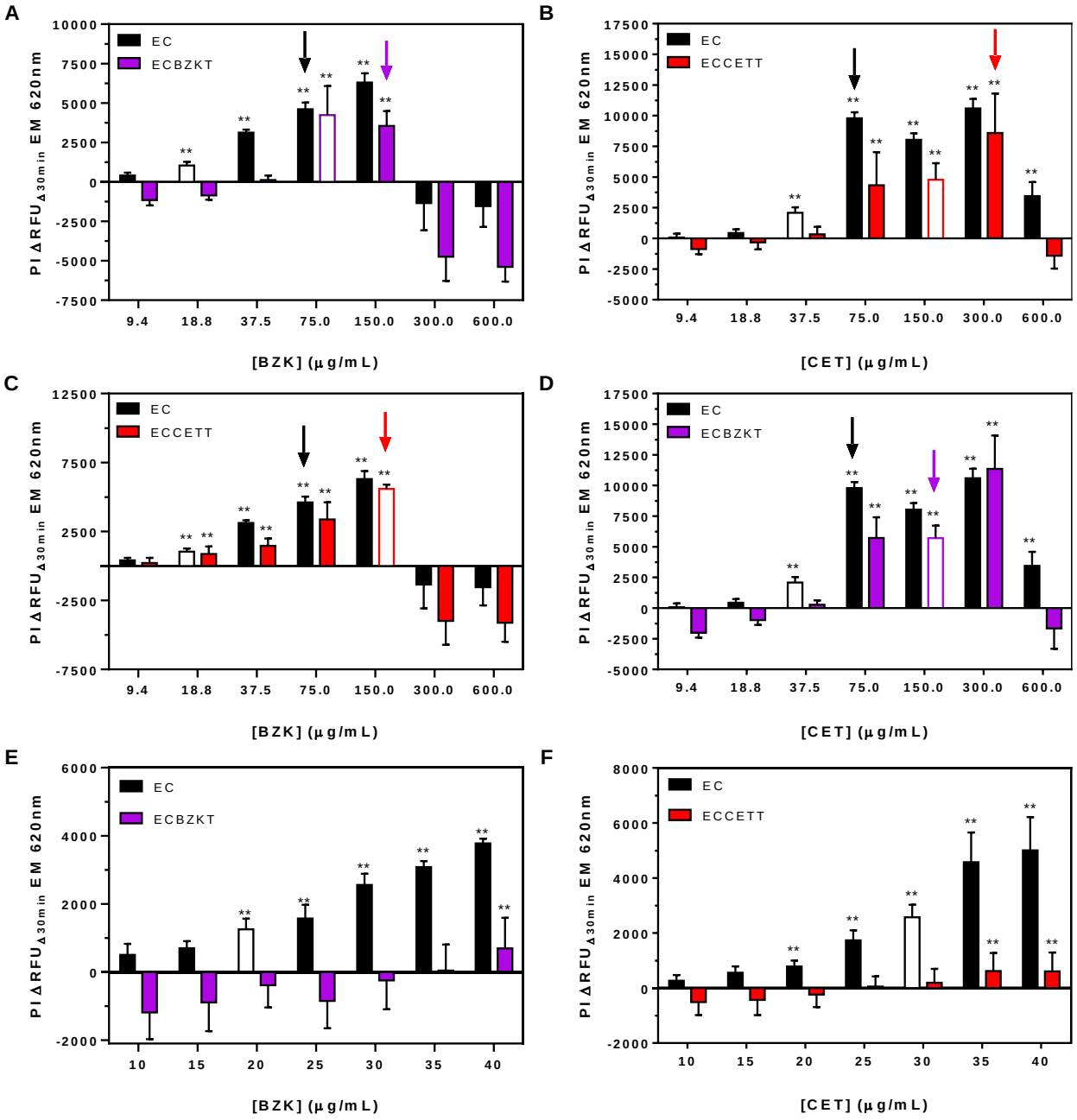


Figure 3.2. RFDMIA of stationary phase *E. coli* K-12 BW25113 (EC, ECBZKT, ECCETT) isolates with increasing concentrations of BZK (A, C, E) or CET (B, D, F). **A)** RFDMIA comparison of EC and ECBZKT replicates exposed to BZK. **B)** Shows RFDMIA results for EC and ECCETT exposed to CET. **C)** RFDMIA results of EC and ECCETT exposed to BZK. **D)** RFDMIA EM values for EC and ECBZKT exposed to CET. **E)** Narrow range RFDMIA of BZK concentrations (10-40 µg/mL). **F)** RFDMIA of EC versus ECCETT exposed to narrow range of CET concentrations (10-40 µg/mL). All graphs are the mean $\Delta RFU_{\Delta 30min}$ EM 620nm values from three biological and three technical replicates at each concentration. Arrows are color coordinated and indicate the 30MBC of each replicate. Unfilled bars indicate the respective MIC of each isolate. Student's t-test were used to determine $\Delta RFU_{\Delta 30min}$ values at each concentration that significantly differed from the lowest QAC concentration value as a double asterisk (**) with $P \leq 0.01$; n=9.

RFDMIA occurred at lowest CET concentration with significantly increased $\Delta RFU_{\Delta 30min}$ value (37.5 µg/mL CET; Fig. 3.2B). This outcome shows that significant increases in RFDMIA $\Delta RFU_{\Delta 30min}$ values correspond to and may predict MIC values for *E. coli* EC and ECBZKT isolates. However, RFDMIA of ECCETT isolates demonstrated that the lowest CET concentration with significantly increased PI $\Delta RFU_{\Delta 30min}$ values occurred at 75 µg/mL CET, which was 4-fold lower than its respective CET MIC value for the ECCETT isolate (Fig. 3.2B; Table 3.1). This indicates that PI dye permeates into ECCETT cells at lower CET concentrations than BZK exposed ECBZKT cells and suggests that ECCETT replicate's cell membranes are more permeable to PI dye as noted by the $\Delta RFU_{\Delta 30min}$ increases. Overall, PI $\Delta RFU_{\Delta 30min}$ values for both ECBZKT and ECCETT isolates were distinguishable from EC $\Delta RFU_{\Delta 30min}$ values at the same QAC concentrations, validating our main study hypothesis that RFDMIA can distinguish between QAC susceptible phenotypes.

A comparison of RFDMIA PI $\Delta RFU_{\Delta 30min}$ and 30MBC values for EC and QAC adapted *E. coli* exposed to BZK or CET demonstrated that the 30MBC often coincided to each respective isolate's maximum PI $\Delta RFU_{\Delta 30min}$ value (Fig. 3.2A-B). The only exception appeared to be EC exposed to BZK, where its 30MBC value occurred at the second highest $\Delta RFU_{\Delta 30min}$ value (75 µg/mL BZK) rather than at its EM maxima (150 µg/mL BZK). This finding suggests that RFDMIA is more accurate for predicting 30MBC values as compared to MIC. Overall, RFDMIA appears to be accurate in estimating QAC-susceptible EC and underpredicts QAC-tolerant ECBZKT and ECCETT MIC values at $\log_2$ QAC dilution ranges when compared to AST methods.

To determine the precision of the RFDMIA, we tested EC, ECCETT, and ECBZKT to a narrow range of BZK or CET concentrations (0-40 µg/mL in 5 µg/mL steps) shown in Figure 3.2C-D. ECBZKT exhibited low but significant gains in PI $\Delta RFU_{\Delta 30min}$ at concentrations of 40 µg/mL BZK, whereas the susceptible EC showed its first significant increase (1.78-fold change from its lowest [QAC]) in PI $\Delta RFU_{\Delta 30min}$ values at 20 µg/mL BZK which corresponded to its respective BZK MIC value (Fig. 3.2C; Table 3.1). Similar to ECCETT, this finding suggests that ECBZKT replicates may also exhibit a low level of PI dye permeability. Using the same narrow range of concentrations for CET (0-40 µg/mL; 5 µg/mL steps), RFDMIA results for ECCETT and EC indicated that EC had low (2.94-fold) but significantly increased PI $\Delta RFU_{\Delta 30min}$ values at 20 µg/mL CET. This indication of MIC value was

17.5 µg/mL lower than the determined value (Fig. 3.2D, Table 3.1) and suggests that RFDMIA is sensitive to QAC induced PI cell permeation in *E. coli*.

3.2.2.1 Discussion of *E. coli* QAC RFDMIA results

It is important to acknowledge here, that RFDMIA of QAC-adapted replicates ECBZKT and ECCETT often demonstrated negative PI $\Delta RFU_{\Delta 30min}$ values at low QAC concentrations below their respective AST MIC values (>75 µg/mL QAC). Additionally, all of the *E. coli* isolates (EC, ECBZKT, ECCETT) we tested with RFDMIA at high concentrations of BZK (>150 µg/mL) and CET (>300 µg/mL) demonstrated a noticeable reduction in PI $\Delta RFU_{\Delta 30min}$ values (Figure 3.1). In our study, the lowest QAC concentrations we measured corresponded to the lowest sub-inhibitory MIC concentration of each replicate at a fixed final concentration of PI dye (2.0 µg/mL PI). It is likely that lower concentrations of QAC may have been detectable, and in future studies, lower QAC concentrations should be explored. RFDMIA does have a maximum detection threshold, which may be linked to the critical micelle concentration (CMC) and/or the increase in counter ions. The high QAC concentrations used in our study correspond to previously reported CET and BZK critical micelle concentration (CMC) values of 750 and 100 µg/mL respectively (171–174). The co-occurrence of RFU_{30min} emission signal loss as QAC CMC values were reached by RFDMIA (Figure 3.1) suggests that QAC micellization may prevent accurate emission detection by RFDMIA. Additionally, high QAC concentrations also increase the concentration of anionic counter ions (Cl^- and Br^-) present in solution which may increase signal quenching (175). Since PI is a structural analog of ethidium bromide, increased counter anion concentrations likely impact emission signal intensity and may contribute to dye EM signal loss and saturation in live versus heat-treated samples measured in our analysis (Fig 3.1). Overall, the range of QAC concentrations we tested in this analysis were sufficient to discriminate between nearly all the QAC-susceptible and QAC-tolerant replicates we tested, indicating the assay is worth pursuing as an antiseptic/disinfectant assay in future applications.

3.2.3 Stationary phase cultures were optimal for RFDMIA QAC susceptibility prediction with *E. coli*

To further investigate the RFDMIA's ability to predict QAC susceptibility by different culturing methods, stationary phase cultures initially tested in section 3.2 were compared to mid-log phase (OD_{600nm}=0.5) samples and LB agar plated colonies resuspended in PBS. RFDMIA were repeated with *E. coli* isolates (EC, ECBZKT, ECCETT) grown to mid-log phase or grown as agar colonies where each replicate was standardized to the same OD_{600nm} 0.2 units as the stationary phase cell experiments. After comparing BZK and CET RFDMIA results (Fig. 3.3), it was evident that stationary phase cultures were the optimal for efficient RFDMIA. Mid-log EC preparation used for RFDMIA demonstrated the assay could predict the MIC values for BZK and CET (Fig. 3.3C, D) with at the same QAC concentrations as stationary phase cells (Fig. 3.3A, B). Mid-log EC also exhibited higher PI $\Delta RFU_{\Delta 30min}$ values for BZK and CET that were 2-3-fold higher $\Delta RFU_{\Delta 30min}$ than stationary phase EC for each QAC tested (Fig. 3.3C-D). However, both mid-log ECBZKT and ECCETT isolate preparations used for RFDMIA resulted in PI $\Delta RFU_{\Delta 30min}$ values that under predicted QAC susceptibility. ECBZKT and ECCETT mid-log RFDMIA demonstrated initial significantly increased PI $\Delta RFU_{\Delta 30min}$ EM values at the lowest QAC concentrations of 37.5 µg/mL BZK for ECBZKT and 37.5 µg/mL CET for ECCETT; much lower concentrations than their respective MIC values (ECBZK: 75 µg/mL BZK; ECCETT: 300 µg/mL CET) (Fig. 3.3C). These findings reveal that mid-log cell preparations were as accurate as stationary phase samples for predicting QAC susceptibility concentrations with RFDMIA, but were less accurate in predicting QAC susceptibility of the QAC-adapted replicates, potentially due to cell morphology alterations exhibited by both adapted isolates observed from SEM data (Figure 3.3, 3.8, 3.10). EC, ECBZKT, and ECCETT isolates prepared directly from agar plated colonies in PBS buffer for RFDMIA demonstrated the least agreement with AST MIC and 30MBC values (Fig. 3.3E, F). RFDMIA comparisons of EC to either ECBZKT or ECCETT using colony cell preparations demonstrated PI $\Delta RFU_{\Delta 30min}$ values that were nearly identical in value at all QAC concentrations tested, preventing accurate differentiation of QAC-susceptible QAC-tolerant phenotypes when compared to AST values (Fig. 3.3E, F). EC colony RFDMIA preparations exposed to CET also underpredicted susceptibility values, where the first significant increase in $\Delta RFU_{\Delta 30min}$ EM values to indicate MIC concentrations were similar

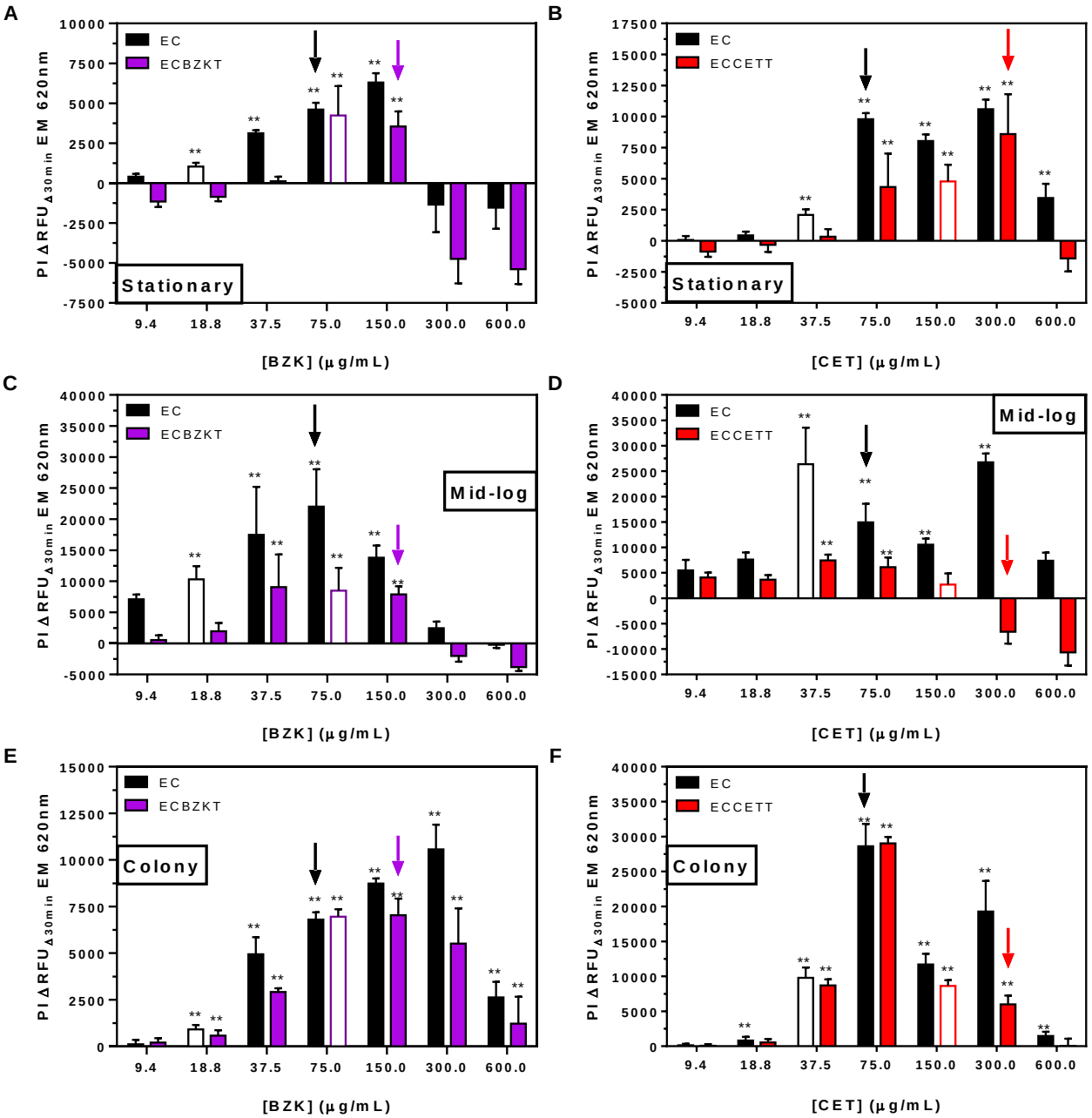


Figure 3.3. RFDMIA results of *E. coli* EC, ECBZKT and ECCETT replicates prepared as stationary phase (**A, B**), mid-log phase (**C, D**), and agar colony (**E, F**) cell PBS-buffered suspensions in the presence of increasing concentrations of BZK (**A, C, E**) and CET (**B, D, F**). RFDMIA data in each panel represents the mean of three biological replicates and three technical replicates. Asterisks (**) shown in each panel indicate significantly increased $\Delta RFU_{\Delta 30min}$ EM values (P<0.01; n=9) from the lowest QAC concentration value as determined by Student's t-test. Arrows represent 30MBC values are color coded. Unfilled bars indicate the MIC value of the isolate.

(Fig. 3.3E, F). Taken together, the fastest and most accurate cell preparation method for RFDMIA to predict MIC values involved the use of stationary phase *E. coli* cultures.

3.2.3.1 Discussion of RFDMIA *E. coli* growth phase results

There are a few explanations for why stationary phase cell preparations are optimal for this assay. 1) Differences in cell envelope composition, capsule thickness (176, 177), lipid composition (147, 178), and membrane protein alterations (177) have all been noted to differ among mid-log, colony, and stationary phase cells (179). Previous studies have shown that the phospholipid composition of the bacteria grown to mid-log or grown on a solid media can differ with alteration in the quantity of phosphatidylethanolamine, phosphatidylglycerol, and cardiolipin (147, 178). Bacterial cells grown as colonies also secrete additional extracellular polymeric substances that prevent their desiccation when growing at solid surface and air interfaces as well as aid the bacteria in adhering to the solid surface (180, 181). The differences in lipids and secreted substances by colonies, or perhaps the fragility of colonies when resuspended into PBS buffer for RFDMIA, likely all obscure the accurate prediction of QAC susceptibility based on PI $\Delta RFU_{\Delta 30min}$ EM 620nm. It is important to note that only a few discrepancies were noted in QAC susceptibility predictions determined by RFDMIA for mid-log and stationary phase *E. coli* isolates preparations. This suggests RFDMIA is feasible for mid-log culture QAC susceptibility predictions but, actively dividing cells found in mid-log cultures may increase cell breakage and result in higher PI $\Delta RFU_{\Delta 30min}$ EM 620nm values, which we observed. Ultimately, actively dividing cells may complicate the application of RFDMIA for mid-log QAC susceptibility predictions. Since mid-log cell preparations add more time to RFDMIA measurements, mid-log cell preparations are less ideal for a rapid fluorescent screening method to detect QAC susceptibility.

3.2.4 RFDMIA can discriminate QAC-tolerant and QAC-susceptible *E. coli* cells for DDAB, CPC, and CDAB

Due to the susceptibility results seen in the MIC AST (Table 3.1) we wanted to verify if the RFDMIA was able to predict the susceptibility of EC, ECBZKT, and ECCETT to additional QACs (DDAB, CPC, and CDAB) (Figure 3.4). RFDMIA was able to discriminate between QAC-susceptible

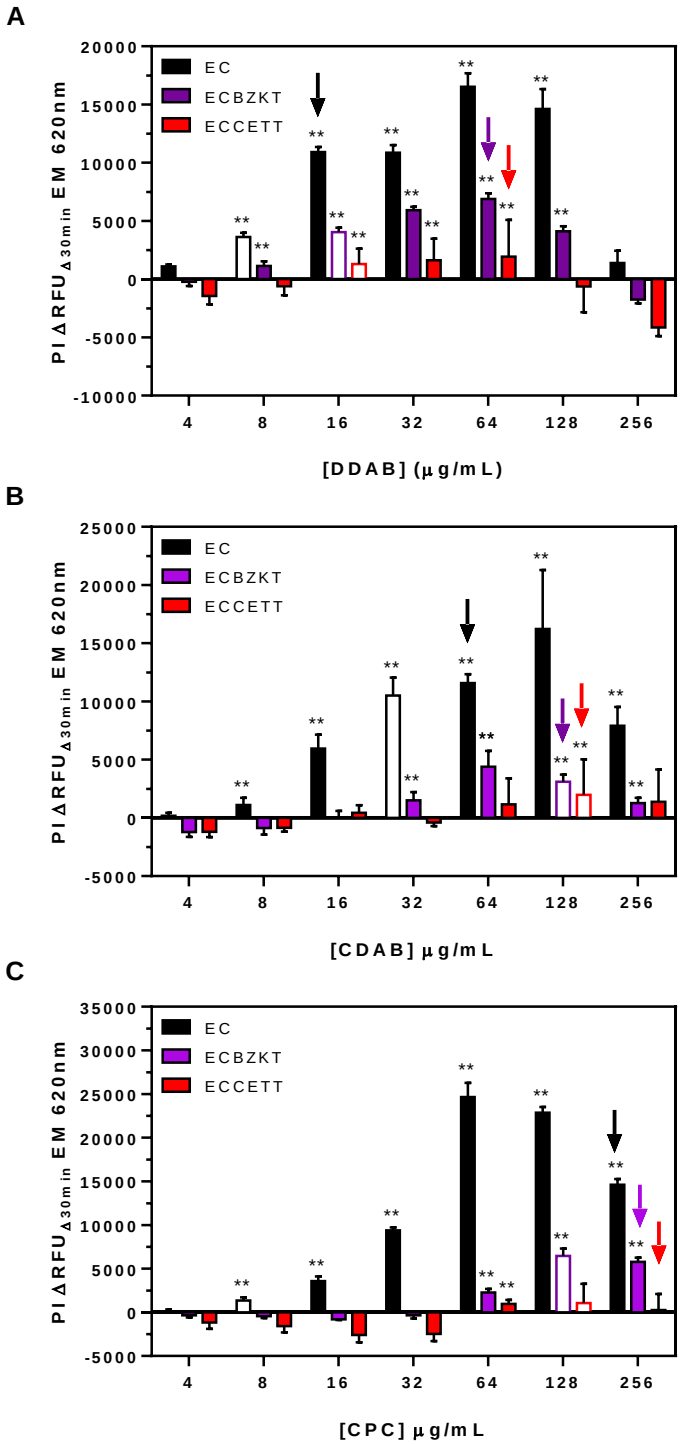


Figure 3.4 RFDMIA results of EC, ECBZKT, and ECCETT with alternative QACs. A) RFDMIA results for exposure to DDAB B) RFDMIA results for exposure to CDAB C) RFDMIA results for exposure to CPC. All graphs are the mean $\Delta RFU_{\Delta 30min}$ EM 620nm values from three biological and three technical replicates at each concentration. Arrows are color coordinated and indicate the 30MBC of each replicate. Unfilled bars indicate the respective MIC of each isolate. Student's t-test were used to determine $\Delta RFU_{\Delta 30min}$ values at each concentration that significantly differed from the lowest QAC concentration value as a double asterisk (**) with $P \leq 0.01$; n=9.

EC strain and both QAC-adapted *E. coli* isolates (ECBZKT and ECCETT). RFDMIA was able to correctly predict the MIC of EC at 8 μg/mL DDAB, however, it under predicted the 30MBC of EC at 64 μg/mL which was 4-fold lower at 16 μg/mL (Fig. 3.4A). Additionally, the assay underpredicted the MIC of ECBZKT as the assay indicated it would be at 8 μg/mL not 16 μg/mL DDAB as we had determined with traditional MIC AST. RFDMIA correctly predicted the 30MBC value of ECBZKT to DDAB which had determined to be 64 μg/mL. For ECCETT, the assay correctly predicted the MIC and 30MBC of DDAB at 16 μg/mL and 64 μg/mL respectively. The significant increase in PI $\Delta RFU_{\Delta 30min}$ values at 8 μg/mL DDAB by ECBZKT indicated that this isolate is more susceptible to DDAB than ECCETT, it's QAC-adapted counterpart. Together, RFDMIAs predicted that EC would be the most susceptible to DDAB, then ECBZKT, and then ECCETT. RFDMIA was unable to predict the precise MIC or 30MBC value for EC and ECBZKT (32 μg/mL and 64 μg/mL; 128 μg/mL) but was able to predict both the MIC and 30MBC values for ECCETT (128 μg/mL) (Fig. 3.4B, Table 3.1). Importantly, it was able to discriminate between QAC-susceptible EC and tolerant QAC-adapted isolates at 8 μg/mL and 16 μg/mL CDAB. As we saw with DDAB, there emerged of susceptibilities for these assayed *E. coli* isolates. The results of the RFDMIA indicate that EC is the most CDAB susceptible, then ECBZKT, and then ECCET as shown by the increase in $\Delta RFU_{\Delta 30min}$ EM values at 8 μg/mL (EC), 32 μg/mL (ECBZKT), and 128 μg/mL (ECCETT) CDAB. Finally, the RFDMIA correctly predicted the MIC value of EC at 8 μg/mL CPC but was underpredicted the 30MBC indicating that it would be at 64 μg/mL CPC, 4-fold lower than the determined 30MBC (Fig. 3.4C). It is important to note that the 30MBC for EC, ECBZKT, and ECCETT all occurred at the same at 256 μg/mL CPC concentration, which differed from all other 30MBC AST measurements as the QAC-adapted *E. coli* consistently had an increased 30MBC concentration as compared to EC (Table 3.1). ECCETT RFDMIA underpredicted the CPC MIC value, where the first significant increase in EM occurred at 64 μg/mL 2-fold lower than the confirmed MIC AST value (Table 3.1) Additionally, the increase in $\Delta RFU_{\Delta 30min}$ EM values for ECCETT were lower than the other isolates tested with the highest $\Delta RFU_{\Delta 30min}$ EM value being 1068.33 (while the highest for EC was 24645.67 units. This may be due to how CPC disrupts the bacterial membrane and potentially the tolerance mechanisms that ECCETT developed during the adaptation process. Importantly, RFDMIA was able to discriminate cross-tolerance of DDAB, CDAB, and CPC between the

susceptible EC and tolerant QAC-adapted replicates (ECBZKT and ECCETT). This gives further evidence that the RFDMIA can differentiate QAC susceptible and tolerant phenotypes in *E. coli*.

3.2.5 RFDMIA can predict QAC susceptibility for *A. baumannii*, *K. pneumoniae*, and *S. sonnei*, but not *P. aeruginosa*.

To examine if the RFDMIA can distinguish susceptibility towards QACs with bacteria other than *E. coli*, we assayed *A. baumannii*, *K. pneumoniae*, *S. sonnei*, and *P. aeruginosa* (Figure 3.5). A discussion of each species RFDMIA results to BZK and CET is provided in sections 3.2.5.1 to 3.2.5.3 below.

3.2.5.1 *A. baumannii* (BZK, CET) RFDMIA

RFDMIA results for *A. baumannii* (AB) exposed to BZK demonstrated a significant increase in PI $\Delta RFU_{\Delta 30min}$ values at 18.75 µg/mL BZK in agreement with its MIC value (Figure 3.5A). When exposed to increasing concentrations of CET, RFDMIAs indicated that AB had its first significant increase in $\Delta RFU_{\Delta 30min}$ EM values at 37.5 µg/mL which was in agreement with its MIC value (Table 3.1, Figure 3.5D).

3.2.5.2 *K. pneumoniae* (BZK) RFDMIA

We found that the RFDMIA was able to differentiate between BZK-tolerant and BZK-susceptible *K. pneumoniae* species. This was seen in the significant increase in $\Delta RFU_{\Delta 30min}$ EM values at 37.5 µg/mL of BZK, where there was a six-fold increase in $\Delta RFU_{\Delta 30min}$ signal between the susceptible (KP) and tolerant *K. pneumoniae* (KPBZKT) isolates (Fig. 3.5B). However, the RFDMIA was unable to correctly predict the MIC value for KP as noted by the incremental increase in $\Delta RFU_{\Delta 30min}$ EM values at 18.8 µg/mL (MIC value for KP). However, the significant increase in $\Delta RFU_{\Delta 30min}$ EM values at 37.5 µg/mL BZK coincided at the 30MBC value for KP. For KPBZKT, RFDMIA was able to correctly predict the MIC value (75 µg/mL BZK) (Figure 3.5B). As seen with the *E. coli* QAC adapted isolates, the RFDMIA was able to discriminate between BZK susceptible *K. pneumoniae* (KP) and BZK tolerant *K. pneumoniae* (KPBZKT) indicating that this assay is a powerful tool to differentiate BZK susceptible and tolerant *K. pneumoniae*.

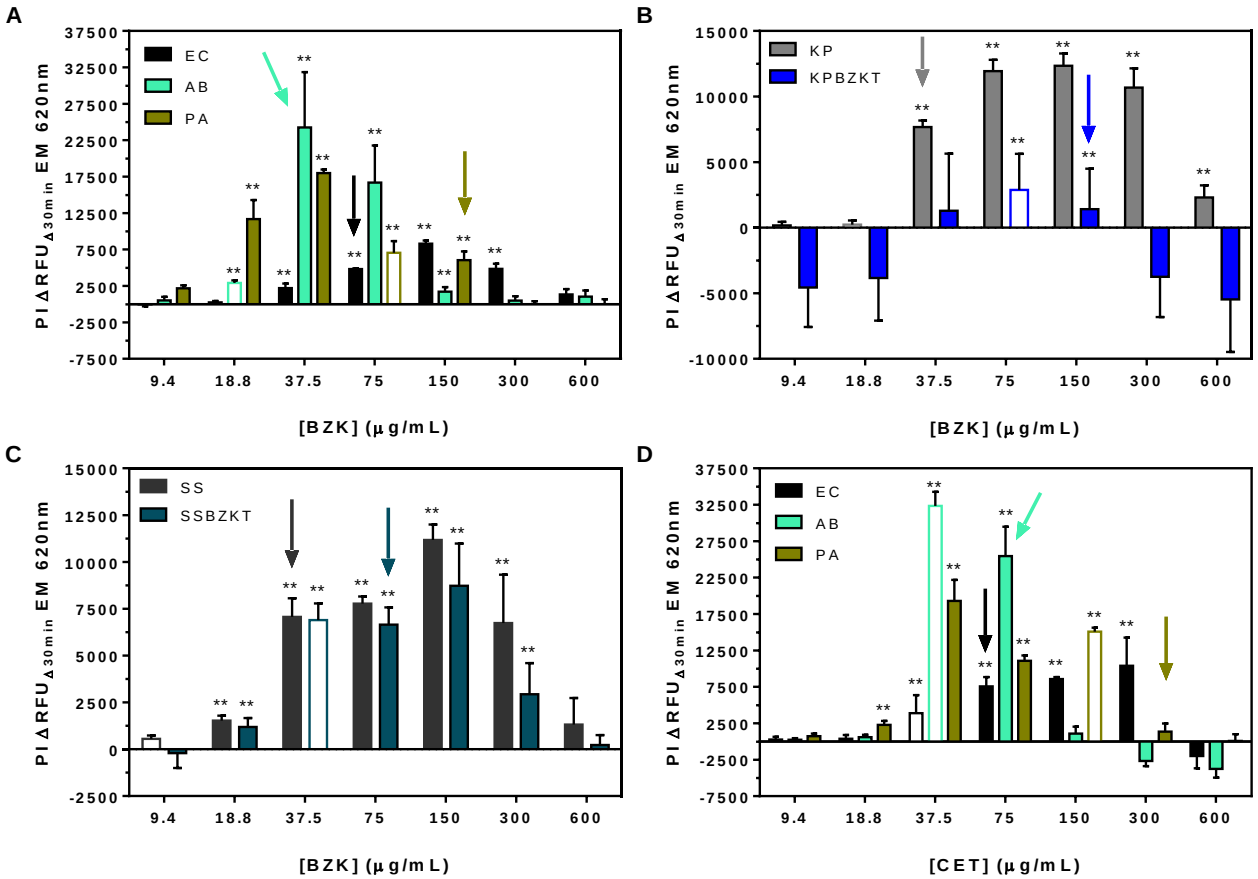


Figure 3.5. RFDMIA results of stationary phase *E. coli* EC (**A, D**), *A. baumannii* (AB) (**A, D**), *P. aeruginosa* (PA) (**A, D**), *S. sonnei* (SS) (**B**), *S. sonnei* BZK-adapted (SSBZKT) (**B**), *K. pneumoniae* (KP) (**C**), and *K. pneumoniae* BZK-adapted (KPBZKT) (**C**) samples exposed to increasing concentrations of QAC. RFDMIA data in each panel represents the mean of 3 biological replicates and 3 technical replicates (n = 9). Asterisks (**) shown in each panel indicate significantly increased $\Delta RFU_{\Delta 30min}$ values (P<0.01) from the lowest QAC concentration $\Delta RFU_{\Delta 30min}$ value as determined by Student's t-test. Arrows represent QAC concentrations that correspond to their respective 30MBC values are color coded; unfilled bars indicate the MIC value of the replicate.

3.2.5.3 *S. sonnei* (BZK) RFDMIA

RFDMIA examination of susceptible (SS) and BZK-tolerant *S. sonnei* (SSBZKT), a closely related *E. coli* pathogen of the Enterobacterales (182) was also compared. Due to the lower MIC value of SS when compared to EC (Table 3.1), RFDMIA was unable to correctly predict SS MICs value as the range used in RFDMIA was too high (the statistical comparison is between the lowest concentration of BZK within the assay). That being said, RFDMIA could still discern the BZK-susceptible from the BZK-tolerant *S. sonnei* isolates. Comparison of $\Delta RFU_{\Delta 30min}$ values at 9.4 µg/mL BZK (Figure 7B), show that the BZK-adapted isolate has a negative $\Delta RFU_{\Delta 30min}$ EM value, however, the susceptible *S. sonnei* (SS) had positive $\Delta RFU_{\Delta 30min}$ EM values indicating the PI dye entered and fluoresced better in SS. These PI EM values were still relatively low as compared to the 30MBC $\Delta RFU_{\Delta 30min}$ values (549.44 units, 7664.78 units respectively). As for SSBZKT, the assay predicted 18.8 µg/mL BZK as the MIC value based on its first significant increase in $\Delta RFU_{\Delta 30min}$, 2-fold lower than its BZK MIC value (37.5 µg/mL). In summary, RFDMIAs were unable to correctly predict precise MIC values for SS and SSBZKT but was able to differentiate between BZK tolerant and susceptible isolates at or around MIC values, specifically at 9.4 µg/mL BZK based on significant differences in $\Delta RFU_{\Delta 30min}$ EM values. These isolates need to be examined at lower BZK concentrations or with arithmetic values for BZK concentrations rather than $\log_2$.

3.2.5.4 *P. aeruginosa* (BZK, CET)

Based on AST MIC values for *P. aeruginosa,* this species was more tolerant to BZK or CET than *A. baumannii* or *E. coli* (Table 3.1). Therefore, we expected to observe RFDMIA PI $\Delta RFU_{\Delta 30min}$ EM 620nm values that coincided with MIC values, but this was not detected for *P. aeruginosa* exposed to either QAC (Figure 3.5A, 3.5D, 3.6C, 3.7C). When *P. aeruginosa* was exposed to either BZK or CET, RFDMIA was not able to determine PA's QAC tolerance, likely due to the fact that this species had significantly high background fluorescence for PI values without any QAC added (Figure 3.6A, 3.7A). Additionally, even exposure to a low concentration of CET or BZK (9.4 µg/mL) caused significant increased in $\Delta RFU_{\Delta 30min}$ PI EM 620nm values (3.5A, 3.5D, 3.6C, 3.7C). To address this, we repeated RFDMIA using an alternative impermeant fluorescent dye, Sytox™ Blue, with EX and EM values outside PI values to determine if another dye could be substituted for PA.

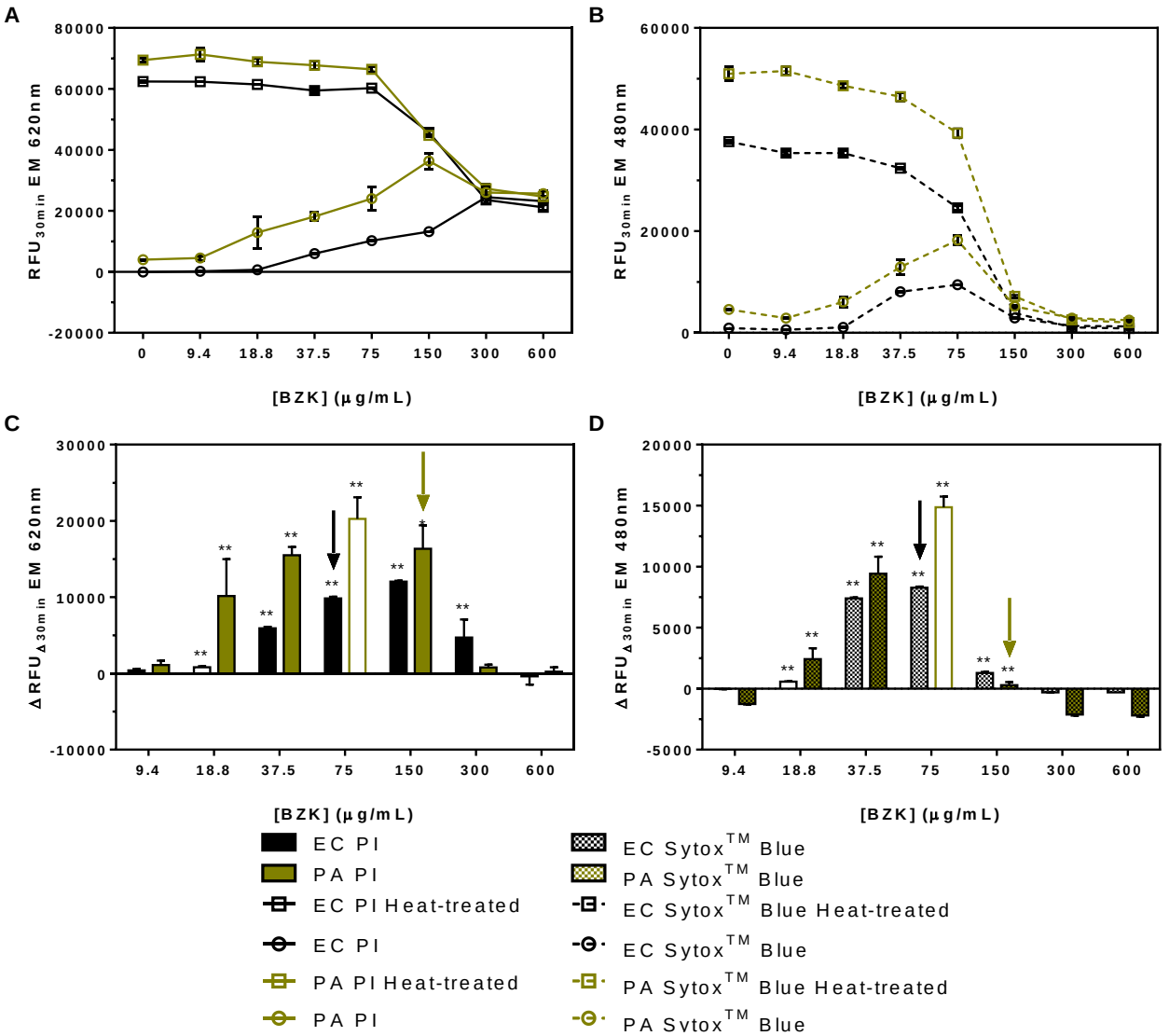


Figure 3.6. RFDMIA results for the comparison between PI (**A**, **C**) and Sytox™ Blue (**B**, **D**) in the presence of increasing concentrations of BZK with EC and PA. Panels A and B show RFU_{30min} EM values demonstrating that there is a loss of signal of the heat-treated samples at 150 µg/mL BZK. Panels C and D show RFDMIA results for $\Delta RFU_{\Delta 30min}$ EM values. Values represent the mean EM values with error bars representing standard deviation of replicates (n=3). Unfilled bars represent the MIC value of each strain; arrows indicate 30MBC values. All data is colour coordinated (Black=EC, Green= PA). Asterisks shown in each panel indicate significantly (P<0.01) increased $\Delta RFU_{\Delta 30min}$ EM values from the lowest QAC concentration as determined by Student's t-test.

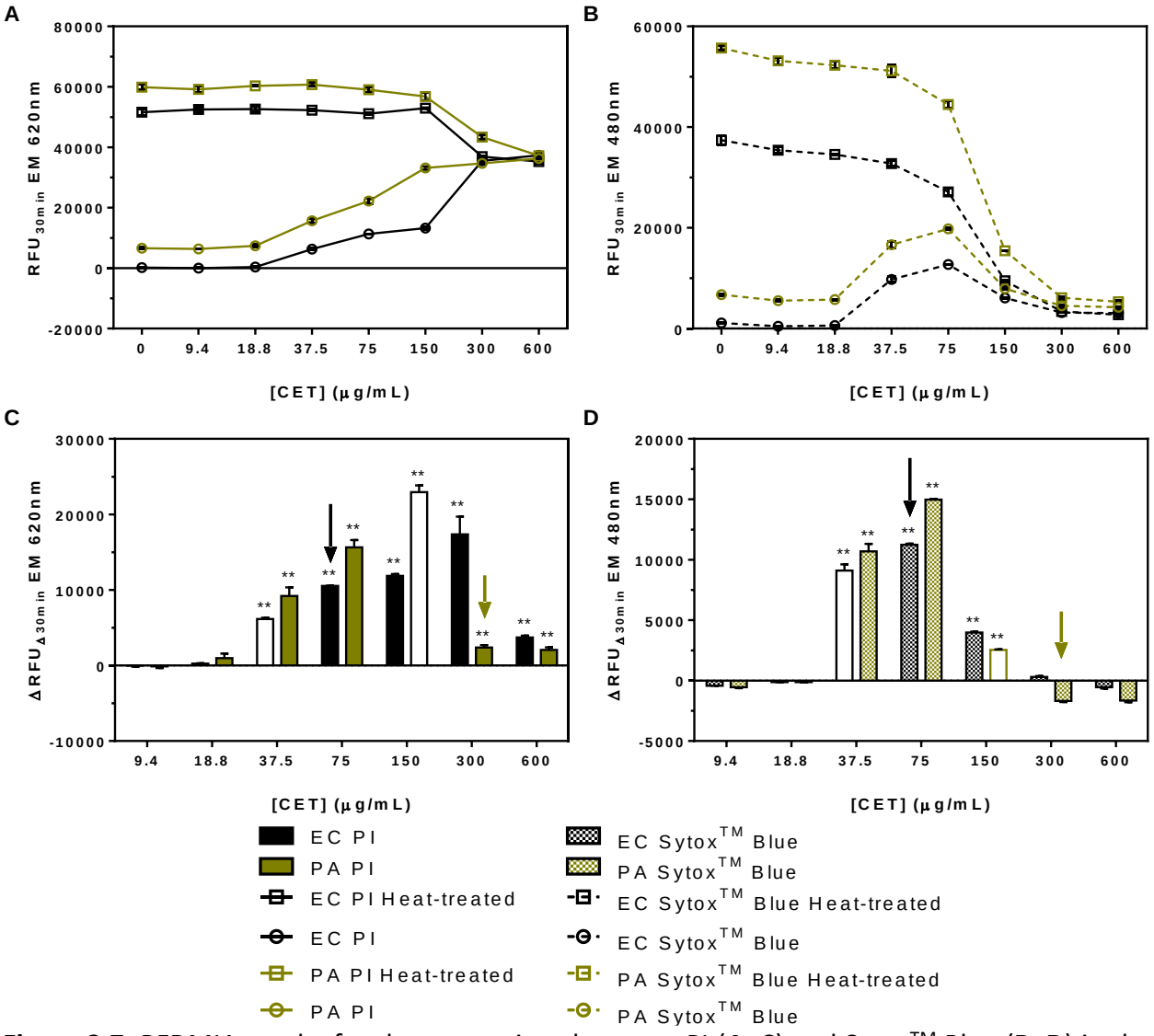


Figure 3.7. RFDMIA results for the comparison between PI (**A**, **C**) and Sytox™ Blue (**B**, **D**) in the presence of increasing concentrations of CET with EC and PA. Panels A and B show RFU_{30min} EM values demonstrating that there is a loss of signal of the heat-treated samples at 150 µg/mL BZK. Panels C and D show RFDMIA results for $\Delta RFU_{\Delta 30min}$ EM values. Values represent the mean EM values with error bars representing standard deviation of replicates (n=3). Unfilled bars represent the MIC value of each strain; arrows indicate 30MBC values. All data is colour coordinated (Black=EC, Green= PA). Asterisks shown in each panel indicate significantly (P<0.01) increased $\Delta RFU_{\Delta 30min}$ EM values from the lowest QAC concentration as determined by Student's t-test

3.2.6 Sytox™ Blue RFDMIA can predict CET and BZK susceptibility in *E. coli* but not *P. aeruginosa*

Following the same method that we employed with the original RFDMIA, we changed our dye from PI to Sytox™ Blue and examined if this dye was better able to predict susceptibly towards CET and BZK in EC, and PA. The results are summarized in Figure 3.6 and Figure 3.7. We found that Sytox™ Blue was able to determine susceptibility of EC towards BZK and CET correctly predicting MIC and 30MBC values (Figure 3.6D, Figure 3.7D). We found that SYTOX™ Blue dye was also unable to accurately predict QAC susceptibility of PA when in the presence of increasing concentrations of CET or BZK. This is shown in the significant increases in $\Delta RFU_{\Delta 30min}$ EM values at subinhibitory concentrations of BZK and CET (Figure 3.6B, D at 18.8 µg/mL; Figure 3.7B, D at 18.8 µg/mL). Interestingly, when comparing PI to Sytox™ Blue, PI showed less EM loss as the QAC concentrations increased. This is seen in Figure 3.6A, B and Figure 3.7A, B where there is a large drop in RFU_{30min} EM signal in the heat-treated samples (150 µg/mL of BZK or CET). This decrease in signal causes the EM of the Live and Heat-treated samples to be indistinguishable from one another. Importantly, Sytox™ Blue demonstrated similar $\Delta RFU_{\Delta 30min}$ EM values as PI at the MIC of EC for both CET and BZK, indicating that the assay was still able to predict susceptibility of EC. Due to the dramatic loss of signal at high QAC concentrations, we concluded that PI is optimal for RFDMIAs as compared to Sytox™ Blue.

3.2.6.1 Discussion of Sytox™ Blue RFDMIA results

For both PI and Sytox™ Blue, the RFDMIA was unable to predict the intrinsic QAC tolerance of PA nor was the assay able to discriminate PA's QAC tolerance from EC's QAC susceptibility. The assay's inability to predict/discriminate PA's QAC tolerance is likely due to the fact that *P. aeruginosa* and other Pseudomonads are capable of producing a variety of fluorescently active pigments. One compound that is enriched in *P. aeruginosa* species is a chromophore molecule known as aeruginosin A (183, 184). Aeruginosin A has fluorescent properties and has a similar emission spectrum as PI (184), and likely explains why RFDMIA PI RFUs we detected were much higher than EC tested by RFDMIA (Figure 3.6A, Figure 3.7A). Further investigation into the specific way in which CET and BZK disrupt PA's membrane may help to elucidate why the RFDMIA is unable to predict *P. aeruginosa*'s QAC susceptibility. For now, the

fluorescent properties of *P. aeruginosa* and potentially other intrinsically fluorescent bacterial species will limit the applicability of RFDMIA.

3.2.7 QAC-adapted *E. coli* demonstrate morphological changes and a type of QAC dependence to maintain membrane morphology

As mentioned in section 3.1, ECBZKT and ECCETT isolate RFDMIA's resulted in one or more negative $\Delta RFU_{\Delta 30min}$ values at low QAC concentrations (9.4 to 75 µg/mL ranges; Figure 3.2). QAC adapted *E. coli* replicates demonstrating negative PI $\Delta RFU_{\Delta 30min}$ EM values at low added QAC concentrations indicate that PI dye permeation was much higher in QAC exposed cell than in cells lacking any added antimicrobial (0 µg/mL QAC; Fig. 3.1). This suggests that QAC-adapted *E. coli* cell integrity may be compromised and more permeant to PI dye than EC. In an effort to explain these negative $\Delta RFU_{\Delta 30min}$ values at 0 to 75 µg/mL QAC with respect to cell morphology, we visualized stationary phase EC, ECBZKT, and ECCETT with SEM analysis to identify QAC concentrations that reduced cell integrity and observe cell morphology alterations after 30 mins of increasing QAC exposure (Fig. 3.8-3.11; Table 3.2, 3.3).

SEM images of EC exposed to increasing BZK concentrations revealed that at low BZK concentrations below its MIC value (9.4 µg/mL BZK), the EC bacteria took on a "flattened" or "deflated" appearance when compared to "plump" bacilliform cells without BZK exposure (Figure 3.8A, C). As the concentration of BZK reached or exceeded its MIC value (18.8 µg/mL BZK), the EC cells became shorter, began fusing together (Figure 3.8E, G, I). In contrast, SEM analysis of ECBZKT revealed that when no BZK was added, the bacteria appeared to be "deflated", opposite to EC at the same concentration (Fig. 3.8B). At BZK concentrations below its MIC value, the overall appearance of ECBZKT cells became "plumper" but also demonstrated an altered elongated morphology when compared to the EC (Figure 3.8D, F; B; Figure 3.9, Table 3.1). As BZK concentrations reached or exceeded the MIC value for ECBZKT, SEM images of these cells appeared to be more fused together and flattened on filters, with more background cell debris on the image filters (Fig. 3.8H, I). These findings indicate that at no or low BZK concentrations, ECBZKT cell morphology was significantly altered when compared to EC cells. Furthermore, ECBZKT cells were more susceptible to SEM fixation dehydration flattening, when no BZK was

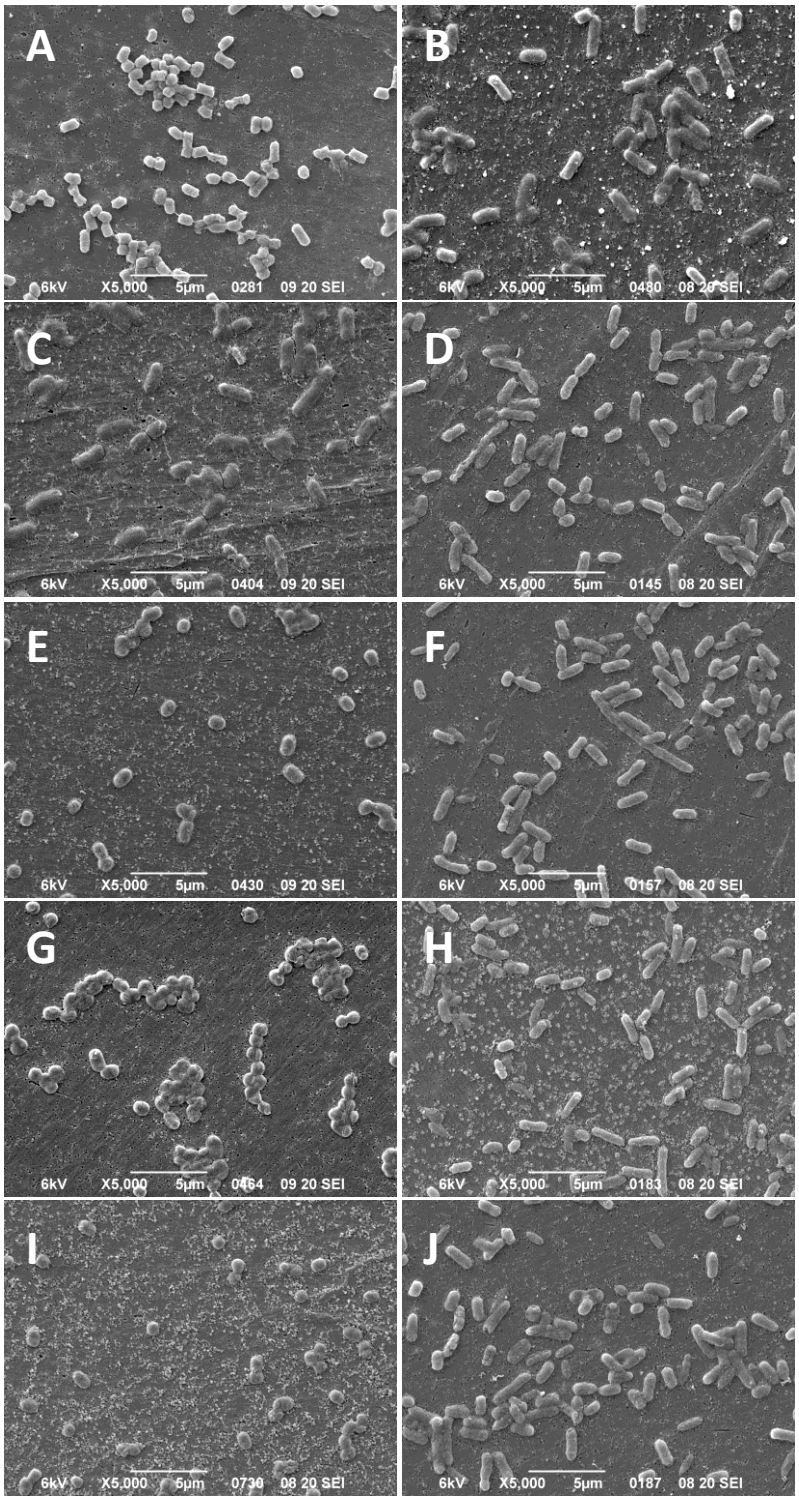


Figure 3.8. SEM images of *E. coli* K-12 BW25113 replicates (EC, ECBZKT) exposed to increasing concentrations of BZK for 30 minutes. Panels **A, C, E, G, I** show EC and panels **B, D, F, H, J** show ECBZKT replicates after 30-minute exposure to BZK at 0 µg/mL (A, B), 9.4 µg/mL (C, D), 18.8 µg/mL (E, F), 75 µg/mL (G, H) and 150 µg/mL (I, J). All images are representative of five SEM images collected at 5000X magnifications and the white scale bar at the bottom of each panel image indicates 5 µm length.

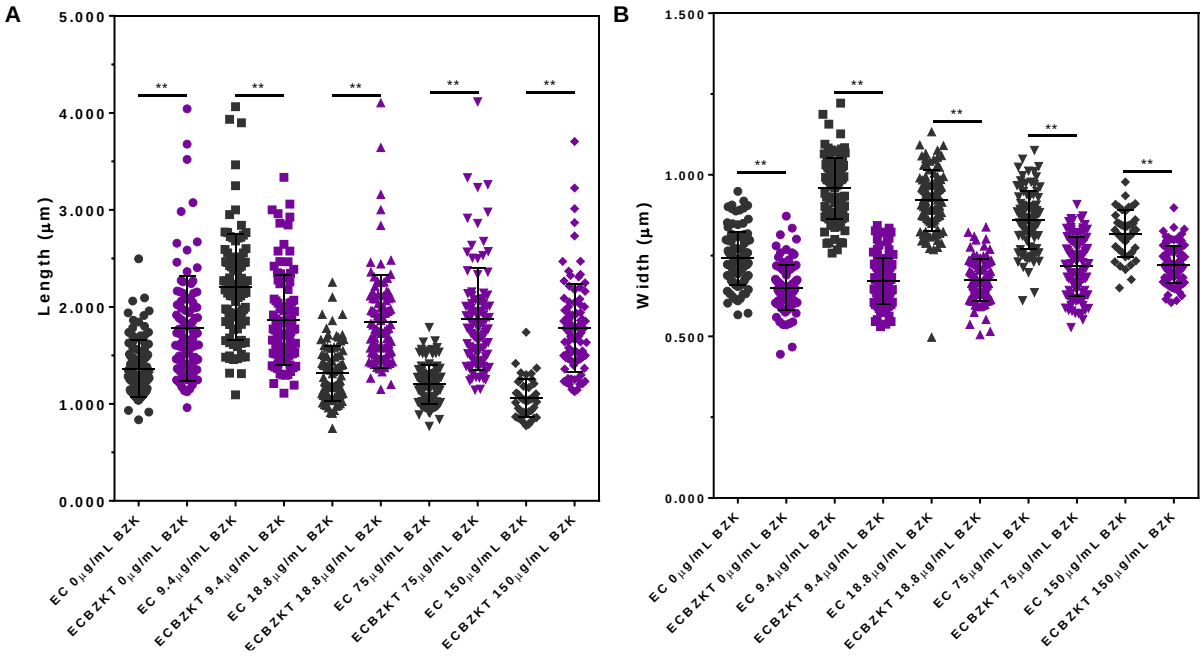


Figure 3.9. A summary of measured *E. coli* K-12 isolates' cell length and width measurements at various QAC concentrations from SEM images. Panels show cell lengths (**A**) and cell width (**B**) measurements in µm using ImageJ (170) for replicates exposed to increasing concentrations of BZK. Asterisks (**) shown above bars in each panel indicate significantly different *P*-values (<0.01) between the samples. Differences in mean length and width are found in **Table 3.2**. Error bars represent standard deviation from the central mean bar.

Table 3.2. Mean length and width values of EC and ECBZKT after 30-minute exposure to BZK at indicated concentrations based off of five 5000X magnification SEM images (n=100)

[BZK] (μg/mL)	Isolate	Length (μm)	Standard deviation	Difference to EC	Width (μm)	Standard deviation	Difference to EC
0	EC	1.363	0.293		0.742	0.083	
	ECBZKT	1.781	0.543	**0.418**	0.651	0.070	**-0.091**
9.4	EC	2.205	0.551		0.958	0.095	
	ECBZKT	1.863	0.467	**-0.342**	0.672	0.072	**-0.286**
18.8	EC	1.313	0.280		0.921	0.095	
	ECBZKT	1.849	0.477	**0.536**	0.676	0.065	**-0.246**
75	EC	1.199	0.202		0.861	0.089	
	ECBZKT	1.874	0.528	**0.675**	0.723	0.114	**-0.138**
150	EC	1.061	0.198		0.818	0.072	
	ECBZKT	1.784	0.450	**0.723**	0.723	0.058	**-0.095**

All bolded values are significant with $P<0.01$ by Student's t-test.

Difference from EC was determined by subtracting mean length or width of EC from mean length or width values of ECBZKT.

added. Taken together with RFDMIA negative $\Delta RFU_{\Delta 30min}$ values (Fig. 3.2), SEM analyses suggests that these BZK-adapted *E. coli* replicates are reliant on or dependant on low concentrations of BZK to maintain a classic bacilliform ECBZKT isolate cell morphology.

Similar trends were noted for EC morphology exposed to CET as we observed for BZK exposure using SEM imaging (Figure 3.10, 3.11; Table 3.3). EC SEM images exposed to no QAC showed plump cells that gradually flattened and dissolved as its respective MIC for CET was reached (Fig. 3.10A, C, E, G, I). ECCETT replicates exhibited a similar flattened cell morphology at no CET concentration (Fig. 3.10B), where cells gradually plumped with added CET (Fig. 3.10D,F), until ECCETT isolates reached or exceeded QAC concentrations close to its CET MIC value (300 µg/mL; Fig. 3.10H,J). In contrast to elongated ECBZKT isolates, SEM images of ECCETT were shorter and wider (Fig. 3.11, Table 3.3), and at sub-inhibitory CET MIC values began to take on a "chain-like" appearance where ECCETT cells became attached at their poles (Fig. 3.10D, F). Altogether, RFDMIA analysis demonstrated sufficient sensitivity to predict the cell membrane integrity differences in QAC-adapted *E. coli* isolates and the EC that were confirmed by SEM analysis.

3.2.7.1 Discussion of SEM

Our study relied on the use of QAC-adapted replicates as there are currently no well-established QAC-tolerant *E. coli* reference strains available for testing, and this resulted in unexpected findings using RFDMIA and SEM. QAC-adapted ECBZKT and ECCETT replicates resuspended in PBS without added QAC resulted in cells with flattened or deflated cell morphologies based on SEM visualization. Using the same SEM fixation conditions, the parental *E. coli* (EC) strain maintained a "rounded" or "plump" morphology. Once exposed to QACs at sub-MIC concentrations, the morphology of both QAC adapted *E. coli* isolates "re-inflated" similar to the non-drug exposed EC. This was especially evident for ECCETT which, as the CET concentrations increased, their overall cell morphology or "plumpness" returned (Fig. 3.10). At sub-MIC levels, the ECCETT started to form chain like structures with very noticeable points at the poles of their membranes. When MIC value of ECCETT was tested, cells began to lose their integrity and started to deflate, appearing to "melt" onto the filter similar to EC cells exposed to

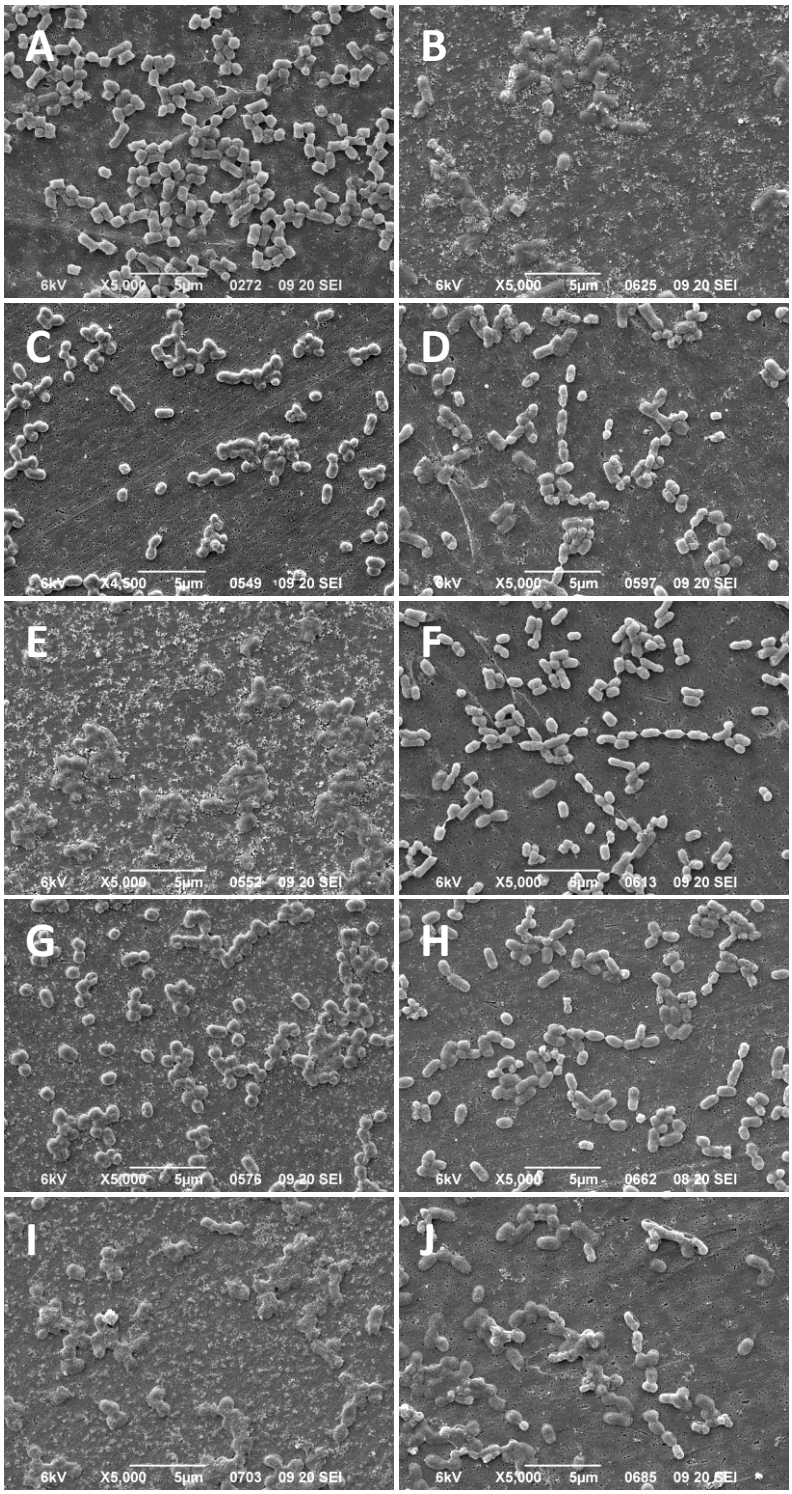


Figure 3.10. SEM images of *E. coli* K-12 BW25113 (EC, ECCETT) isolates exposed to increasing concentrations of CET for 30 minutes. Panels **A, C, E, G, I** show EC replicates and panels **B, D, F, H, J** show ECCETT isolates after 30-minute exposure to CET at 0 µg/mL (A, B), 18.8 µg/mL (C, D), 37.5 µg/mL (E, F), 75 µg/mL (G, H) and 300 µg/mL (I, J). All images are representative of 5 SEM images collected at 5000X magnifications and the white scale bar at the bottom of each panel image indicates 5 µm length.

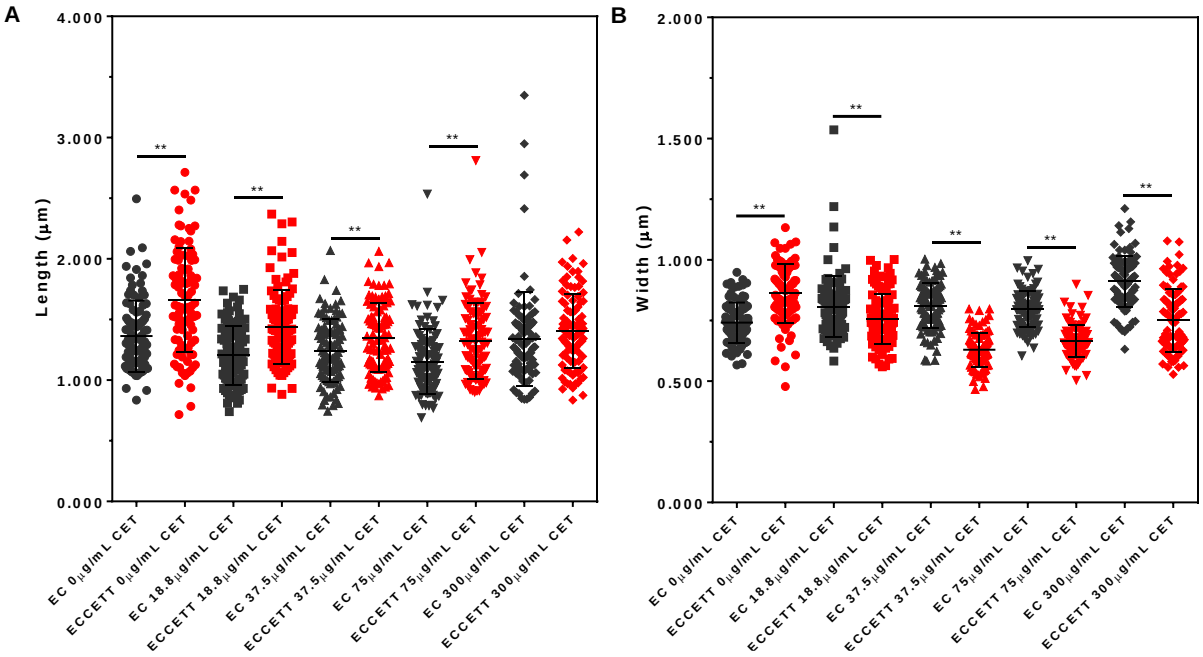


Figure 3.11. A summary of measured *E. coli* K-12 isolates' cell length and width measurements at various QAC concentrations from SEM images. Panels show cell lengths (**A**) and cell width (**B**) measurements in µm using ImageJ (170) for isolates exposed to increasing concentrations of CET. Asterisks (**) shown above bars in each panel indicate significantly different *P*-values (<0.01) between the samples. Differences in mean length and width are found in **Table 3.3**. Error bars represent standard deviation from the central mean bar.

Table 3.3. Mean length and width values of EC and ECCETT after 30-minute exposure to CET at indicated concentrations based off of five 5000X magnification SEM images (n=100).

[CET] (μg/mL)	Isolate	Length (μm)	Standard deviation	Difference to EC	Width (μm)	Standard deviation	Difference to EC
0	EC	1.363	0.293		0.742	0.083	
	ECCETT	1.657	0.429	**0.294**	0.862	0.120	**0.120**
18.8	EC	1.205	0.247		0.808	0.126	
	ECCETT	1.441	0.306	**0.236**	0.757	0.104	**-0.051**
37.5	EC	1.242	0.259		0.811	0.094	
	ECCETT	1.351	0.286	**0.109**	0.629	0.070	**-0.182**
75	EC	1.153	0.266		0.797	0.075	
	ECCETT	1.324	0.316	**0.171**	0.665	0.066	**-0.132**
300	EC	1.342	0.388		0.912	0.106	
	ECCETT	1.405	0.305	0.063	0.751	0.130	**-0.161**

All bolded values are significant with $P<0.01$ by Student's t-test.

Difference from EC was determined by subtracting mean length or width of EC from mean length or width values of ECCETT.

QAC concentrations at their MIC. A similar trend was seen when ECBZKT were in the presence of PBS alone; the membranes began to stick together (Figure 3.8B). When BZK was introduced, the overall plumpness did increase (Figure 3.8D). Interestingly, instead of the development of chains, ECBZKT showed an elongated phenotype (Figure 3.8D, F) being, on average, 40% longer than EC. This type of dependence has not been seen in previous studies to date, making this a novel finding for QAC adapted *E. coli*. Based on the few studies that do examine electron microscopy images of bacteria exposed to QACs, most indicate that the cell membrane(s) of bacteria (*P. fluorescens* (185), *P. aeruginosa* (185–187), *S. aureus* (43), and *E. coli* (43)) is "stripped off" in the presence of QACs, which we did not see in our EC SEM images. Our results do show that, despite the mechanism of action for QACs being similar, the morphology of each QAC-adapted *E. coli* replicate is different (ECBZKT is longer; ECCETT forms chains). Together, RFMID shows additional application potential for it to not only predict QAC tolerance of bacteria from an overnight culture but also to probe deeper into cell permeability using impermeant fluorescent dyes.

Chapter 4: Examination of chlorhexidine adapted *Escherichia coli* membrane permeance and morphology using a rapid fluorescent dye-based membrane impermeant assay and scanning electron microscopy

The findings in this chapter will be submitted to Antimicrobial Agents and Chemotherapy. To accomplish the aims and hypotheses laid out in section 4.1, we employed the techniques described in chapter 2 (2.1.1, 2.2-2.5). MIC AST data collection was initially performed by Dr. Nicola Cartwright and Kari Green and was followed up by Branden Gregorchuk. 30MBC AST, RFDMIA, data analysis, and data processing was performed by Branden Gregorchuk. SEM imaging was done by Branden Gregorchuk and Shelby Reimer, guided by Dr. Dan Beniac and Shannon Heibert. SEM length and width measurements were accomplished by Branden Gregorchuk and Shelby Reimer. SEM image analysis was performed in coordination with Branden Gregorchuk, Shelby Reimer, Dr. Dan Beniac, Shannon Heibert and Dr. Denice Bay. Thesis writing and manuscript writing was done by primarily done Branden Gregorchuk with editing provided by Dr. Denice Bay and Shelby Reimer.

4.1 Aims and Hypotheses of Chapter 4

After completion of QAC RFDMIA, we investigated if the RFDMIA could be applied to detect different classes of biocide CAs (bisbiguanides). We chose chlorhexidine (Figure 1.1) based on its related antimicrobial mechanism of action to QACs (Section 1.2.1.2). We hypothesized that, similar to the QAC RFDMIA in chapter 3, RFDMIA would be able to discriminate between the CHX-susceptible EC and the CHX-tolerant ECCHXT with EC demonstrating a significant (P<0.01) increase in $\Delta RFU_{\Delta 30min}$ EM 620nm values at a lower CHX concentration than ECCHXT. We also wanted to determine if RFDMIA would be able to predict the CHX MIC value of ECCHXT and EC. To verify bacterial cell integrity and morphology at various CHX concentrations used in the RFDMIA, SEM was performed to visualize CHX-adapted and unadapted *E. coli* isolates. Our results identified that RFDMIA could differentiate CHX-tolerant and CHX-susceptible *E. coli*, in a in 30-minute drug exposure timeframe. Our collected SEM images confirmed that MIC and 30MBC CHX concentrations cell disruption and the RFDMIA susceptibility results as well as the membrane disruptive actions of CHX. Additionally, SEM image analysis revealed that CHX-adapted *E. coli* (ECCHXT) was significantly longer than the control (EC), indicating that CHX adaptation alters *E.*

coli cell morphology. SEM images suggested a type of CHX dependence for the CHX-tolerant replicate with it requiring sub-inhibitory concentrations of CHX to maintain a classic bacilliform appearance. Overall, this demonstrates that RFDMIA is suitable to rapidly discriminate CHX susceptibility *E. coli*, providing an additional biocide CA that can be detected by this technique.

4.2 Results and Discussion

4.2.1 AST of tested isolates

Prior to RFDMIA and SEM analyses, we determined CHX AST (MIC and 30MBC) values for EC and ECCHXT was performed as per section 2.3. MIC values determined by AST of ECCHXT demonstrated a 5-fold increase in CHX tolerance as compared to EC (Table 4.1).

4.2.2 RFDMIA can detect CHX susceptibility

To determine if RFDMIA values can accurately predict MIC values and 30MBC values, we compared RFDMIA to AST measurements. Figure 4.1C, revealed that RFDMIA could significantly (P<0.01 indicated with bar) discriminate CHX-susceptible from CHX-tolerant *E. coli* isolates $\Delta RFU_{\Delta 30min}$ values at 16 µg/mL CHX. RFDMIA overpredicted the CHX MIC values of both EC and ECCHXT by 8-fold and 4-fold respectively (Fig. 4.1A). As expected, 30MBC values coincided with the first or second highest significant increase $\Delta RFU_{\Delta 30min}$ EM values for EC and ECCHXT. To compare the extent that PI permeated into live versus heat-treated cells by RFDMIA, their respective RFU_{30min} values were plotted at increasing CHX concentrations (Fig. 4.1B). A comparison of heat-treated with live cell suspensions RFU_{30min} values for EC and ECCHXT demonstrated that both had a significant differences in RFU_{30min} EM values at each CHX concentration tested; only the mean heat-treated RFU_{30min} EM values showed a slight (EC: -4831.7 SD: +/- 534.0; ECCHXT: -4902.6 SD: +/- 1103.6) but significant (P<0.01, n=9) reduction at the highest measured CHX concentration (64 µg/mL CHX; Fig. 4.1B). This result indicates that, at the highest CHX concentration we tested, PI dye emission did not reach the maximum EM values detected for heat-treated cells. This also suggests that CHX-exposed live cells were less permeant to PI or, conversely, the live cells were more intact by comparison to the heat-treated cells as expected.

Table 4.1. Summary of mean MIC and 30MBC values of CHX for isolates in Chapter 4.

Bacterial isolates tested in this study; isolate abbreviation	MIC (µg/mL) (n=9)*	30MBC (µg/mL) (n=9)*
	CHX	CHX
Escherichia coli K-12 BW25113; **EC**[a]	2	32
Escherichia coli K-12 BW25113; **ECCHXT**[b]	10**	64

* n=9 refers to 3 biological replicate cultures and 3 technical replicate dilutions used for AST.

** This is the exact MIC as determined by Dr. Nicola Cartwright (166), in the 2-fold range employed for RFDMIA analysis the MIC value is 16 µg/mL CHX

a. Strain sourced from the Yale Coli Genetic Stock Centre; CGSC (https://cgsc.biology.yale.edu/)

b. CHX-adapted BW25113 isolate, tolerant to 9.6 µg/mL CHX (166).

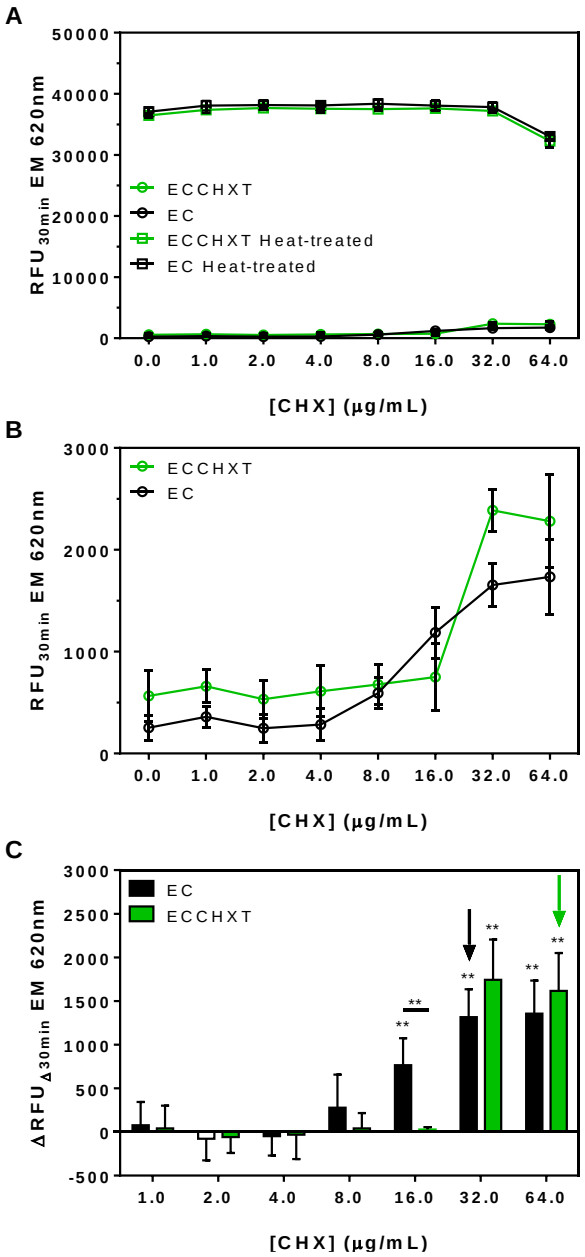


Figure 4.1. RFDMIA of *E. coli* K-12 BW25113 (EC, ECCHXT) incubated with increasing concentrations of CHX. **A)** Shows RFDMIA RFU_{30min} value comparisons of sample and heat-treated EC and ECCHXT replicates exposed to increasing CHX concentrations. **B**) Shows RFDMIA RFU_{30min} value comparisons of sample EC and ECCHXT exposed to increasing CHX concentrations **C)** Shows $\Delta RFU_{\Delta 30min}$ values for live sample EC and ECCHXT exposed to CHX. Graphs represent the mean EM values from three biological and three technical replicates for each concentration. Arrows are color coordinated and indicate the 30MBC of each isolate; unfilled bars indicate the MIC of each isolate. *NB:* Due to the $\log_2$ dilution range, MIC value of ECHXT was considered 16 µg/mL CHX for the purposes of this assay. Students t-test were used to determine $\Delta RFU_{\Delta 30min}$ values at each concentration that significantly differed from the lowest CHX concentration value (**:$P \leq 0.01$). Bar with double asterisk is the comparison between EC and ECCHXT at a given CHX concentration utilizing a Student's t-test to determine significance ($P \leq 0.01$).

4.2.2.1 Discussion of CHX RFDMIA Results

There are a number of reasons that may explain why CHX MIC values could not be accurately predicted. First, CHX concentrations below or at MIC values of EC and ECCHXT may arrest cell growth but may be insufficient to disrupt bacterial membranes. Second, MIC and 30MBC values determined by approved AST measurements require a loss of cell growth measurable over a 18-24-hour CHX exposure as opposed to RFDMIA (16). Similar to antibiotics, CHX susceptibility is often only reliably measured when cells are growing (188), and it may be that at lower CHX concentrations, the membrane disruptive capabilities of CHX at the MIC value concentrations may be more pronounced when the cells are actively growing. For RFDMIA, *E. coli* cells are resuspended into PBS buffer to prevent their growth and based on QAC analyses can involve the use of either stationary phase cells or mid-log. We chose stationary phase cells to determine if CHX disrupted *E. coli* cell integrity in established cultures rather than in cells actively dividing. Using stationary phase cultures in RFDMIA avoids variations in PI dye fluorescence that may be caused by higher PI penetration into cells in the midst of cell division. As it stands, there is little research into the differences between CHX exposure at mid-log and stationary phase cells. In a study by Cheung *et al*. 2012, *E. coli* strains exposed to CHX after 3 hrs exhibited a significant increase in intracellular phosphorus at their respective CHX MIC values(189). It may be that 30 minutes of CHX drug exposure may be too short of a time frame to accurately predict the CHX MIC value by RFDMIA if growth is an important consideration for CHX's mechanism of action. Furthermore, the mechanism of action and chemical structure of CHX differs from the detergent-like QACs explored in Chapter 3. Together, this section demonstrates that the RFDMIA was able to discriminate between EC and ECCHXT at 16 μg/mL.

4.2.3 SEM imaging of CHX adapted *E. coli* reveals that have longer cell lengths but variable width morphologies

To visualize cell morphology at relevant CHX exposure concentrations, EC and ECCHXT cells exposed to increasing concentrations of CHX for 30-minutes were measured by SEM (Figure 4.2.-4.4, Table 4.2). The cell morphologies of all EC and ECCHXT appear intact at low CHX concentrations tested in agreement with our RFDMIA findings that show live cells exposed to CHX below 8 μg/mL have very EM 620nm values. This observation is reaffirmed when we

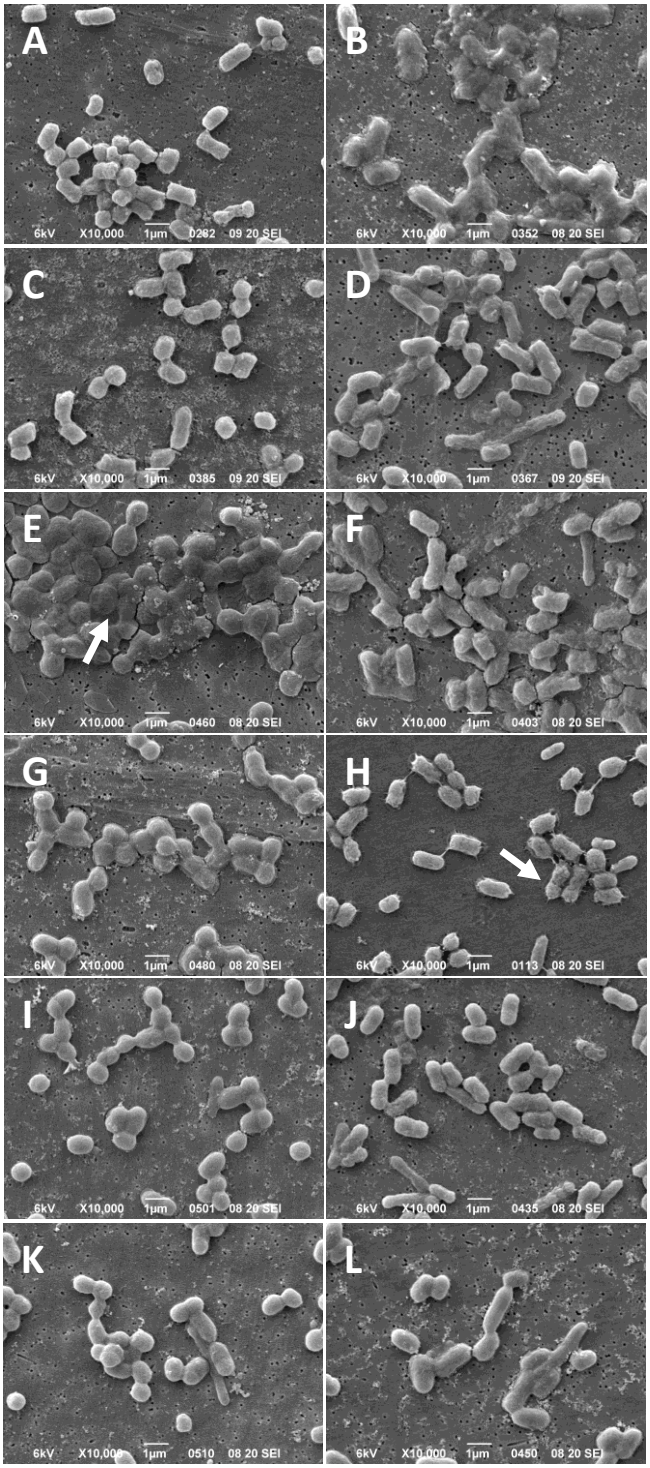


Figure 4.2. SEM images of *E. coli* K-12 BW25113 (EC, ECCHXT) replicates exposed to increasing concentrations of CHX for 30 minutes. Panels **A, C, E, G, I, K** shows EC and panels **B, D, F, H, J, L** show ECCHXT after 30-minute exposure to CHX at 0 µg/mL (A,B), 1 µg/mL (C,D), 2 µg/mL (E,F), 10 µg/mL (G,H), and 32 µg/mL (I,J), 64 µg/mL. All images are representative of 5 SEM images collected at 10,000X magnifications and the white scale bar at the bottom of each panel image indicates 1 µm length. Arrows show wrinkling and pitting or the bacteria.

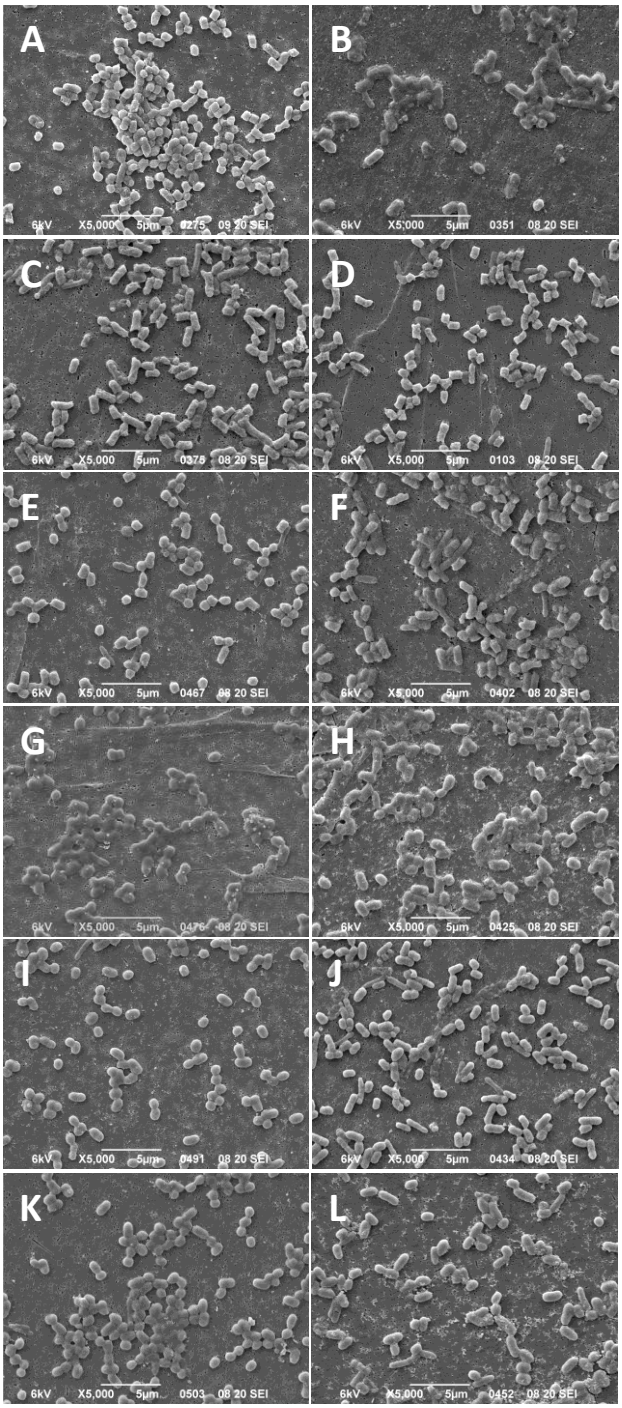


Figure 4.3. SEM images of *E. coli* K-12 BW25113 (EC, ECCHXT) isolates exposed to increasing concentrations of CHX for 30 minutes. Panels **A, C, E, G, I, K** shows EC and panels **B, D, F, H, J, L** show ECCHXT after 30-minute exposure to CHX at 0 µg/mL (Control) (A,B), 1 µg/mL (Sub-MIC EC) (C,D), 2 µg/mL (MIC EC) (E,F), 10 µg/mL (MIC ECCHXT) (G,H), and 32 µg/mL (30MBC EC) (I,J), 64 µg/mL (30MBC ECCHXT). All images are representative of 5 SEM images collected at 5000X magnification and the white scale bar at the bottom of each panel image indicates 5 µm length.

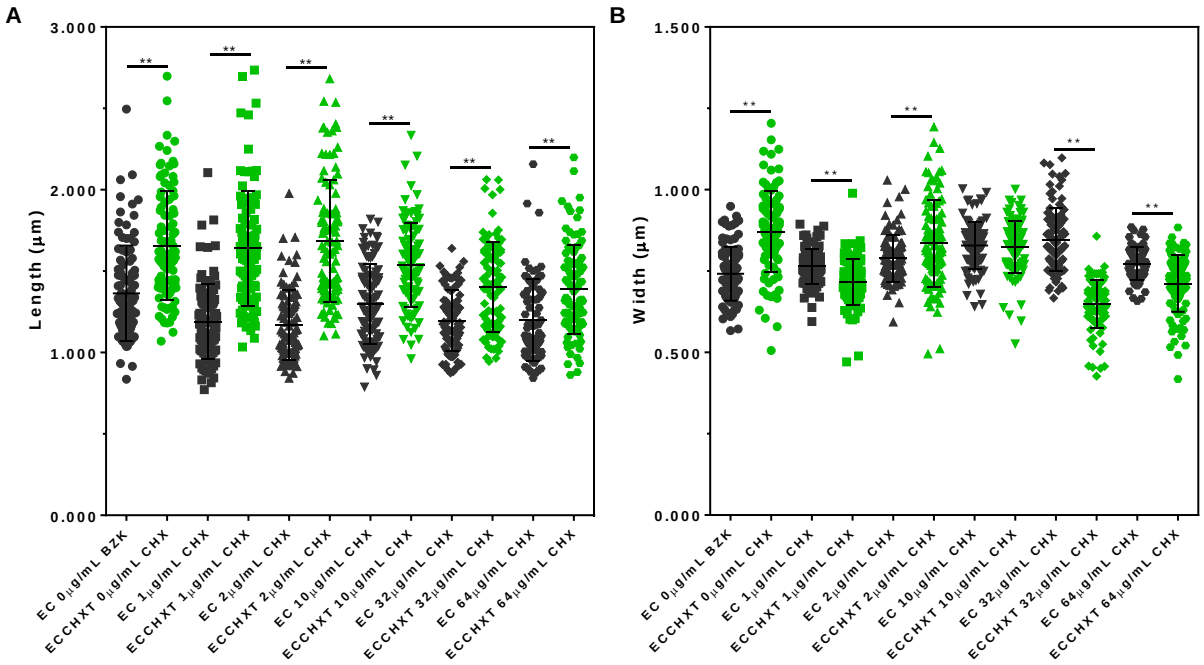


Figure 4.4. A summary of measured EC and ECCHXT cell length and width measurements at various CHX concentrations from SEM images. Panels show cell lengths (**A**) and cell width (**B**) measurements in µm using ImageJ (170) for isolates exposed to increasing concentrations of. Asterisks (**) shown above bars in each panel indicate significantly different *P*-values (<0.01) between the samples. Differences in mean length and width are found in **Table 4.2**. Error bars represent standard deviation from the central mean bar.

Table 4.2. Mean length and width measurements of EC and ECCHXT after 30-minute exposure to CHX based on individual cells visualized from five SEM images collected at 5000X magnification.

[CHX] (µg/mL)	Isolate	Length (µm)	Standard deviation	Length Difference to EC	Width (µm)	Standard deviation	Width Difference to EC
0	EC	1.363	0.293	**0.294**	0.742	0.083	**0.129**
	ECCHXT	1.657	0.337		0.871	0.124	
1	EC	1.189	0.230	**0.450**	0.765	0.054	**-0.048**
	ECCHXT	1.639	0.356		0.717	0.070	
2	EC	1.169	0.215	**0.517**	0.789	0.072	**-0.046**
	ECCHXT	1.686	0.373		0.835	0.134	
10	EC	1.299	0.246	**0.241**	0.829	0.072	-0.005
	ECCHXT	1.540	0.258		0.824	0.081	
32	EC	1.196	0.186	**0.206**	0.847	0.096	**-0.199**
	ECCHXT	1.402	0.274		0.648	0.074	
64	EC	1.342	0.241	**0.186**	0.773	0.051	**-0.062**
	ECCHXT	1.388	0.274		0.712	0.087	

All bolded values are significant with $P<0.01$ by Student's t-test.
Difference from EC was determined by subtracting mean length or width of EC from mean length or width values of ECCHXT.

compared our live cell images to heat-treated *E. coli* cell preparations (Fig. 4.5). EC cells that were not exposed to CHX had a classical bacilliform morphology that became increasingly deflated and flattened in morphology at sub-inhibitory CHX concentrations at its CHX MIC (≤ 2.0 µg/mL; Figure 4.2A, C, E; Figure 4.3 A, C, E). In contrast to EC at the same CHX concentrations, ECCHXT at 0 µg/mL had a deflated bacilliform morphology (similar to EC exposed to CHX at its MIC) that gradually re-inflated when CHX concentrations increased to its CHX MIC value of 10 µg/mL (Figure 4.2B, D, F, Figure 4.3B, D, F). Similar to findings observed for QAC-adapted *E. coli* isolates (Chapter 3), these images suggest that CHX-adapted *E. coli* have a dependence on added CHX concentrations for proper cell morphology and membrane stability. At higher CHX concentrations approaching their respective 30MBC values, EC cells were more fused and rounded in appearance when compared to EC cells exposed to no CHX or sub-inhibitory CHX values (Figure 4.2G, I, K, Figure 4.3G, I, K) or ECCHXT at the same concentrations (Figure 2H, J, L, Figure 4.3H, J, L). Finally, at the 30MBC of ECHXT (64 µg/mL), both EC and ECCHXT took on a more rounded (Figure 4.2K, L, Figure 4.3K, L, Figure 4.4,), but ECCHXT remained significantly longer than EC cells (+0.186 µm) and more narrow in width (-0.062 µm) (Table 4.2). Measurements of cell length from SEM images showed that ECCHXT had more heterogenous cell lengths than EC cells that were on average longer than EC at all CHX concentrations measured (Fig. 4.4, Table 4.2). No noticeable trends were observed for EC or ECCHXT with respect to measured cell widths from SEM images, except that both isolates had cell widths that diminished as the concentration of CHX increased. Therefore, SEM analysis is in agreement with RFDMIA findings indicating that CHX exposure measurably alters cell morphology over 30 minutes. Both SEM and RFDMIA analyses demonstrated that all concentrations of CHX tested do not disrupt cell integrity as compared to a heat-treated control suggesting that CHX's mechanism of action may not result in substantial cell disruption as we observed for QACs at sub 30MBC concentrations.

4.2.3.1 Discussion of SEM results

In Chapter 3, we observed that the QAC-adapted isolates had a dependence phenotype requiring a sub-inhibitory concentration of BZK or CET to maintain an EC-like cell morphology. Here in Chapter 4, SEM data supports EC-like cell morphology of ECCHXT cells when exposed to

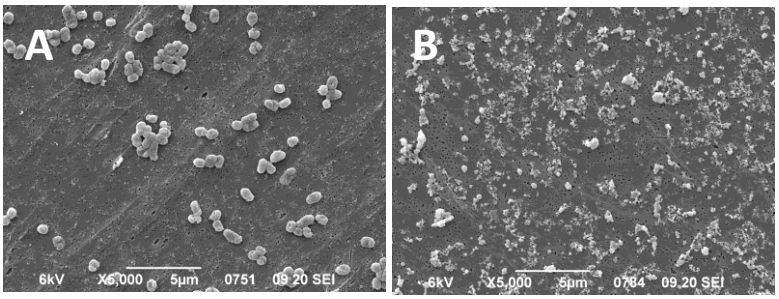


Figure 4.5. SEM images of *E coli* isolates EC (A) and PBS (B) controls after heat-treatment. All images are representative of five SEM images collected at 5000X magnifications and the white scale bar at the bottom of each panel image indicates 5 µm length.

sub-inhibitory concentrations of CHX. Upon SEM imaging, ECCHXT displayed the similar characteristics of CHX dependence we observed for QAC-adapted *E. coli* (Figure 3.8, 3.10). This is seen at 0 μg/mL CHX where ECCHXT appears deflated (Figure 2B) and, as sub-inhibitory concentrations of CHX were added (Figure 2D, F), the observed cells began to round out, no longer being faded onto the membrane. This suggests that, similar to QAC dependence observed in Chapter 3, there may be a CHX dependence generated during the CHX adaptation process. It is important to note that, despite both CHX and QACs being members of cationic antimicrobials and having similar broad mechanisms of action involving membrane disruption, the specific way by which CHX exerts its antimicrobial action is different than QACs; CHX binds anionic phospholipids and proteins rather than solubilizing lipids and membrane proteins into micelles like QACs (11). CHX is unable to solubilize within the hydrophobic core of the bacterial membrane similar to QACs (11). This may explain why there was a difference within the magnitude of negative ΔRFUΔ30min EM values for both EC and ECCHXT as compared to Chapter 3. It may be that the negative ΔRFUΔ30min EM values of the RFDMIA are revealing subtle perturbations in PI dye penetration based on CHX's mechanism of action for both EC as well as ECCHXT at sub-inhibitory CHX concentrations. To resolve this, future RFDMIA studies at CHX concentrations below 1.0 μg/ml and determine if these negative ΔRFUΔ30min EM values are due to RFDMIA reaching a limit of detection for CHX or a genuine alteration of cell envelope interaction allowing greater PI dye cell incorporation. Additionally, the ECCHXT were adapted over 20 generations as compared to 40 generations for our QAC-adapted replicates. This shorter adaptation time course may be influencing the degree of dependence that was able to develop within our CHX-adapted replicates. SEM analyses of EC and ECCHX exposed to increasing CHX concentrations provided a unique opportunity to observe morphological changes to cell surfaces and overall *E. coli* morphology and revealed differences in CHX mechanism of action between adapted and unadapted *E. coli*. At 0 μg/ml CHX our SEM images revealed that without CHX, CHX adapted *E. coli* cells were far more susceptible to the fixative used to image the cells, where cells were flattened and deflated by comparison to EC (Fig. 2A-B); this suggests that CHX adapted *E. coli* likely has substantial differences in cell envelope stability. Whole genome sequencing of the ECCHXT was recently performed and identified single nucleotide alterations in a number of genes

related to cell envelope stress (*marR*, *lon*, *yfdC*) and lipid alterations (*mlaA*, *ybjG*, *eutE*) (166). Based on negative values for RFDMIA and SEM images, this may be an indication that the adapted replicate of EC has a CHX dependence as we observed in Chapter 3. As we increased the CHX concentration, we saw the characteristic noticeable pitting (Figure 4.2E, H) and membrane fusion (Fig. 4.2G, L), which was seen in other electron microscopy studies discussed below. In the study by Cheung *et al*. 2012 (189), both pitting, cell "dents" and cell to cell fusion were observed for cells exposed to CHX, by scanning electron microscopy, though the location does vary among bacteria due to differences in lipid content of their membranes (189). Another study by Shalamanov 2005 (190) who examined *Pseudomonas aeruginosa*, *Enterobacter cloacae*, and Serratia marcescens exposed to Hibitane gluconate 20% (active ingredient is CHX), showed heterogeneous population of cells that showed increased cell clustering and aggregation after exposure to inhibitory concentrations of this mixed CHX containing antimicrobial solution. Our SEM images show similar results to these previous studies, in that EC cells are progressively more wrinkled, become smaller, cell surface pitted, as inhibitory concentrations of CHX were reached. We also measured 100 cells to estimate the extent of changes in cell morphology based on cell width and lengths (Figure 4.3, 4.4). We do note that were unable to find any previous studies that quantified these length and width changes due to CHX exposure. This type of fusion and cell aggregation/clustering may influence how effective RFDMIA PI dye may penetrate cells, since more cell fusion may reduce the overall cell surface area for PI dye to penetrate and bind to DNA/RNA thereby increasing dye fluorescence. Our observation that only ECCHXT cells were elongated when compared to EC cells (Fig. 4.4), is likely a result of genetic alterations observed from CHX-adaptation as described in recent work from our lab (166). Investigation into the genomics and proteomics of ECCHXT is ongoing and will clarify how antiseptic adaptation may influence *E. coli* cell morphology.

Chapter 5. Antibiotic CAs cause minimal membrane disruption as revealed by indirect measurement of a membrane impermeant dye

This chapter will be submitted in addition to secondary research involving phenotypic, genotypic, and proteomic analysis of the ECCOLR replicates to Antimicrobial Agents and Chemotherapy. COL MIC AST was initially performed by Dr. Nicola Cartwright and Kari Green and was repeated by Branden Gregorchuk. Aminoglycoside MIC AST was performed by Andy Seo, Michelle Wuzinski, and Branden Gregorchuk. COL RFDMIA and their subsequent 30MBC and 60MBC analysis was performed by Branden Gregorchuk and Michelle Wuzinski. GNT and TOB RFDMIA as well as their respective 30MBCs was performed by Michelle Wuzinski and Andy Seo. SEM imaging was performed by Branden Gregorchuk and Shelby Reimer with assistance from Dr. Dan Beniac and Shannon Heibert. SEM image data analysis and processing were done by Branden Gregorchuk with assistance from Shelby Reimer, Dr. Dan Beniac, Shannon Heibert, and Dr. Denice Bay. Thesis chapter writing was done by Branden Gregorchuk with editing help by Dr. Denice Bay. All methods listed in Chapter 2 have been used in this section.

5.1 Chapter 5 Aims, hypotheses, and approaches

This chapter determines if the RFDMIA was able to discriminate between antibiotic CA (COL, GENT, TOB) susceptible and resistant isolates and if it can predict the MIC values for a collection of antibiotic CA resistant isolates (Table 5.1). To this end, we examined two RFDMIA datasets of antibiotic CAs and their corresponding antibiotic CA resistant isolates. The first set focused on COL, where we examined EC, a COL resistant adapted isolate (ECCOLR), and an EC strain transformed with an expression plasmid containing the *mcr1* gene (MCR1). The second antibiotic CA RFDMIA dataset set was centered on examining aminoglycoside resistance and used Cadham Provincial Lab clinical isolates (Table 5.1) that were resistant to TOB or GNT. As with Chapters 3 and 4, we hypothesized that the RFDMIA would be able to predict the MIC value of antibiotic CAs in 30 minutes by the first significant increase in $\Delta RFU_{\Delta 30min}$. Additionally, we hypothesized that the RFDMIA would be able to discern the susceptible control (EC) from the resistant *E. coli* (ECCOLR and MCR1) as determined by the significant difference of $\Delta RFU_{\Delta 30min}$ between the tested replicates. In an effort to visualize the morphological changes caused by COL adaptation as well as the effects of 30 minutes of COL exposure, we performed SEM to analyse

the changes in cell length, width, as well as the overall morphologies of the COL resistant set of bacteria. Similar to what was seen in Chapters 3 and 4, we expected to see a difference within the length and width measurements of ECCOLR at all COL concentrations. Furthermore, we proposed that EC and MCR1 would have similar length, width, and morphological appearances at their respective sub-MIC and MIC value COL concentrations. RFDMIA was unable to reliably predict the MIC values of all COL resistant or susceptible *E. coli* within 30 minutes. Therefore, we investigated if the 30-minute exposure time was insufficient by performing a 60-minute RFDMIA, which revealed that this longer COL exposure time could differentiate between some COL resistant *E. coli* but still underpredicted the MICs value of the *E. coli* MCR1 transformant isolate. Finally, we moved onto examining the effects that COL adaptation had on *E. coli* as well as the membrane disruptive capabilities of COL with the use of SEM. SEM analysis revealed that ECCOLR was significantly shorter and thinner than EC and MCR1. In contrast to the dependant phenotypes seen with biocide CA adaptation, ECCOLR displayed no dependence suggesting that this phenomenon may be more associated with biocide CAs rather than antibiotic CAs. Next, we examined if RFDMIA was able to predict aminoglycoside resistance of aminoglycoside resistant clinical *E. coli* isolates. RFDMIA was unable to predict aminoglycoside resistance and failed at discriminating between the susceptible control and the resistant *E. coli* isolates for both TOB and GNT RFDMIA suggesting that the membrane disruptive capabilities of aminoglycosides may be more subtle than other CAs tested in this thesis or not detectable by this method. Together, this chapter demonstrates that detection of antibiotic CA susceptibility is unreliable within a 30-minute timeframe, that COL dependence was not found, and further investigation into the mechanism of action for COL is necessary based on RFDMIA and SEM findings.

5.2 Results and discussions

5.2.1 AST of various *E. coli* isolates verifies MIC and 30MBC values for colistin and aminoglycosides.

To determine if antibiotic CA resistant and susceptible *E. coli* be can rapidly detected using the RFDMIA technique developed for biocide CAs in Chapters 3-4, the antimicrobial susceptibilities of the various *E. coli* replicates adapted to COL or clinical isolates tested with aminoglycoside resistance in Table 5.1 were performed by AST. ECCOLR selected for this study

Table 5.1 A summary of mean MIC and 30MBC values for COL and aminoglycoside susceptibility for strains used in Chapter 5.

Bacterial strains tested in this study; strain abbreviation	MIC (μg/mL) (n=9)*			30MBC (μg/mL) (n=9)*		
	TOB	GNT	COL	TOB	GNT	COL
Escherichia coli K-12 BW25113; **EC**[a]	8	8	1	128	256	16**
Escherichia coli K-12 BW25113+pMS119EG; **ECP**[b]	-	-	1	-	-	16**
Escherichia coli K-12 BW25113; **ECCOLR**[c]	-	-	>450	-	-	>1024
Escherichia coli K-12 BW25113+pMCR1; **MCR1**[d]	-	-	8	-	-	256**
Escherichia coli Clinical isolate 93; **EC93**[e]	32	-	-	>512	-	-
Escherichia coli Clinical isolate 96*;* **EC96**[e]	128	-	-	>512	-	-
Escherichia coli Clinical isolate 97*;* **EC97**[e]	-	512	-	-	>2048	-
Escherichia coli Clinical isolate 102*;* **EC102**[e]	-	64	-	-	1024	-

* n=9 refers to 3 biological replicate cultures and 3 technical replicate dilutions used for AST.

** 30MBC and 60MBC values for these strains were identical.

a. Strain sourced from the Yale Coli Genetic Stock Centre; CGSC (https://cgsc.biology.yale.edu/).
b. Transformed BW25113strain with pMS119EH (167) empty vector.
c. COL adapted BW25113 isolate, tolerant to 300 μg/mL COL.
d. BW25113 strain with pMS119EH-*mcr-1* plasmid providing COL resistance.
e. Clinical isolates donated from Cadham provincial labs by Dr. David Alexander.

was generated by a previous by Bay lab member (Dr. N Cartwright) by continually sub-culturing *E. coli* BW25113 to increasing COL concentrations (166). After 32 sub-cultured generations, the COL adapted *E. coli* was resistant to a surprisingly high final concentration of COL (>450 µg/mL COL; Table 5.1) (166). It is important to note here that MIC values for ECCOLR are much higher (900-fold increase in MIC from EC) than in previously generated COL-adapted isolates as reported in other studies (125, 135, 191, 192). It also represents one of highest published MIC resistance profiles for a COL-adapted isolate without possessing the *mcr-1* gene. In an effort to compare this extremely resistant COL-adapted isolate to COL resistance more commonly observed in clinical isolates a *mcr-1* was cloned into a low copy expression vector pMS119EH (167) and transformed into *E. coli* BW25113 generating the transformant MCR1 (Table 5.1). MCR1 demonstrated an 8-fold increase in MIC as compared to its control (Table 5.1), in agreement with previously published findings of clinical COL resistant *E. coli* isolates (39, 135, 191, 193). This indicates that our *mcr-1* plasmid expression is similar to clinical *mcr-1* resistant isolate phenotypes when expressed by the *E. coli* K-12 strain used in this study. The MIC and 30MBC value for ECCOLR was also considerably higher than MCR1's (>50-fold and >128-fold respectively; Table 5.1). Based on this AST data, both ECCOLR and MCR1 were selected for further RFDMIA analysis.

Two clinical *E. coli* isolates with resistance to GNT (EC97, EC102) or TOB (EC93, EC96) were selected to test RFDMIA aminoglycoside resistance and their AST MIC values are listed in Table 5.1. MIC values of the aminoglycoside resistant isolates varied from a 4-fold (EC93) to 64-fold (EC97) as compared to EC. The 30MBC for the aminoglycoside resistant isolates demonstrated a 4-fold to 8-fold increase in resistance. For EC93, EC96, EC97, the 30MBC occurred at aminoglycoside concentrations that were beyond the ranges tested by RFDMIA. Based on this AST data, EC93, EC96, EC97, EC102 were selected for aminoglycoside RFDMIA analysis.

5.2.2 RFDMIA cannot reliably discriminate antibiotic CA susceptibility or resistance in *E. coli*

5.2.2.1 Colistin

To examine if RFDMIAs can detect and/or predict COL resistance, we tested and compared ECCOLR and MCR1 to its respective susceptible control strain (EC). It should be noted that EC and the EC empty plasmid control (ECP) had the same susceptibility profile which allowed

us to move forward with just EC as a control (Table 5.1). Based on our analysis, RFDMIA was unable to accurately predict COL susceptibility or MIC values in the replicates we tested. Based on RFDMIA results, the assay predicted that the MIC of EC would occur at 4 μg/mL, while the MIC for MCR1 would be 1 μg/mL based on the first significant increase in $\Delta RFU_{\Delta 30min}$ values; this is inaccurate based on MIC AST susceptibility values in Table 5.1. However, RFDMIA correctly predicted the 30MBC of EC which corresponded with the largest increase in $\Delta RFU_{\Delta 30min}$ value (Figure 5.1A). The assay was not able to predict the 30MBC of either MCR1 or ECCOLR due to the lower range examined ($\leq$16 μg/mL COL). At higher concentrations of COL (Figure 5.1B), we found that the assay underpredicted the MIC and the 30MBC of MCR1 by predicting its susceptibility at 16 μg/mL and 128 μg/mL COL respectively. At this increased COL range, RFDMIA was unable to predict the MIC value for EC. Hence, RFDMIA was unable to differentiate susceptible EC from resistant MCR1, as the resistant isolate maintained an increased $\Delta RFU_{\Delta 30min}$ EM values at the majority of the COL concentrations tested (Figure 5.1A, B).In both the low range and increased range 30-minute RFDMIA (Figure 5.1A, B) ECCOLR demonstrated constant negative $\Delta RFU_{\Delta 30min}$ EM values in both low and high concentrations of COL; this was not unexpected as the MIC and 30MBC values were outside the concentrations tested (Table 5.1).

As COL may potentially act over longer timeframes as compared to biocide CAs necessitating a longer drug exposure time 30-minutes may be an insufficient timeframe to detect COL resistance. Therefore, a high COL concentration longer RFDMIA experiment was measured over 60 minutes (Figure 5.1C). For EC, there was no significant increase in $\Delta RFU_{\Delta 60min}$ EM values at the higher concentration range, indicating that cell membranes may already be disrupted. After 60 minutes, RFDMIA was unable to predict the MIC value of MCR1 to COL as indicated by the first significant increase in $\Delta RFU_{\Delta 60min}$ at 32 μg/mL COL; this concentration of COL was 4-fold larger than the MIC of MCR1 (8 μg/mL COL; Table 5.1). RFDMIA was able to correctly predict the 60MBC of MCR1 as the largest gain in $\Delta RFU_{\Delta 60min}$ EM value and it occurred at 256 μg/mL COL which coincides with its 60MBC. Due to the concentration range used, the assay was not able to predict the MIC value of EC (MIC: 1 μg/mL COL) nor ECCOLR (MIC: >450 μg/mL). Importantly, the 60-minute COL RFDMIA was able to discriminate between EC and MCR1, EC and ECCOLR, and MCR1 and ECCOLR after a 60-minute exposure (Figure 5.1C). This was seen in Figure 5.1C where

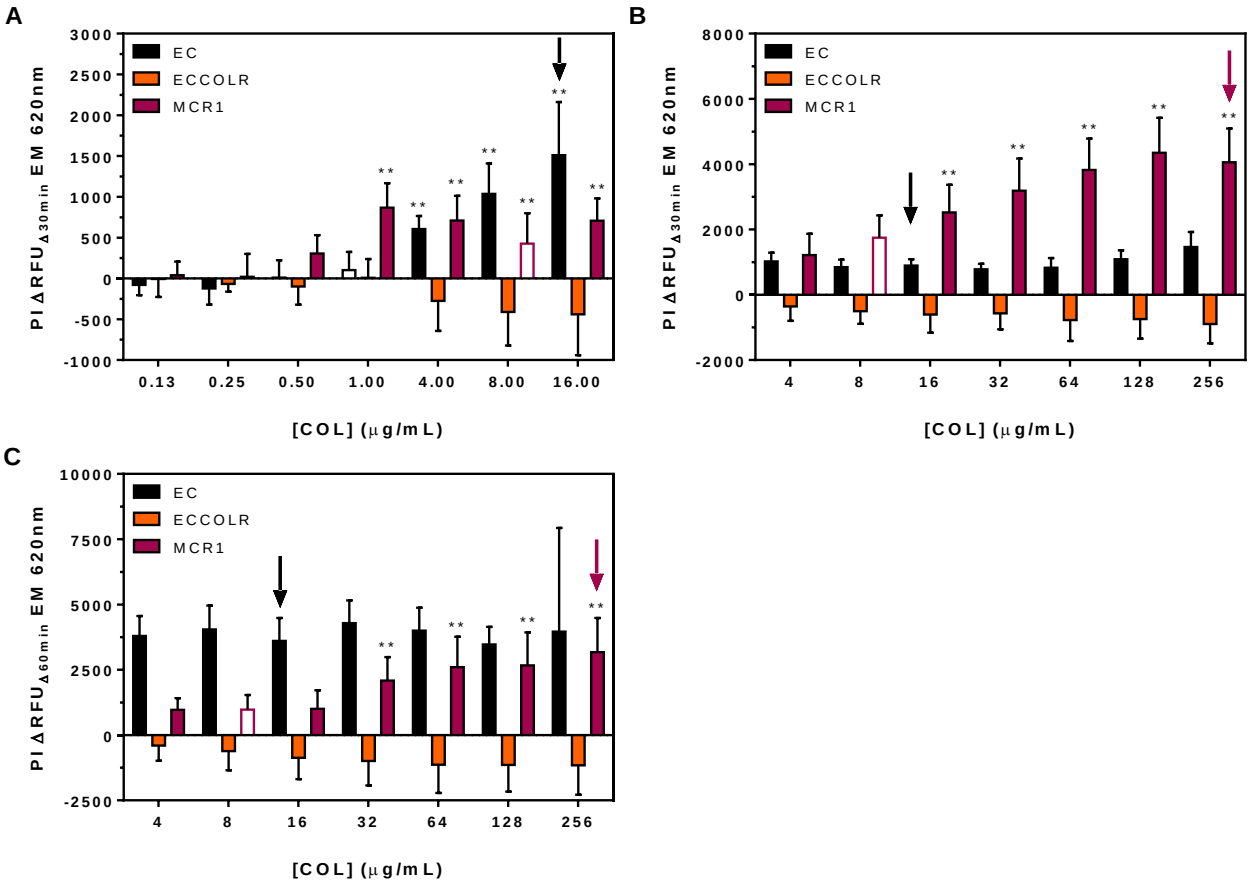


Figure 5.1. RFDMIA results of *E. coli* K-12 isolates adapted to COL (ECCOLR) or transformed with *mcr-1* containing plasmid (MCR1). All RFDMIA was performed using stationary phase cells with 2.0 µg/ml PI dye. **A)** RFDMIA $\Delta RFU_{\Delta 30min}$ EM values for EC, MCR1, and ECCOLR at a low range COL after 30 minutes. **B)** RFDMIA $\Delta RFU_{\Delta 30min}$ EM values of EC, MCR1, and ECCOLR exposed to intermediate COL log_2 concentration range. Graphs A and B represent the mean $\Delta RFU_{\Delta 30min}$ values from three biological and three technical replicates for each concentration. Arrows are color coordinated and indicate the 30MBC of each isolate. **C)** RFDMIA $\Delta RFU_{\Delta 60min}$ of EC, MCR1, and ECCOLR exposed to COL over 60 minutes. Graph C shows the mean $\Delta RFU_{\Delta 60min}$ values from three biological and three technical replicates for each concentration. Arrows are color coordinated and indicate the 60-minute MBC (60MBC) of each isolate. For all graphs a Students t-test were used to determine if $\Delta RFU_{\Delta min}$ value at each concentration significantly differed from the lowest measured COL concentration $\Delta RFU_{\Delta min}$ value (**:*P* <0.01). For all graphs, unfilled bars indicate the MIC of each isolate and are colour coordinated to the isolate (EC=Black, MCR1=dark pink, ECCOLR=Orange).

EC maintained high $\Delta RFU_{\Delta 60min}$ EM, while MCR1 had a low $\Delta RFU_{\Delta 60min}$ EM values below 32 µg/mL. After 32 µg/mL COL, there were significant increase in $\Delta RFU_{\Delta 60min}$ EM for MCR1 which eventually achieved similar values to EC.

In summary, only at 60 minutes could the RFDMIA discriminate COL resistances of EC, ECCOLR, and MCR1, when compared together. After 30-minute exposure, the assay was unable to discriminate between MCR1 and EC with MCR1 having higher $\Delta RFU_{\Delta 30min}$ EM values which is discordant with our AST.

5.2.2.1.1 Discussion of COL RFDMIA

The inability to detect COL susceptibility in a 30-minute RFDMIA timeframe, but the ability to discriminate EC, MCR1, and ECCOLR susceptibility at 60-minutes may suggest that COL needs a longer exposure time to act and be detectable by PI dye. Although the mechanism of COL action is still debated (34, 39, 63) RFDMIA analyses indicate that COL requires more time to act on bacterial membranes as compared to biocide CAs which act quickly. Further, this may suggest that for COL, membrane disruption may not be solely responsible for growth inhibition and cell death in *E. coli* (39). In *A. baumannii*, polymyxin exposure also generated hydroxyl radicals which ultimately contributed to bacterial cell death (34, 194). The balance between COL's membrane disruption activity and the generation of hydroxyl radicals as part of its mechanism of action may influence RFDMIA's results, however, hydroxy radical formation cannot be measured in this assay. Secondly, there has been some research suggesting that COL causes a pronounced disruption of the outer membrane of *E. coli* and *P. aeruginosa* but minimal cytoplasmic membrane damage (63). If this is the case, it is another explanation for why RFDMIA is not able to predict COL susceptibility, as the dye (PI) requires access to the DNA/RNA of the bacterium. If the cytoplasmic membrane is not disrupted sufficiently for PI to enter, no fluorescent signal would be detected and, therefore, the assay would underpredict COL susceptibility.

5.2.2.2 Gentamicin and tobramycin RFDMIA of clinical *E. coli* isolates

To examine if RFDMIA can be used to predict aminoglycoside CA susceptibility, GNT resistant and TOB resistant clinical isolates were investigated. At high concentrations these antimicrobials are proposed to cause a type of membrane disruption due to their self promoted

uptake and protein misfolding (33, 36). Overall, RFDMIA was unable to predict either TOB or GNT susceptibilities of the respective resistant clinical isolates (EC93, EC96, EC97, EC102) and susceptible *E. coli* (EC) isolates tested (Figure 5.2). A significant increase in $\Delta RFU_{\Delta 30min}$ EM values for EC at 64 μg/mL TOB, well beyond (8-fold increase) the MIC of this isolate (Figure 5.2A). Further, EC96 failed to have its MIC correctly predicted at 128 μg/mL TOB and EC93 had no significant increase in $\Delta RFU_{\Delta 30min}$ EM values at any TOB concentration tested. RFDMIA was also unable to predict the 30MBC of EC at 128 μg/mL TOB, where the 30MBC of EC93 and EC93 were beyond the drug concentrations ranges tested. Due to the minimal changes in $\Delta RFU_{\Delta 30min}$ EM values, examination of additional TOB concentrations was not followed up any further by 30-min or 60-min RFDMIA. RFDMIAs showed almost no increases in $\Delta RFU_{\Delta 30min}$ EM values at any GNT concentration, with the exception of MIC values for isolates EC97 and EC102 being found within the range of concentrations (512 μg/mL and 64 μg/mL respectively; Table 5.1, Fig. 5.2B). In addition, at GNT 30MBC concentrations of EC and EC102, no increase in $\Delta RFU_{\Delta 30min}$ EM values was observed. Even the differentiation between GNT susceptible and resistant *E. coli* could not be determined due to the lack of differences in $\Delta RFU_{\Delta 30min}$ EM values between EC and the resistant isolates.

5.2.2.2.1 Discussion of GNT and TOB resistant *E. coli* isolates' RFDMIA

Similar to COL at 30-min exposure, GNT and TOB susceptibility could not be detected by RFDMIA. Unfortunately, 60-min RFDMIA was not performed to determine drug exposure as timeframes were a factor. Increasing exposure time, may improve the membrane disruptive capabilities of GNT and TOB. However, the primary mechanism of action for aminoglycosides is protein inhibition, which necessitates drug incorporation in actively growing cells (57). Since the assay was designed to look at cell disruption cells were resuspended in PBS, there are no nutrient and carbon sources that would allow bacterial growth (except the PI and antimicrobial). Additionally, aminoglycosides are able to pass through the outer membrane by porins (81, 195). This means that, if the aminoglycoside molecule accesses the cytoplasm without membrane disruption (inner or outer membrane), the cell is not disrupted, and the dye will not be able to bind to DNA or RNA leading to no detectible EM.

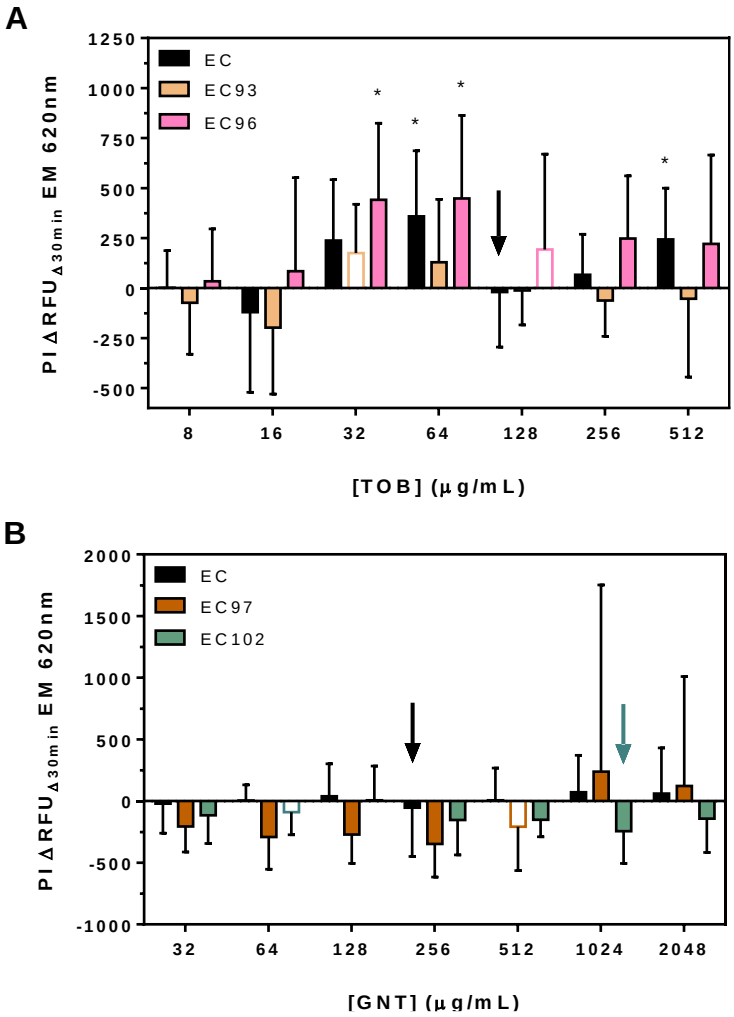


Figure 5.2. RFDMIA results of *E. coli* K12 BW25113 (EC), TOB resistant clinical isolates (EC93, EC96), and GNT resistant clinical isolates (EC97, EC102) after 30-minute exposure to increasing concentrations of aminoglycosides. **A**) RFDMIA results for 30-minute TOB exposure **B**) RFDMIA results for 30-minute GNT exposure. All graphs represent the mean $\Delta RFU_{\Delta 30min}$ values from three biological and three technical replicates for each concentration. Arrows are color coordinated and indicate the 30MBC of each isolate. For all graphs, unfilled bars indicate the MIC of each isolate, 30MBC is indicated by arrows, and are colour coordinated to the isolate (EC=black, EC93=beige, EC96=pink, EC97=orange, EC102=light green). Students t-test were used to determine $\Delta RFU_{\Delta 30min}$ values at each concentration that significantly differed from the lowest aminoglycoside concentration value (*: $P<0.05$). *NB*: EC's MIC for both GNT and TOB are well below the tested concentrations but, even at these elevated concentrations, we did not see and increase in $\Delta RFU_{\Delta 30min}$ EM values.

5.2.3 COL adaptation causes a reduction in length and width in *E. coli* but no COL dependence.

As with the biocide CA-adapted *E. coli*, we wanted to visualize the membrane changes that exposure to COL would have on the *E. coli* isolates tested by RFDMIA as well as what morphology changes were caused by COL adaptation and drug exposure. To this end, EC, MCR1, and ECCOLR was exposed to increasing concentrations of COL to observe their morphological changes (Figure 5.3). For EC, it was apparent that, as the concentration of COL increased, the membrane became deflated and where cells started to fuse together, particularly when the MIC concentration of COL was reached (Figure 5.3G). As the concentration of COL increased above the MIC value for EC, increased cell fusion was observed where the cells appeared to be further deflated (Fig. 5.3J). For MCR1, we saw a similar morphology as for EC cells, which was not unexpected as this replicate differed from EC by the expression of a single gene (*mcr-1*). As with EC, MCR1's cell integrity appeared to diminish once its COL MIC was achieved (Figure 5.3K). At the MIC value, the cells appeared to be fused together and cells became more deflated in appearance on the SEM filter. Additionally, at higher COL concentrations the formation of large cell agglomerates appears where cells are stuck together (Fig. 5.3K). Examination of ECCOLR by SEM revealed that its cells did not have any observable cell integrity problems as the concentration of COL increased; this was to be expected as its COL MIC value of ECCOLR was >450 µg/mL. Unlike the biocide CA-adapted isolates, we did not observe any COL dependence, despite ECCOLR being highly resistant to COL.

5.2.3.1 Discussion of COL SEM images

Unlike what had been seen with our SEM images of biocide CA-adapted *E. coli* (Chapter 3, Chapter 4) we did not observe a COL dependant phenotype. This finding was unexpected as, unlike biocide CA dependence which have no studies, previous AST studies with COL-adapted *A. baumannii* displayed a COL dependant phenotype (196, 197). Additionally, upon further examination of our SEM images, we found that there was a mixed population of cells within the SEM images for ECCOLR, where some appeared to be deflated, even at low (0.13 µg/mL) COL concentrations (Fig. 5.3C, F, I, L). The mixed population of cell morphologies we observed for ECCOLR may explained by a concept known as "heteroresistance" described for other COL-resistant isolates (192). This concept is anchored on the idea that bacteria, even if it was derived

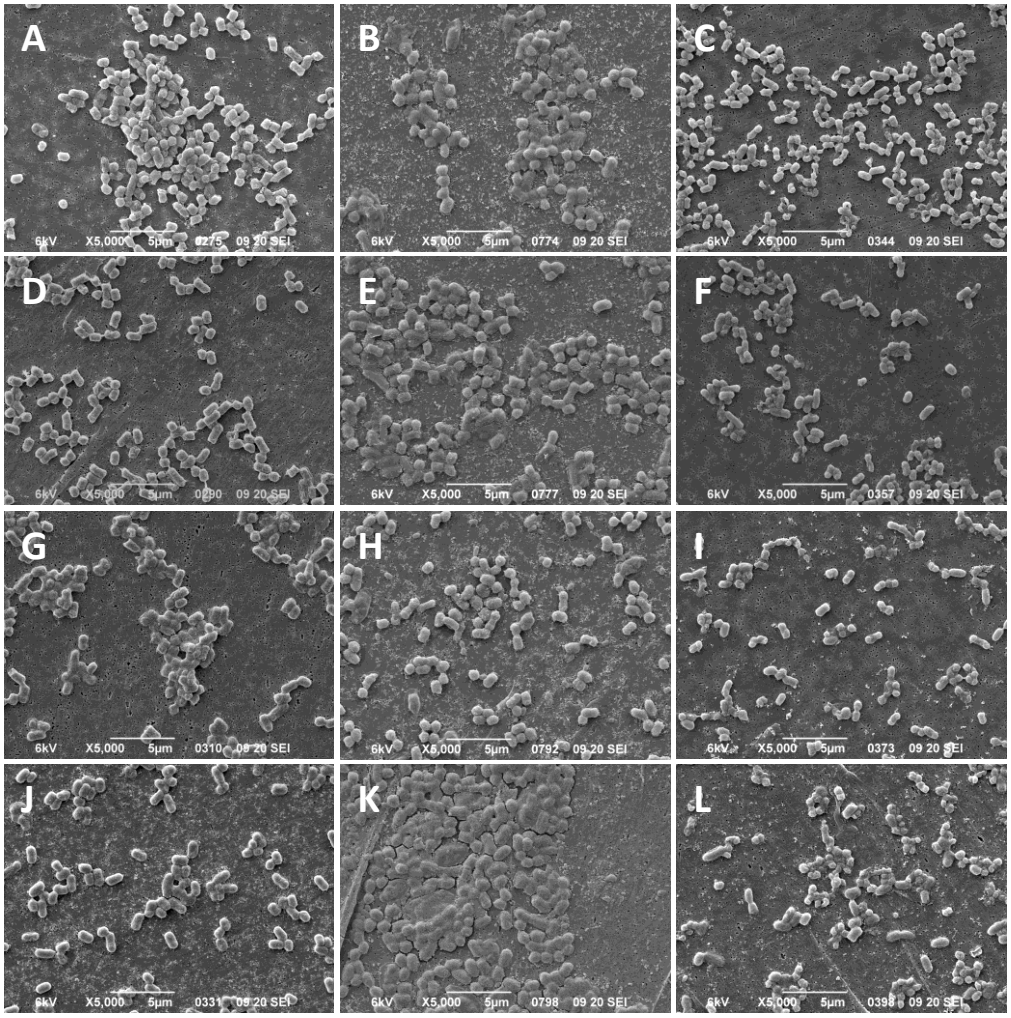


Figure 5.3. SEM images of *E. coli* K-12 BW25113 (EC, MCR1, ECCOLR) isolates exposed to increasing concentrations of COL for 30 minutes. Panels **A, D, G, J** shows EC, panels **B, E, H, K** shows MCR1, and panels **C**, **F**, **I**, **L** shows ECCOLR after 30-minute exposure to COL at 0.00 µg/mL (A, B, C), 0.13 µg/mL (D, E, F), 1.00 µg/mL (G, H, I), and 8.00 µg/mL (G,H). All images are representative of 5 SEM images collected at 5000X magnifications and the white scale bar at the bottom of each panel image indicates 5 µm length. Summary length and width measurements can be found in **Figure 5.4** and **Table 5.2**.

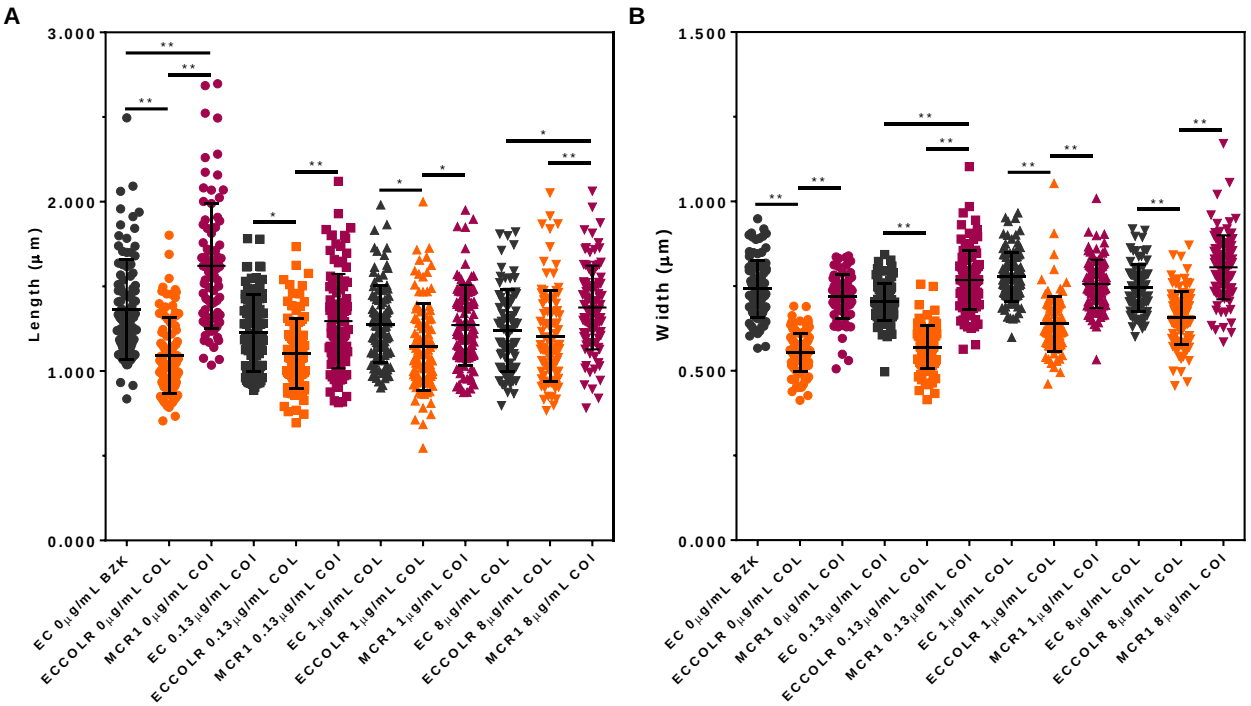


Figure 5.4. A summary of measured EC, MCR1, and ECCOLR cell length and width measurements at indicated COL concentrations from SEM images. Panels show cell lengths (**A**) and cell width (**B**) measurements in µm using ImageJ (170) for isolates exposed to increasing concentrations of. Asterisks (**) shown above bars in each panel indicate significantly different *P*-values (*P*<0.01) between the samples. Differences in mean length and width are found in **Table 5.2**. Error bars represent standard deviation from the central mean bar (n=100).

Table 5.2. Mean length and width values of *E. coli* EC, MCR1, and ECCOLR after 30-minute exposure to COL at indicated concentrations based off of five 5000X magnification SEM images (n=100).

[COL] (μg/mL)	Isolate	Length (μm)	Standard deviation	Difference to EC	Difference to MCR1	Width (μm)	Standard deviation	Difference to EC	Difference to MCR1
0.00	EC	1.363	0.293	-	-	0.742	0.083	-	-
	MCR1	1.621	0.371	**0.258**	-	0.719	0.066	-0.023	-
	ECCOLR	1.094	0.223	**-0.269**	**-0.527**	0.554	0.057	**-0.188**	**-0.165**
0.13	EC	1.226	0.226	-	-	0.703	0.054	-	-
	MCR1	1.295	0.278	0.069	-	0.768	0.087	**0.065**	-
	ECCOLR	1.104	0.206	**-0.122**	**-0.191**	0.570	0.063	**-0.133**	**-0.198**
1.00	EC	1.278	0.229	-	-	0.778	0.073	-	-
	MCR1	1.272	0.237	-0.006	-	0.757	0.071	-0.021	-
	ECCOLR	1.143	0.258	**-0.135**	**-0.129**	0.639	0.082	**-0.139**	**-0.118**
8.00	EC	1.245	0.249	-	-	0.745	0.070	-	-
	MCR1	1.375	0.247	**0.130**	-	0.806	0.094	**0.061**	-
	ECCOLR	1.206	0.268	-0.039	**-0.169**	0.657	0.079	**-0.088**	**-0.149**

All bolded values are significant with $P<0.01$ by Student's t-test.
Difference from EC was determined by subtracting mean length or width of EC from mean length or width values of ECCHXT or MCR1
Difference from MCR1 was determined by subtracting mean length or width of MCR1 from mean length or width values of ECCHXT

from a single isolate, demonstrate various susceptibilities to an antibiotic (192). This can result in the misinterpretation of AST breakpoints for “susceptible” and “resistant” isolates.

When examining the length and width measurements of our COL exposed *E. coli* (Figure 5.4), we found that at many of the COL concentrations tested, EC and MCR1 were not significantly different in terms of their overall length and width, however, ECCOLR was consistently shorter and thinner than EC and MCR1 (Table 5.2). Overall, our SEM images are some of the few that exist showing a COL-adapted replicates exposed to increasing COL concentrations. Additionally, these SEM images also visualize the cell membrane perturbations caused by a 30-minute COL exposure. Similar findings were reported in a study by Mohamed *et al.* 2016, who found that 1 hr COL exposure did cause membrane permeabilization of *A. baumannii* and *P. aeruginosa* by transmission electron microscopy (198). A study by O’Driscoll *et al.* 2018, found that *E. coli* and *P. aeruginosa* after 1 hour of COL exposure caused a pronounced clumping of the cells, where the cells became fused together after COL exposure (63) which we also observed in our MCR1 and EC. In conclusion, our 30-minute SEM images of EC, MCR1, and ECCOLR confirmed cell disruption despite the assay indicating minimal disruption at the MIC values for EC and MCR1 (1 μg/mL and 8 μg/mL, respectively). Additionally, we found that, to discriminate COL RFDMIA susceptibility in *E. coli* requires 1 hour of exposure time. SEM confirmed that COL exposure caused clumping of cells as seen in previous research.

Chapter 6 Final Discussion and Summary

In an attempt to summarize all the findings of this thesis, this section provides a brief discussion of the results from Chapters 3-5, to unify the various discussion sections.

6.1 RFDMIA's benefits and limitations

This project has allowed for the development of a rapid detection assay capable of detecting biocide CA susceptibility and, with extended measurement timeframes, COL susceptibility. We have shown that the RFDMIA was unable to consistently predict MIC or 30MBC values, however, this technique is different than traditional AST methods as it does not measure growth; the assay focuses on rapid membrane perturbations caused by CAs. We found that the assay was sensitive in that it was able to differentiate between QAC and CHX susceptible (EC, SS, KP) and tolerant/adapted bacteria (ECBZKT, ECCETT, SSBZKT, KPBZKT, ECCHXT) in the presence of increasing biocide CA concentrations. Importantly, this assay can use a very narrow range of BZK or CET (20 μg/mL; Figure 3.2E, F) to differentiate between biocide CA susceptible and tolerant *E. coli* isolates. Additionally, we found that we could swap out the membrane impermeant fluorescent dye with a secondary fluorescent dye and still predict susceptibility in *E. coli* (Figure 3.6, 3.7). The RFDMIA was able to also foreshadow the BZK, CET, and CHX dependant phenotypes indicated by the negative $\Delta RFU_{\Delta 30min}$ EM values (Figure 3.2, 4.1.). We also confirmed that biocide CA tolerance and susceptibility of many enterobacteria and non-fluorescent pseudomonads can be detected in 30 minutes with a suitable control species. This technique may provide an additional method to detect membrane perturbations caused by other cationic or uncharged biocides, though, this will need to be explored further. Finally, RFDMIA may be able to reveal mechanism of action of other membrane disruptive antimicrobials.

There were some noted downsides to the assay. First, we were unable to predict *P. aeruginosa*'s intrinsic tolerance to BZK and CET (Figure 3.5-3.7) with either one of the dyes though, this may be due to the intrinsic fluorescent properties of PA (183, 184). This will limit the detection of bacteria with fluorescent properties close to the EX/EM of the chosen impermeant dye in the assay. Secondly, we found that high concentrations of some QACs did lead to a loss of EM signal seen in our assay's heat-treated samples and this phenomenon did vary depending on the impermeant dye used (Figure 3.1; 3.6A, B; 3.7A, B). This means that, if the tested

strain/isolate is extremely tolerant to a biocide CA (*e.g.* >300 µg/mL BZK) detection at or above that concentration will not be possible; this may be a dye dependant phenomenon as we saw a greater loss in EM values for Sytox^{TM} Blue than PI (Figure 3.6, 3.7). We found that the 30-minute RFDMIA was unable to predict the COL MIC value for the isolates tested but its maximum EM values coincided with the 30MBC of EC and MCR1 as well as the 60MBC of MCR1 (Figure 5.1A, B). We also noted that for COL, cell membrane disruption is more pronounced after 1-hour exposure not 30 minutes as with the biocide CAs (Figure 5.1C) suggesting that time is an important parameter to consider. As for aminoglycoside resistance, the assay was unable to predict MIC values or 30MBC values of the isolates tested (Figure 5.2). This could be due to the longer (>30mins) time aminoglycosides require to exert their mechanism of action or due to the mechanisms by which the bacterial membrane is compromised by aminoglycosides versus biocide CAs.

6.2 RFDMIA insights into CA mechanisms of action

This brings forth the question of how the membrane is being disrupted. As noted in a review by Gilbert and Moore, 2005 (11), the specific mechanism by which Gram-negative bacterial membranes are destroyed is dependant on the CA used. For the QACs, the membrane blebs off creating micelles of the membrane and phospholipids (11). For CHX, it follows a similar pattern of binding to the bacterial membrane but, instead of creating micelles, bridges the gap between the polar head groups of the lipids and forces them apart due to CHX's inflexibility (11). For COL, the exact mechanism that it kills bacteria is still unclear, but it proposed to be "detergent-like" (34). Based on our assay's results, it suggests that COL does change the membrane integrity for *E. coli* though, it is still unclear as to how it destroys the membrane and how "detergent-like" this disruption may be (34). Comparison between EC and MCR1 with RFDMIA revealed profound changes in $\Delta RFU_{\Delta 30min}$ EM values, highlighting the potential to quickly screen for membrane based molecular mechanisms of resistance. Furthermore, we were able to visualize the membrane disruption due to COL and we saw that there was membrane damage but that the type of perturbations caused differed between our EC and MCR1 (Figure 5.3K, G). EC did not show the type of membrane fusion seen in the MCR1 images at their respective MIC values (EC: 1 µg/mL COL; MCR1: 8 µg/mL COL; Table 5.1).

Finally, there are many different mechanisms of CA tolerance/resistance that a bacterium can employ (efflux pumps, porin loss, lipid modifications) to become CA resistant/tolerant that will need to be further investigated as it is currently unknown which specific mechanisms can be detected (i.e. can it detect efflux pump activity). As seen with antibiotic resistance, when a system is targeted (peptidoglycan synthesis of the β-lactams), bacteria can adapt by making very specific changes (production of β-lactamases) that directly affect the destructive capabilities of the antibiotic. With CAs, their broad mechanism of action (membrane disruption) adaptation to these molecules will also have to be quite broad. In other words, for bacteria to adapt to a molecule that disrupts membranes, many outer membrane systems need to be modified to become resistant/tolerant (*e.g.* lipid content alterations (34, 145–147, 199), porin expression (51, 81, 105, 148), efflux pump activity (21, 31, 39, 57, 149, 150)) as compared to antibiotics which generally target one specific aspect (protein synthesis, DNA synthesis, cell wall formation, etc.(200) .

6.3 Dependence phenotype seen in SEM images

During the development of the RFDMIA, we decided to utilize SEM to visualize the membrane disruption caused by CA exposure. We found that we could see the membrane of the bacteria become compromised as the CA concentration increased. Unexpectedly, we saw that our biocide CA-adapted tolerant isolates (ECBZKT, ECCETT, and ECCHXT) required a low concentration of their respective CAs to maintain a wild type bacilliform cell appearance (Figure 3.8, 3.10, 4.3) which is novel for research involving biocide CA-adapted *E. coli*. The closest result similar to our findings is was published by Hawlet and Murray 2007 (197). In this study, an *A. baumannii* clinical isolate displayed enhanced growth after subcultures in the presence of high (8 µg/mL) COL concentration, that would have been inhibitory for the non-drug exposed baseline culture. In this thesis, our COL-adapted *E. coli* did not display any noticeable traits of the COL-dependant phenotype reported by Hawlet and Murray 2007 (Figure 5.3). This difference may be due to multiple factors such as bacterial species we employed (Enterobacterales *vs.* Pseudomonad), that their study examined a clinical isolate, and that our COL-adapted *E. coli* was exposed to more than 30 days to increasing concentrations of COL resulting in a significantly higher resistance (>450 µg/mL COL). To date, there is relatively little research in the field of

antimicrobial dependence, so our research offers more data to further this topic. CA dependence is an interesting phenomenon with regards to AMR. Additionally, our SEM images of ECBZKT, ECCETT, and ECCHXT demonstrate a biocide CA-dependant phenotype as, without biocide CA exposure, the membrane is deflated (Figure 3.8, 3.10, 4.3). As more biocide CA is added, this adapted *E. coli* become more bacilliform in cell shape until there a critical breaking point is reached and the membrane becomes overwhelmed and ruptures (Figure 3.8, 3.10, 4.3). Together, our SEM images suggest that CA-adaptation can cause profound morphological changes in length and width of the bacterial cell (Figure 3.9, 3.11, 4.4, 5.4; Table 3.2, 3.3, 4.2, 5.2). For all our CA-adapted isolates, there was noticeable differences in length and width as compared to the baseline *E. coli* (Figure 3.9, 3.11, 4.4, 5.4; Table 3.2, 3.3, 4.2, 5.2).

6.4 Thesis conclusions

This thesis proposed a main hypothesis that cells incubated with increasing concentrations of CAs in the presence of a membrane impermeant dye, propidium iodide (PI), can be fluorescently monitored to detect bacterial CA susceptibility. Based on this hypothesis, we expected that a CA resistant/tolerant bacterial isolate will exhibit a lower level of relative fluorescent units (RFUs) from the excited dye when compared to a CA susceptible isolate exposed to the same CA concentration. To address this overarching hypothesis, we proposed 5 questions which we answer below.

1) *What growth phase (mid-log, stationary phase broth cultures or agar colony) is most efficiently used to accurately discriminate CA susceptibility in E. coli?*

As described in Chapter 3, we found that the ideal growth phase for *E. coli* was stationary phase cultures, with the use of mid-log cells being possible, but colony resuspensions were unsuccessful.

2) *Can RFDMIA differentiate CA susceptible from CA tolerant E. coli BW25113 adapted to various biocide CAs when compared to MIC or MBC values?*

As addressed in Chapter 3 and Chapter 4, we found that we were able to differentiate between CA susceptibilities of tolerant and susceptible *E. coli* towards CHX, BZK, and CET within a 30-minute timeframe by examining changes in $\Delta RFU_{\Delta 30min}$ EM values. Prediction of MIC or 30MBC values were inconsistent for biocide CAs.

3) *Does RFDMIA predicted E. coli cell/membrane disruption at increasing biocide or antibiotic CA concentrations agree with bacterial cells imaged by scanning electron microscopy?*

In Chapters 3, 4, and 5, we confirmed that *E. coli* cell integrity was lost at expected MIC and 30MBC CA concentrations. Unexpectedly, SEM images revealed a biocide CA dependant phenotype within our biocide CA-adapted *E. coli*.

4) *Can RFDMIA differentiate CA susceptibilities of critical priority Gram-negative species E. coli, K. pneumoniae, S. sonnei, A. baumannii, and P. aeruginosa exposed to biocide CAs?*

As discussed primarily in Chapter 3 and Chapter 4, we found that RFDMIA was able to discern the cross-tolerance of our CET-adapted and BZK-adapted *E. coli* from the susceptible EC. Additionally, we confirmed the discriminatory abilities of RFDMIA for *A. baumannii*, *K. pneumoniae*, *S. sonnei*, However, *P. aeruginosa* susceptibility was unable to be predicted, even with an alternative membrane impermeant dye.

5) *Can RFDMIA can predict antibiotic CA resistance in colistin-adapted, colistin resistant, tobramycin-resistant, and gentamicin-resistant E. coli isolates?*

As described in Chapter 5, we were unable to discriminate antibiotic CA resistance towards COL, GNT, or TOB within 30 minutes. A 1-hour RFDMIA for COL was able to discern between the COL-adapted, COL resistant, and COL susceptible *E. coli* isolates.

Based on the results of this thesis, we have shown that RFDMIA can rapidly discriminate biocide CA susceptibilities for various antimicrobials in a variety of critical priority Gram-negative bacteria. The technique developed here represents a more rapid way to discern biocide CA susceptibilities than current methods available (Figure 6.1).

6.4 Future Directions of RFDMIA

RFDMIA offers a rapid method to discriminate biocide CA susceptibilities. This technique could potentially be employed as a quick and straightforward method to screen a large collection of clinical isolates to discern biocide CA susceptibilities. The RFDMIA tolerant signal values of tested isolates can be followed up with traditional AST methods to confirm precise MIC/MBC concentrations if desired. By investigating the molecular mechanisms of CA cross-resistance and

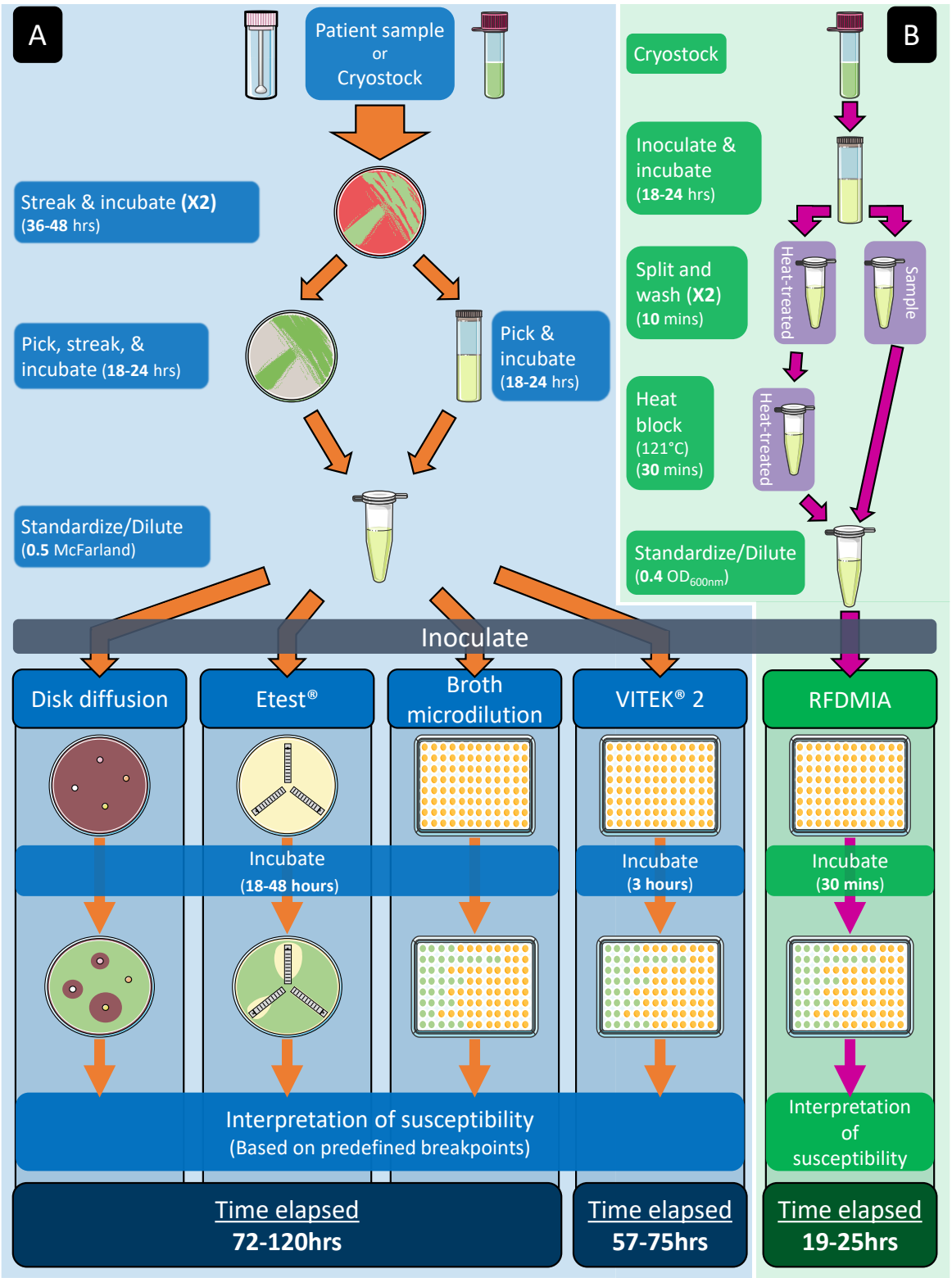


Figure 6.1. Comparison of traditional MIC AST assays (A) to RFDMIA (B). **A**) Shows traditional MIC AST methods used to determine CA susceptibility and their total time elapsed. Note that only broth microdilution method is used for determining biocide CA susceptibility **B**) Shows the RFDMIA process from start to finish for determining CA tolerance/resistance.

cross-tolerance focusing on specific cell membrane changes (*i.e.* Porin loss, efflux pump activity, and individual lipid modifications) it may provide additional insights into how resistance/tolerance emerge. Finally, with the use of the RFDMIA, there is now a straightforward method to start monitoring biocide CA tolerance that can be standardized and widely employed. In doing so, there is the potential to uncover the real prevalence of biocide CA tolerance in clinical and environmental isolates.

References

1. CDC. 2019. Antibiotic resistance threats in the United StatesAntibiotic Resistance Coordination and Strategy Unit within the Division of Healthcare Quality Promotion, National Center for Emerging and Zoonotic Infectious Diseases, Centers for Disease Control and Prevention. Atlanta, GA.

2. Marshall BM, Levy SB. 2011. Food animals and antimicrobials: Impacts on human health. Clin Microbiol Rev 24:718–733.

3. Mahlapuu M, Håkansson J, Ringstad L, Björn C. 2016. Antimicrobial peptides: An emerging category of therapeutic agents. Front Cell Infect Microbiol 6:194.

4. Gnanadhas DP, Marathe SA, Chakravortty D. 2013. Biocides – resistance, cross-resistance mechanisms and assessment. Expert Opin Investig Drugs 22:191–206.

5. Maillard J-Y. 2005. Antimicrobial biocides in the healthcare environment: Efficacy, usage, policies, and perceived problems. Ther Clin Risk Manag 1:307–320.

6. Davies J, Davies D. 2010. Origins and evolution of antibiotic resistance. Microbiol Mol Biol Rev 74:417–433.

7. Nicolaou KC, Rigol S. 2018. A brief history of antibiotics and select advances in their synthesis. J Antibiot (Tokyo) 71:153–184.

8. Aminov RI. 2010. A brief history of the antibiotic era: lessons learned and challenges for the future. Front Microbiol 1:134.

9. Pankey GA, Sabath LD. 2004. Clinical relevance of bacteriostatic versus bactericidal mechanisms of action in the treatment of Gram-positive bacterial infections. Clin Infect Dis 38:864–870.

10. Mcdonnell G, Russell AD. 1999. Antiseptics and disinfectants: Activity, action, and resistance. Clin Microbiol Rev 12:147–179.

11. Gilbert P, Moore LE. 2005. Cationic antiseptics: Diversity of action under a common epithet. J Appl Microbiol 99:703–715.

12. Government of Canada. 2014. Antibiotic resistance and risks to human health.

13. WHO. 2018. Antibiotic resistance.

14. Boucher HW, Talbot GH, Bradley JS, Edwards JE, Gilbert D, Rice LB, Scheld M, Spellberg B, Bartlett J. 2009. Bad bugs, no drugs: No ESKAPE! An update from the infectious diseases society of America. Clin Infect Dis 48:1–12.

15. World Health Organization. 2017. Global priority list of antibiotic-resistant bacteria to guide research, discovery, and development of new antibiotics.

16. Clinical Laboratory Standards Institude. 2016. M100S: Performance standards for antimicrobial susceptibility testingM100S, 26th Edition.

17. EUCAST. 2018. European committee on antimicrobial susceptibility testing breakpoint tables for interpretation of MICs and zone diametersThe European Committee on Antimicrobial Susceptibility Testing.

18. Cerf O, Carpentier B, Sanders P. 2010. Tests for determining in-use concentrations of antibiotics and disinfectants are based on entirely different concepts : “Resistance” has different meanings. Int J Food Microbiol 136:247–254.

19. Gilbert P, McBain AJ. 2003. Potential impact of increased use of biocides in consumer products on prevalence of antibiotic resistance. Clin Microbiol Rev 16:189–208.

20. Ortega Morente E, Fernandez-Fuentes MA, Grande Burgos MJ, Abriouel H, Perez Pulido R, Galvez A. 2013. Biocide tolerance in bacteria. Int J Food Microbiol 162:13–25.

21. Slipski CJ, Zhanel GG, Bay DC. 2018. Biocide selective TolC-independent efflux pumps in Enterobacteriaceae. J Membr Biol 251:15–33.

22. Maillard JY. 2007. Bacterial resistance to biocides in the healthcare environment: Should it be of genuine concern? J Hosp Infect 65:60–72.

23. Davin-Regli A, Pagès JM. 2012. Cross-resistance between biocides and antimicrobials: an emerging question. RevSciTech 31:89–104.

24. Bloomfield SF. 2002. Significance of biocide usage and antimicrobial resistance in domiciliary environments. J Appl Microbiol Symp Suppl 92:144S-157S.

25. Sheldon Jr. AT. 2005. Antiseptic “resistance”: Real or perceived threat? Clin Infect Dis 40:1650–1656.

26. Russell AD. 2004. Bacterial adaptation and resistance to antiseptics, disinfectants and preservatives is not a new phenomenon. J Hosp Infect 57:97–104.

27. Soumet C, Fourreau E, Legrandois P, Maris P. 2012. Resistance to phenicol compounds following adaptation to quaternary ammonium compounds in Escherichia coli NC. Vet Microbiol 158:147–152.

28. Loughlin MF, Jones M V, Lambert P a. 2002. Pseudomonas aeruginosa cells adapted to benzalkonium chloride show resistance to other membrane-active agents but not to clinically relevant antibiotics. J Antimicrob Chemother 49:631–639.

29. Wand ME, Bock LJ, Bonney LC, Sutton JM. 2015. Retention of virulence following adaptation to colistin in Acinetobacter baumannii reflects the mechanism of resistance. J Antimicrob Chemother 70:2209–2216.

30. Langsrud S, Sundheim G, Holck AL. 2004. Cross-resistance to antibiotics of Escherichia coli adapted to benzalkonium chloride or exposed to stress-inducers. J Appl Microbiol 96:201–208.

31. Hegstad K, Langsrud S, Lunestad BT, Scheie AA, Sunde M, Yazdankhah SP. 2010. Does the wide use of quaternary ammonium compounds enhance the selection and spread of antimicrobial resistance and thus threaten our health? Microb Drug Resist 16:91–104.

32. Kawamura-Sato K, Wachino JI, Kondo T, Ito H, Arakawa Y. 2010. Correlation between reduced susceptibility to disinfectants and multidrug resistance among clinical isolates of Acinetobacter species. J Antimicrob Chemother 65:1975–1983.

33. Mingeot-Leclercq M-P, Glupczynski Y, Tulkens PM. 1999. Aminoglycosides: Activity and Resistance. Antimicrob Agents Chemother 43:727–737.

34. Bialvaei AZ, Samadi Kafil H. 2015. Colistin, mechanisms and prevalence of resistance. Curr Med Res Opin 31:707–721.

35. Babaei M, Sulong A, Hamat R, Nordin S, Neela V. 2015. Extremely high prevalence of antiseptic resistant Quaternary Ammonium Compound E gene among clinical isolates of multiple drug resistant Acinetobacter baumannii in Malaysia. Ann Clin Microbiol Antimicrob 14:11.

36. Hancock REW, Farmer SW, Li Z, Poole K. 1991. Interaction of aminoglycosides with the outer membranes and purified lipopolysaccharide and OmpF porin of Escherichia coli. Antimicrob Agents Chemother 37:1309–1314.

37. Epand RM, Walker C, Epand RF, Magarvey NA. 2016. Molecular mechanisms of membrane targeting antibiotics. Biochim Biophys Acta - Biomembr 1858:980–987.

38. Nayyar AS. 2015. Chlorhexidine: A cationic bisbiguanide, membrane active drug in periodontal medicine, structure advantages and associated adverse effects, a brief communication. World J Pharm Pharm Sci 4:37–392.

39. Olaitan AO, Morand S, Rolain JM. 2014. Mechanisms of polymyxin resistance: Acquired and intrinsic resistance in bacteria. Front Microbiol.

40. Shakil S, Khan R, Zarrilli R, Khan AU, Yang M, Wang J, Shen H, Zhou X, Ma X, Shakil S, Khan R, Zarrilli R, Khan A, Jana S, Deb J, Kotra L, Haddad J, Mobashery S, Ramirez M, Tolmasky M, Yamane K, Wachino J, Doi Y, Kurokawa H, Arakawa Y, O'Connor M, Stasio E De, Dahlberg A, Beauclerk A, Cundliffe E, Zarubica T, Baker M, Wright H, Rife J, Galimand M, Courvalin P, Lambert T, Wachino J, Shibayama K, Kurokawa H, Kimura K, Yamane K, Suzuki S, Shibata N, Ike Y, Arakawa Y, Magnet S, Courvalin P, Lambert T, Kim C, Mobashery S, Yan J, Wu J, Ko W, Tsai S, Chuang C, Wu H, Lu Y, Li J, Ma L, Lin C, Chen J, Fung C, Chang F, Lai Y, Lin J, Siu L, Xiao Y, Hu Y, Vaziri F, Peerayeh S, Nejad Q, Farhadian A, Xia Q, Wang H, Zhang A, Wang T, Zhang Y, Yu F, Yao D, Pan J, Chen C, Qin Z, Parsons C, Yang L, Li Q, Zhang X, Qu D, Yu Y, Zhou H, Yang Q, Chen Y, Li L, Clark N, Olsvik O, Swenson J, Spiegel C, Tenover F, Vakulenko S, Donabedian S, Voskresenskiy A, Zervos M, Lerner S, Chow J, Disney M, Magnet S,

Blanchard J, Seeberger P, Chen S, Zhao S, McDermott P, Schroeder C, White D, Meng J, Qin M, Wang D, Huang F, Nie K, Qu M, Wang M, Shu Y, Ma X, Yang M, Luo L, Nie K, Wang M, Zhang C, Li J, Ma X, Li J, Mao N, Zhang C, Yang M, Wang M, Xu W, Ma X, Hu X, Zhang Y, Zhou X, Xu B, Yang M, Wang M, Zhang C, Li J, Bai R, Xu W, Strahilevitz J, Jacoby G, Hooper D, Robicsek A, Tabone T, Mather D, Hayden M, Rai A, Kamath R, Gerald W, Fleisher M, Arpin C, Dubois V, Coulange L, Andre C, Fischer I, Noury P, Grobost F, Brochet J, Jullin J, Dutilh B, Park C, Robicsek A, Jacoby G, Sahm D, Hooper D, Gow S, Waldner C, Harel J, Boerlin P, Torres C, Perlin M, Baquero F, Lerner D, Lerner S, Kim J, Park Y, Kwon H, Han K, Kang M, Woo G. 2007. Aminoglycosides versus bacteria – A description of the action, resistance mechanism, and nosocomial battleground. J Biomed Sci 15:5–14.

41. Tezel U, Pavlostathis SG. 2011. Role of quaternary ammonium compounds on antimicrobial resistance in the environment, p. 349–387. *In* Keen, PL, Montforts, MHMM (eds.), Antimicrobial Resistance in the Environment, 1st ed. John Wiley & Sons, Inc., New York.

42. Jennings MC, Minbiole KPC, Wuest WM. 2016. Quaternary ammonium compounds: An antimicrobial mainstay and platform for innovation to address bacterial resistance. ACS Infect Dis 1:288–303.

43. Ma J, Liu N, Huang M, Wang L, Han J, Qian H, Che F. 2019. Synthesis, physicochemical and antimicrobial properties of cardanol-derived quaternary ammonium compounds (QACs) with heterocyclic polar head. J Mol Liq 294:874–882.

44. Mulder I, Siemens J, Sentek V, Amelung W, Smalla K, Jechalke S. 2018. Quaternary ammonium compounds in soil: Implications for antibiotic resistance development. Rev Environ Sci Bio/Technology 17:159–185.

45. Gerba CP. 2015. Quaternary ammonium biocides: Efficacy in application. Appl Environ Microbiol 81:464–469.

46. Tezel U, Pavlostathis SG. 2015. Quaternary ammonium disinfectants: Microbial adaptation, degradation and ecology. Curr Opin Biotechnol 33:296–304.

47. Lee JY, Wang B -J. 1995. Contact dermatitis caused by cetrimide in antiseptics. Contact Dermatitis 33:168–171.

48. Tattawasart U, Maillard JY, Furr JR, Russell AD. 2000. Outer membrane changes in *Pseudomonas stutzeri* resistant to chlorhexidine diacetate and cetylpyridinium chloride. Int J Antimicrob Agents 16:233–238.

49. Méchin L, Dubois-Brissonnet F, Heyd B, Leveau JY. 1999. Adaptation of Pseudomonas aeruginosa ATCC 15442 to didecyldimethylammonium bromide induces changes in membrane fatty acid composition and in resistance of cells. J Appl Microbiol 86:859–866.

50. Ayfer B, Dizman B, Elasri MO, Mathias LJ, Avci D. 2005. Synthesis and antibacterial activities of new quaternary ammonium monomers. Des Monomers Polym 8:437–451.

51. Delcour AH. 2009. Outer membrane permeability and antibiotic resistance. Biochim Biophys Acta 1794:808–816.

52. Graling PR, Vasaly FW. 2013. Effectiveness of 2% CHG cloth bathing for reducing surgical site infections. AORN J 97:547–551.

53. Edmiston CE, Bruden B, Rucinski MC, Henen C, Graham MB, Lewis BL. 2013. Reducing the risk of surgical site infections: Does chlorhexidine gluconate provide a risk reduction benefit? Am J Infect Control 41:S49–S55.

54. Brooks SE, Walczak MA, Hameed R, Coonan P. 2002. Chlorhexidine resistance in antibiotic-resistant bacteria isolated from the surfaces of dispensers of soap containing chlorhexidine. Infect Control Hosp Epidemiol 23:692–695.

55. Wand ME, Bock LJ, Bonney LC, Sutton JM. 2016. Mechanisms of increased resistance to chlorhexidine and cross-resistance to colistin following exposure of Klebsiella pneumoniae clinical isolates to chlorhexidine. Antimicrob Agents Chemother 61:1–12.

56. Jana S, Deb JK. 2006. Molecular understanding of aminoglycoside action and resistance. Appl Microbiol Biotechnol 70:140–150.

57. Shakil S, Khan R, Zarrilli R, Khan AU. 2008. Aminoglycosides versus bacteria - A description

of the action, resistance mechanism, and nosocomial battleground. J Biomed Sci 15:5–14.

58. Li J, Nation RL, Milne RW, Turnidge JD, Coulthard K. 2005. Evaluation of colistin as an agent against multi-resistant Gram-negative bacteria. Int J Antimicrob Agents 25:11–25.

59. Gupta S, Govil D, Kakar P, Prakash O, Arora D, Das S, Govil P, Malhotra A. 2009. Colistin and polymyxin B: A re-emergence. Indian J Crit Care Med 13:49.

60. Fernández L, Gooderham WJ, Bains M, McPhee JB, Wiegand I, Hancock REW. 2010. Adaptive resistance to the “last hope” antibiotics polymyxin B and colistin in Pseudomonas aeruginosa is mediated by the novel two-component regulatory system ParR-ParS. Antimicrob Agents Chemother 54:3372–3382.

61. Huang X, Yu L, Chen X, Zhi C, Yao X, Liu Y, Wu S, Guo Z, Yi L, Zeng Z, Liu JH. 2017. High prevalence of colistin resistance and mcr-1 gene in Escherichia coli isolated from food animals in China. Front Microbiol 8:1–5.

62. Watkins RR, Smith TC, Bonomo RA. 2016. On the path to untreatable infections: Colistin use in agriculture and the end of ‘last resort’ antibiotics. Expert Rev Anti Infect Ther 14:785–788.

63. O’Driscoll NH, Cushnie TPT, Matthews KH, Lamb AJ. 2018. Colistin causes profound morphological alteration but minimal cytoplasmic membrane perforation in populations of Escherichia coli and Pseudomonas aeruginosa. Arch Microbiol 200:793–802.

64. Sabnis A, Klöckner A, Becce M, Evans LE, Furniss RCD, Mavridou DAI, Stevens MM, Edwards AM. 2018. Colistin kills bacteria by targeting lipopolysaccharide in the cytoplasmic membrane. bioRxiv 479618.

65. Romero JL, Grande Burgos MJ, Pérez-Pulido R, Gálvez A, Lucas R. 2017. Resistance to Antibiotics, Biocides, Preservatives and Metals in Bacteria Isolated from Seafoods: Co-Selection of Strains Resistant or Tolerant to Different Classes of Compounds. Front Microbiol 8:1–16.

66. Hacker J, Carniel E, Achtmann M, Zurth K, Morelli G, Torrea G, Guiyoule A, Carniel E, Arber

W, Bach S, Almeida A de, Carniel E, Blum G, Ott M, Lischewski A, Ritter A, Imrich H, Tschäpe H, Hacker J, Buchrieser C, Brosch R, Bach S, Guiyoule A, Carniel E, Carniel E, Guilvout I, Prentice M, Cesini S, Cornelis GR, Cruz F de la, Davies J, Solar G del, Alonso JC, Espinosa M, Diaz-Orejas R, Doolittle WF, Finlay BB, Falkow S, Galán JE, Collmer A, Groisman EA, Ochman H, Hacker J, Kaper JB, Hacker J, Blum-Oehler G, Mühldorfer I, Tschäpe H, Hentschel U, Steinert M, Hacker J, Hochhut B, Jahreis K, Lengeler JW, Schmid K, Ito T, Katayama Y, Hiramatsu K, Karaolis DKR, Johnson JA, Bailey CC, Boedeker EC, Kaper JB, Reeves PR, Khan AS, Kniep B, Ölschläger AT, Die I Van, Korhonen T, Hacker J, Kurland CG, Lawrence JG, Ochman H, Lee N, Bakkeren G, Wong K, Sherwood JE, Kronstad JW, Ochman H, Lawrence JG, Groisman EA, Ravatn R, Studer S, Springael D, Zehnder AJB, Meer JR van der, Schubert S, Rakin A, Karch H, Carniel E, Heesemann J, Strauss EJ, Falkow S, Sullivan JT, Ronson CW, Vogel JP, Andrews HL, Wong SK, Isberg RR, Waldor MK, Mekalanos JJ. 2001. Ecological fitness, genomic islands and bacterial pathogenicity A Darwinian view of the evolution of microbes. EMBO Rep 2:376–381.

67. Condell O, Iversen C, Cooney S, Power KA, Walsh C, Burgess C, Fanning S. 2012. Efficacy of biocides used in the modern food industry to control Salmonella enterica, and links between biocide tolerance and resistance to clinically relevant antimicrobial compounds. Appl Environ Microbiol 78:3087–3097.

68. Zhanel GG, DeCorby M, Adam H, Mulvey MR, McCracken M, Lagacé-Wiens P, Nichol KA, Wierzbowski A, Baudry PJ, Tailor F, Karlowsky JA, Walkty A, Schweizer F, Johnson J, Hoban DJ. 2010. Prevalence of antimicrobial-resistant pathogens in Canadian hospitals: Results of the Canadian Ward Surveillance study (CANWARD 2008). Antimicrob Agents Chemother 54:4684–4693.

69. Serrano PH. 2005. Responsible use of antibiotics in aquaculture, p. 11–40. *In* Responsable use of antibiotics in aquaculture. Food and Agriculture Organization of the United Nations, Rome.

70. Wales A, Davies R. 2015. Co-selection of resistance to antibiotics, biocides and heavy metals, and its relevance to foodborne pathogens. Antibiotics 4:567–604.

71. Wessels S, Ingmer H. 2013. Modes of action of three disinfectant active substances: A review. Regul Toxicol Pharmacol 67:456–467.

72. Cole EC, Addison RM, Rubino JR, Leese KE, Dulaney PD, Newell MS, Wilkins J, Gaber DJ, Wineinger T, Criger DA. 2003. Investigation of antibiotic and antibacterial agent cross-resistance in target bacteria from homes of antibacterial product users and nonusers. J Appl Microbiol 95:664–676.

73. Aslam B, Wang W, Arshad MI, Khurshid M, Muzammil S, Rasool MH, Nisar MA, Alvi RF, Aslam MA, Qamar MU, Salamat MKF, Baloch Z. 2018. Antibiotic resistance: a rundown of a global crisis. Infect Drug Resist 11:1645–1658.

74. Ferri M, Ranucci E, Romagnoli P, Giaccone V. 2017. Antimicrobial resistance: A global emerging threat to public health systems. Crit Rev Food Sci Nutr 57:2857–2876.

75. Poole K. 2005. Efflux-mediated antimicrobial resistance. J Antimicrob Chemother 56:20–51.

76. Levy SB, Bonnie M. 2004. Antibacterial resistance worldwide: Causes, challenges and responses. Nat Med 10:S122–S129.

77. Peterson E, Kaur P. 2018. Antibiotic resistance mechanisms in bacteria: Relationships between resistance determinants of antibiotic producers, environmental bacteria, and clinical pathogens. Front Microbiol 9:2928.

78. Reygaert WC. 2018. An overview of the antimicrobial resistance mechanisms of bacteria. AIMS Microbiol 4:482–501.

79. Denyer SP, Maillard JY. 2002. Cellullar impermeability and uptake of biocides and antibiotics in Gram-negative bacteria. J Appl Microbiol Symp Suppl 92:35S-45S.

80. Bos MP, Robert V, Tommassen J. 2007. Biogenesis of the Gram-negative bacterial outer membrane. Annu Rev Microbiol 61:191–214.

81. Fernandez L, Hancock REW, Fernández L, Hancock REW. 2012. Adaptive and mutational resistance: Role of porins and efflux pumps in drug resistance. Clin Microbiol

Rev2012/10/05. 25:661–681.

82. Gillings MR. 2013. Evolutionary consequences of antibiotic use for the resistome, mobilome, and microbial pangenome. Front Microbiol 4:1–10.

83. Hibbing ME, Fuqua C, Parsek MR, Peterson SB. 2010. Bacterial competition: Surviving and thriving in the microbial jungle. Natl Rev Microbiol 8:15–25.

84. Ignak S, Nakipoglu Y, Gurler B. 2017. Frequency of antiseptic resistance genes in clinical staphycocci and enterococci isolates in Turkey. Antimicrob Resist Infect Control 6:88.

85. Bjorland J, Steinum T, Kvitle B, Waage S, Sunde M, Heir E. 2005. Widespread distribution of disinfectant resistance genes among Staphylococci of bovine and caprine origin in Norway. J Clin Microbiol 43:4363–4368.

86. Sidhu MS, Heir E, Leegaard T, Wiger K, Holck A. 2002. Frequency of disinfectant resistance genes and genetic linkage with β-lactamase transposon Tn552 among clinical Staphylococci. Antimicrob Agents Chemother 46:2797–2803.

87. Vali L, Davies SE, Lai LLG, Dave J, Amyes SGB. 2008. Frequency of biocide resistance genes, antibiotic resistance and the effect of chlorhexidine exposure on clinical methicillin-resistant Staphylococcus aureus isolates. J Antimicrob Chemother 61:524–532.

88. Deus D, Krischek C, Pfeifer Y, Sharifi AR, Fiegen U, Reich F, Klein G, Kehrenberg C. 2017. Comparative analysis of the susceptibility to biocides and heavy metals of extended-spectrum β-lactamase-producing Escherichia coli isolates of human and avian origin, Germany. Diagn Microbiol Infect Dis 88:88–92.

89. Grare M, Dibama HM, Lafosse S, Ribon A, Mourer M, Regnouf-de-Vains JB, Finance C, Duval RE. 2010. Cationic compounds with activity against multidrug-resistant bacteria: Interest of a new compound compared with two older antiseptics, hexamidine and chlorhexidine. Clin Microbiol Infect 16:432–438.

90. Abuzaid AA, Amyes SGB. 2015. The genetic environment of the antiseptic resistance genes qacEΔ1 and cepA in Klebsiella pneumoniae. J Chemother 27:139–144.

91. Wang R, van Dorp L, Shaw LP, Bradley P, Wang Q, Wang X, Jin L, Zhang Q, Liu Y, Rieux A, Dorai-Schneiders T, Weinert LA, Iqbal Z, Didelot X, Wang H, Balloux F. 2018. The global distribution and spread of the mobilized colistin resistance gene mcr-1. Nat Commun 9:1179.

92. Maciuca IE, Cummins ML, Cozma AP, Rimbu CM, Guguianu E, Panzaru C, Licker M, Szekely E, Flonta M, Djordjevic SP, Timofte D. 2019. Genetic features of mcr-1 mediated colistin resistance in CMY-2-Producing Escherichia coli From romanian poultry. Front Microbiol 10:2267.

93. Liu YY, Wang Y, Walsh TR, Yi LX, Zhang R, Spencer J, Doi Y, Tian G, Dong B, Huang X, Yu LF, Gu D, Ren H, Chen X, Lv L, He D, Zhou H, Liang Z, Liu JH, Shen J. 2016. Emergence of plasmid-mediated colistin resistance mechanism MCR-1 in animals and human beings in China: A microbiological and molecular biological study. Lancet Infect Dis 16:161–168.

94. Chen C-W, Tang H-J, Chen C-C, Lu Y-C, Chen H-J, Su B-A, Weng T-C, Chuang Y-C, Lai C-C. 2019. The microbiological characteristics of carbapenem-resistant Enterobacteriaceae carrying the mcr-1 gene. J Clin Med 8:261.

95. Arabacı Ç, Dal T, Başyiğit T, Genişel N, Durmaz R. 2019. Investigation of carbapenemase and mcr-1 genes in carbapenem-resistant Klebsiella pneumoniae isolates. J Infect Dev Ctries 13:504–509.

96. Iglewski BH. 1996. Pseudomonas, p. . *In* Baron, S (ed.), Medical Microbiology, 4th ed. University of Texas Medical Branch at Galveston, Galveston, TX.

97. Streeter K, Katouli M. 2016. Pseudomonas aeruginosa: A review of their pathogenesis and prevalence in clinical settings and the environment. Infect Epidemiol Med 2:25–32.

98. Garvey MI, Bradley CW, Tracey J, Oppenheim B. 2016. Continued transmission of Pseudomonas aeruginosa from a wash hand basin tap in a critical care unit. J Hosp Infect 94:8–12.

99. Lister PD, Wolter DJ, Hanson ND. 2009. Antibacterial-resistant Pseudomonas aeruginosa:

Clinical impact and complex regulation of chromosomally encoded resistance mechanisms. Clin Microbiol Rev 22:582–610.

100. Ciofu O, Tolker-Nielsen T. 2019. Tolerance and resistance of Pseudomonas aeruginosa biofilms to antimicrobial agents—How P. aeruginosa can escape antibiotics. Front Microbiol 10:913.

101. Moradali MF, Ghods S, Rehm BHA. 2017. Pseudomonas aeruginosa lifestyle: A paradigm for adaptation, survival, and persistence. Front Cell Infect Microbiol 7:39.

102. Tümmler B, Klockgether J. 2017. Recent advances in understanding Pseudomonas aeruginosa as a pathogen [version 1; peer review: 3 approved]. F1000Research 6:1261.

103. Gellatly SL, Hancock REW. 2013. Pseudomonas aeruginosa: New insights into pathogenesis and host defenses. Pathog Dis 67:159–173.

104. Bhagirath AY, Li Y, Somayajula D, Dadashi M, Badr S, Duan K. 2016. Cystic fibrosis lung environment and Pseudomonas aeruginosa infection. BMC Pulm Med 16:1–22.

105. Driscoll JA, Brody SL, Kollef MH. 2007. The epidemiology, pathogenesis and treatment of Pseudomonas aeruginosa infections. Drugs 67:351–368.

106. Strateva T, Yordanov D. 2009. Pseudomonas aeruginosa - A phenomenon of bacterial resistance. J Med Microbiol 58:1133–1148.

107. Minagawa S, Inami H, Kato T, Sawada S, Yasuki T, Miyairi S, Horikawa M, Okuda J, Gotoh N. 2012. RND type efflux pump system MexAB-OprM of Pseudomonas aeruginosa selects bacterial languages, 3-oxo-acyl-homoserine lactones, for cell-to-cell communication. BMC Microbiol 12:1–10.

108. Denisuik AJ, Garbutt LA, Golden AR, Adam HJ, Baxter M, Nichol KA, Lagacé-Wiens P, Walkty AJ, Karlowsky JA, Hoban DJ, Mulvey MR, Zhanel GG. 2019. Antimicrobial-resistant pathogens in Canadian ICUs: Results of the CANWARD 2007 to 2016 study. J Antimicrob Chemother 74:645–653.

109. Magiorakos AP, Srinivasan A, Carey RB, Carmeli Y, Falagas ME, Giske CG, Harbarth S,

Hindler JF, Kahlmeter G, Olsson-Liljequist B, Paterson DL, Rice LB, Stelling J, Struelens MJ, Vatopoulos A, Weber JT, Monnet DL. 2012. Multidrug-resistant, extensively drug-resistant and pandrug-resistant bacteria: An international expert proposal for interim standard definitions for acquired resistance. Clin Microbiol Infect 18:268–281.

110. Asif M, Alvi IA, Ur Rehman S. 2018. Insight into Acinetobacter baumannii: Pathogenesis, global resistance, mechanisms of resistance, treatment options, and alternative modalities. Infect Drug Resist 11:1249–1260.

111. Peleg AY, Seifert H, Paterson DL. 2008. Acinetobacter baumannii: Emergence of a successful pathogen. Clin Microbiol Rev 21:538–582.

112. Neonakis IK, Spandidos DA, Petinaki E. 2011. Confronting multidrug-resistant Acinetobacter baumannii: A review. Int J Antimicrob Agents 37:102–109.

113. Doi Y, Murray GL, Peleg AY. 2015. Acinetobacter baumannii: Evolution of antimicrobial resistance-treatment options. Semin Respir Crit Care Med 36:85–98.

114. Boyd DA, Mataseje LF, Pelude L, Mitchell R, Bryce E, Roscoe D, Embree J, Katz K, Kibsey P, Lavallee C, Simor AE, Taylor G, Turgeon N, Langley JM, Amaratunga K, Mulvey MR. 2019. Results from the Canadian Nosocomial Infection Surveillance Program for detection of carbapenemase-producing Acinetobacter spp. in Canadian hospitals, 2010-16. J Antimicrob Chemother 74:315–320.

115. Zhanel GG, Adam HJ, Baxter MR, Fuller J, Nichol KA, Denisuik AJ, Golden AR, Hink R, Lagacé-Wiens PRS, Walkty A, Mulvey MR, Schweizer F, Bay D, Hoban DJ, Karlowsky JA. 2019. 42936 pathogens from Canadian hospitals: 10 years of results (2007-16) from the CANWARD surveillance study. J Antimicrob Chemother 74:iv5–iv21.

116. Fernández-Cuenca F, Tomás M, Caballero-Moyano FJ, Bou G, Martínez-Martínez L, Vila J, Pachón J, Cisneros JM, Rodríguez-Baño J, Pascual Á. 2015. Reduced susceptibility to biocides in Acinetobacter baumannii: association with resistance to antimicrobials, epidemiological behaviour, biological cost and effect on the expression of genes encoding porins and efflux pumps. J Antimicrob Chemother 70:3222–3229.

117. Vila J, Sáez-López E, Johnson JR, Römling U, Dobrindt U, Cantón R, Giske CG, Naas T, Carattoli A, Martínez-Medina M, Bosch J, Retamar P, Rodríguez-Bañõ J, Baquero F, Soto SM. 2016. Escherichia coli: An old friend with new tidings. FEMS Microbiol Rev 40:437–463.

118. Guentzel NM. 1996. Escherichia, Klebsiella, Enterobacter, Serratia, Citrobacter, and Proteus, p. . *In* Baron, S (ed.), Medical Microbiology, 4th ed. University of Texas Medical Branch at Galveston, Galveston, TX.

119. Kaper JB, Nataro JP, Mobley HLT. 2004. Pathogenic Escherichia coli. Nat Rev Microbiol 2:123–140.

120. Denisuik AJ, Karlowsky JA, Adam HJ, Baxter MR, Lagacé-Wiens PRS, Mulvey MR, Hoban DJ, Zhanel GG. 2019. Dramatic rise in the proportion of ESBL-producing Escherichia coli and Klebsiella pneumoniae among clinical isolates identified in Canadian hospital laboratories from 2007 to 2016. J Antimicrob Chemother 74:iv64–iv71.

121. Shafaati M, Boroumand M, Nowroozi J, Amiri P, Kazemian H. 2016. Correlation between qacE and qacEΔ1 efflux pump genes, antibiotic and disinfectant resistant among clinical isolates of E. coli. Recent Pat Antiinfect Drug Discov 11:189–195.

122. Martin RM, Bachman MA. 2018. Colonization, infection, and the accessory genome of Klebsiella pneumoniae. Front Cell Infect Microbiol 8:4.

123. Paczosa MK, Mecsas J. 2016. Klebsiella pneumoniae: Going on the offense with a strong defense. Microbiol Mol Biol Rev 80:629–661.

124. Effah CY, Sun T, Liu S, Wu Y. 2020. Klebsiella pneumoniae: An increasing threat to public health. Ann Clin Microbiol Antimicrob 19:1–9.

125. Wand ME, Bock LJ, Mark Sutton J. 2017. Retention of virulence following colistin adaptation in Klebsiella pneumoniae is strain-dependent rather than associated with specific mutations. J Med Microbiol 66:959–964.

126. Lampel KA, Formal SB, Maurelli AT. 2018. A Brief History of Shigella. EcoSal Plus 8:ESP-

0006-2017.

127. Baker S, Chung H. 2018. Recent insights into Shigella : A major contributor to the global diarrhoeal disease burden. Curr Opin Infect Dis 31:449–454.

128. Kotloff KL, Riddle MS, Platts-Mills JA, Pavlinac P, Zaidi AKM. 2018. Shigellosis. Lancet 391:801–812.

129. Carayol N, Nhieu GT Van. 2013. Tips and tricks about Shigella invasion of epithelial cells. Curr Opin Microbiol 16:32–37.

130. Ranjbar R, Farahani A. 2019. Shigella: Antibiotic-Resistance Mechanisms And New Horizons For Treatment. Infect Drug Resist 12:3137–3167.

131. Vincent J-L, Rello J, Marshall J, Silva E, Anzueto A, Martin CD, Moreno R, Lipman J, Gomersall C, Sakr Y, Reinhart K, EPIC II Group of Investigators for the. 2009. International study of the prevalence and outcomes of infection in intensive care units. JAMA 302:2323–2329.

132. Evans HL, Lefrak SN, Lyman J, Smith RL, Chong TW, McElearney ST, Schulman AR, Hughes MG, Raymond DP, Pruett TL, Sawyer RG. 2007. Cost of Gram-negative resistance. Crit Care Med 35:89–95.

133. Dadgostar P. 2019. Antimicrobial resistance: Implications and costs. Infect Drug Resist 12:3903–3910.

134. McEwen SA, Collignon PJ. 2018. Antimicrobial resistance: A One Health perspective. Microbiol Spectr 6:ARBA-009-2017.

135. Aghapour Z, Gholizadeh P, Ganbarov K, Bialvaei AZ, Mahmood SS, Tanomand A, Yousefi M, Asgharzadeh M, Yousefi B, Kafil HS. 2019. Molecular mechanisms related to colistin resistance in enterobacteriaceae. Infect Drug Resist 12:965–975.

136. Pati SG, Arnold WA. 2020. Comprehensive screening of quaternary ammonium surfactants and ionic liquids in wastewater effluents and lake sediments. Environ Sci Process Impacts 22:430–441.

137. Nhung NT, Thuy CT, Trung N V, Campbell J, Baker S, Thwaites G, Hoa NT, Carrique-mas J. 2015. Induction of antimicrobial resistance in Escherichia coli and non-typhoidal Salmonella strains after adaptation to disinfectant commonly used on farms in Vietnam. Antibiotics 4:480–494.

138. Buffet-Bataillon S, Le jeune A, Gall-David S Le, Bonnaure-Mallet M, Jolivet-Gougeon A. 2012. Molecular mechanisms of higher MICs of antibiotics and quaternary ammonium compounds for Escherichia coli isolated from bacteraemia. J Antimicrob Chemother 67:2837–2842.

139. Joynson JA, Forbes B, Lambert RJW. 2002. Adaptive resistance to benzalkonium chloride, amikacin and tobramycin: The effect on susceptibility to other antimicrobials. J Appl Microbiol 93:96–107.

140. Environment and Climate Change Canada. 2019. Screening assessment - Chlorhexidine and its salts.

141. Williamson DA, Carter GP, Howden BP. 2017. Current and emerging topical antibacterials and antiseptics: Agents, action, and resistance patterns. Clin Microbiol Rev 30:827–860.

142. Punina N V., Makridakis NM, Remnev MA, Topunov AF. 2015. Whole-genome sequencing targets drug-resistant bacterial infections. Hum Genomics 9.

143. Ruppé E, Cherkaoui A, Lazarevic V, Emonet S, Schrenzel J. 2017. Establishing genotype-to-rhenotype relationships in bacteria causing hospital-acquired pneumonia: A prelude to the application of clinical metagenomics. Antibiot 6:30.

144. Chapman JS. 2003. Disinfectant resistance mechanisms, cross-resistance, and co-resistance. Int Biodeterior Biodegrad 51:271–276.

145. Raetz CRH, Reynolds CM, Trent MS, Bishop RE. 2007. Lipid A modification systems in Gram-negative bacteria. Annu Rev Biochem 76:295–329.

146. Guo L, Lim KB, Poduje CM, Daniel M, Gunn JS, Hackett M, Miller SI. 1998. Lipid A acylation and bacterial resistance against vertebrate antimicrobial peptides. Cell 95:189–198.

147. Rowlett VW, Mallampalli VKPS, Karlstaedt A, Dowhan W, Taegtmeyer H, Margolin W, Vitrac H. 2017. The impact of membrane phospholipid alterations in Escherichia coli on cellular function. J Bacteriol 199:1–22.

148. Moya-Torres A, Mulvey MR, Kumar A, Oresnik IJ, Brassinga AK aren C. 2014. The lack of OmpF, but not OmpC, contributes to increased antibiotic resistance in Serratia marcescens. Microbiology 160:1882–1892.

149. Blanco P, Hernando-Amado S, Reales-Calderon J, Corona F, Lira F, Alcalde-Rico M, Bernardini A, Sanchez M, Martinez J. 2016. Bacterial multidrug efflux pumps: Much more than antibiotic resistance determinants. Microorganisms 4:14.

150. Tandukar M, Oh S, Tezel U, Konstantinidis KT, Pavlostathis SG. 2013. Long-term exposure to benzalkonium chloride disinfectants results in change of microbial community structure and increased antimicrobial resistance. Environ Sci Technol 47:9730–9738.

151. Du D, Wang-Kan X, Neuberger A, van Veen HW, Pos KM, Piddock LJ V, Luisi BF. 2018. Multidrug efflux pumps: Structure, function and regulation. Nat Rev Microbiol 16:523–539.

152. Aulawi K, Junko N, Okada S. 2018. Relationship between resistance to antibiotics and insusceptibility to biocides of Staphylococcus aureus and Pseudomonas aeruginosa isolated in Indonesian hospitals 6:1890–1897.

153. Braoudaki M, Hilton AC. 2004. Adaptive resistance to biocides in Salmonella enterica and Escherichia coli O157 and cross-resistance to antimicrobial agents. J Clin Microbiol 42:73–78.

154. Zhang C, Cui F, Zeng G ming, Jiang M, Yang Z zhu, Yu Z gang, Zhu M ying, Shen L qing. 2015. Quaternary ammonium compounds (QACs): A review on occurrence, fate and toxicity in the environment. Sci Total Environ.

155. Lasek F, Karpel Vel Leitner N, Rauwel G, Blanchier L, Castel O, Ayraud-Thevenot S, Deborde M. 2019. Discharge of biocidal products from healthcare activities into a sewage system

— A case study at a French university hospital. Environ Sci Pollut Res 26:4938–4951.

156. Van Boeckel TP, Gandra S, Ashok A, Caudron Q, Grenfell BT, Levin SA, Laxminarayan R. 2014. Global antibiotic consumption 2000 to 2010: An analysis of national pharmaceutical sales data. Lancet Infect Dis 14:742–750.

157. Ishikawa S, Matsumura Y, Yoshizako F, Tsuchido T. 2002. Characterization of a cationic surfactant-resistant mutant isolated spontaneously from Escherichia coli. J Appl Microbiol 92:261–268.

158. Abdelaziz A, Sonbol F, Elbanna T, El-Ekhnawy E. 2019. Exposure to sublethal concentrations of benzalkonium chloride induces antimicrobial resistance and cellular changes in Klebsiellae pneumoniae clinical isolates. Microb drug Resist 25:631–638.

159. Kampf G. 2018. Biocidal Agents Used for Disinfection Can Enhance Antibiotic Resistance in Gram-Negative Species. Antibiotics 7.

160. Mc Cay PH, Ocampo-Sosa AA, Fleming GTA. 2010. Effect of subinhibitory concentrations of benzalkonium chloride on the competitiveness of Pseudomonas aeruginosa grown in continuous culture. Microbiology 156:30–38.

161. Balouiri M, Sadiki M, Ibnsouda SK. 2016. Methods for in vitro evaluating antimicrobial activity: A review. J Pharm Anal 6:71–79.

162. Langsrud S, Sidhu MS, Heir E, Holck AL. 2003. Bacterial disinfectant resistance - A challenge for the food industry. Int Biodeterior Biodegrad 51:283–290.

163. Baba T, Ara T, Hasegawa M, Takai Y, Okumura Y, Baba M, Datsenko KA, Tomita M, Wanner BL, Mori H. 2006. Construction of Escherichia coli K-12 in-frame, single-gene knockout mutants: The Keio collection. Mol Syst Biol 21:2006.0008.

164. Bore E, Hébraud M, Chafsey I, Chambon C, Skjæret C, Moen B, Møretrø T, Langsrud Ø, Rudi K, Langsrud S. 2007. Adapted tolerance to benzalkonium chloride in Escherichia coli K-12 studied by transcriptome and proteome analyses. Microbiology 153:935–946.

165. Cold Spring Harbour Laborator Press. 2018. LB Liquid Medium II.

166. Cartwright N. 2019. Examination of cationic antimicrobial tolerance in Escherichia coli to identify phenotypic and genotypic adaptations. University of Manitoba.

167. Fürste JP, Pansegrau W, Frank R, Blöcker H, Scholz P, Bagdasarian M, Lanka E. 1986. Molecular cloning of the plasmid RP4 primase region in a multi-host-range tacP expression vector. Gene 48:119–131.

168. Sambrook J, Russell DW. 2001. Molecular cloning : A laboratory manual3rd ed. Cold Spring Harbor Laboratory Press, Cold Spring Harbor, N.Y.

169. Golding CG, Lamboo LL, Beniac DR, Booth TF. 2016. The scanning electron microscope in microbiology and diagnosis of infectious disease. Sci Rep 6:26516.

170. Abràmoff MD, Magalhães PJ, Ram SJ. 2007. Image Processing with ImageJ. Biophotonics Int 11:36–42.

171. Shanthi PMSL, Mangalaraja R V, Uthirakumar AP, Velmathi S, Balasubramanian T, Ashok M. 2010. Synthesis and characterization of porous shell-like nano hydroxyapatite using cetrimide as template. J Colloid Interface Sci 350:39–43.

172. Duquemin SJ, Nixon JR. 1985. The effect of sodium lauryl sulphate, cetrimide and polysorbate 20 surfactants on complex coacervate volume and droplet size. J Pharm Pharmacol 37:698–702.

173. Georgiev GA, Yokoi N, Koev K, Kutsarova E, Ivanova S, Kyumurkov A, Jordanova A, Krastev R, Lalchev Z. 2011. Surface chemistry study of the interactions of benzalkonium chloride with films of meibum, corneal cells lipids, and whole tears. Invest Ophthalmol Vis Sci 52:4645–4654.

174. Kato Y, Yagi H, Kaji Y, Oshika T, Goto Y. 2013. Benzalkonium chloride accelerates the formation of the amyloid fibrils of corneal dystrophy-associated peptides. J Biol Chem 288:25109–25118.

175. Geddes CD. 2001. Optical halide sensing using fluorescence quenching: Theory, simulations and applications - A review. Meas Sci Technol 12:R53–R88.

176. Cunnion KM, Lee JC, Frank MM. 2001. Capsule production and growth phase influence binding of complement to Staphylococcus aureus. Infect Immun 69:6796–6803.

177. Navarro Llorens JM, Tormo A, Martínez-García E. 2010. Stationary phase in Gram-negative bacteria. FEMS Microbiol Rev 34:476–495.

178. Salanitro JP, Wegener WS. 1971. Growth of Escherichia coli on short-chain fatty acids: growth characteristics of mutants. J Bacteriol 102:885–892.

179. Whitfield C, Roberts IS. 1999. Structure, assembly and regulation of expression of capsules in Escherichia coli. Mol Microbiol 31:1307–1319.

180. Gilbert P, Evans DJ, Evans E, Duguid IG, Brown MRW. 1991. Surface characteristics and adhesion of Escherichia coli and Staphylococcus epidermidis. J Appl Bacteriol 71:72–77.

181. Bales PM, Renke EM, May SL, Shen Y, Nelson DC. 2013. Purification and characterization of biofilm-associated EPS exopolysaccharides from ESKAPE organisms and other pathogens. PLoS One 8:e67950.

182. Chattaway MA, Schaefer U, Tewolde R, Dallman TJ, Jenkins C. 2017. Identification of Escherichia coli and shigella species from whole-genome sequences. J Clin Microbiol.

183. Meyer JM. 2000. Pyoverdines: Pigments, siderophores and potential taxonomic markers of fluorescent pseudomonas species. Arch Microbiol 174:135–142.

184. Abu EA, Su S, Sallans L, Boissy RE, Greatens A, Heineman WR, Hassett DJ. 2013. Cyclic voltammetric , fluorescence and biological analysis of purified aeruginosin A , a secreted red pigment of Pseudomonas aeruginosa PAO1. Microbiology 159:1736–1747.

185. Langsrud S, Sundheim G, Borgmann-Strahsen R. 2003. Intrinsic and acquired resistance to quaternary ammonium compounds in food-related Pseudomonas spp. J Appl Microbiol 94:874–882.

186. Rutala W a, Stiegel MM, Sarubbi F a, Weber DJ. 1997. Susceptibility of antibiotic-susceptible and antibiotic-resistant hospital bacteria to disinfectants. Infect Control Hosp Epidemiol 18:417–21.

187. Washam CJ, Sandine WE, Elliker PR. 1976. A strain of Pseudomonas aeruginosa resistant to a quaternary ammonium compound. J Milk Food Technol 39:546–550.

188. Corona F, Martinez JL. 2013. Phenotypic Resistance to Antibiotics. Antibiot 2:237–255.

189. Cheung HY, Wong MMK, Cheung SH, Liang LY, Lam YW, Chiu SK. 2012. Differential actions of chlorhexidine on the cell wall of Bacillus subtilis and Escherichia coli. PLoS One 7:e36659.

190. Shalamanov DS. 2005. Chlorhexidine gluconate-induced morphological changes in Gram negative microorganisms. Biotechnol Biotechnol Equip 19:121–124.

191. Li J, Rayner CR, Nation RL, Owen RJ, Spelman D, Tan KE, Liolios L. 2006. Heteroresistance to colistin in multidrug-resistant Acinetobacter baumannii. Antimicrob Agents Chemother 50:2946–2950.

192. Martínez-Servat S, Yero D, Huedo P, Marquez R, Molina G, Daura X, Gibert I. 2018. Heterogeneous colistin-resistance Phenotypes coexisting in Stenotrophomonas maltophilia isolates influence colistin susceptibility testing. Front Microbiol 9:2871.

193. Jayol A, Nordmann P, Brink A, Villegas MV, Dubois V, Poirela L. 2017. High-level resistance to colistin mediated by various mutations in the crrB gene among carbapenemase-producing Klebsiella pneumoniae. Antimicrob Agents Chemother 61:e01423-17.

194. Sampson TR, Liu X, Schroeder MR, Kraft CS, Burd EM, Weiss DS. 2012. Rapid killing of Acinetobacter baumannii by polymyxins is mediated by a hydroxyl radical death pathway. Antimicrob Agents Chemother 56:5642–5649.

195. Nakae R, Nakae T. 1982. Diffusion of aminoglycoside antibiotics across the outer membrane of Escherichia coli. Antimicrob Agents Chemother 22:554–559.

196. Lee JY, Chung ES, Ko KS. 2017. Transition of colistin dependence into colistin resistance in Acinetobacter baumannii. Sci Rep 7:1–11.

197. Hawley JS, Murray CK, Jorgensen JH. 2007. Development of colistin-dependent Acinetobacter baumannii-Acinetobacter calcoaceticus complex. Antimicrob Agents Chemother 51:4529–4530.

198. Mohamed YF, Abou-Shleib HM, Khalil AM, El-Guink NM, El-Nakeeb MA. 2016. Membrane permeabilization of colistin toward pan-drug resistant Gram-negative isolates. Brazilian J Microbiol 47:381–388.

199. Baron S, Hadjadj L, Rolain JM, Olaitan AO. 2016. Molecular mechanisms of polymyxin resistance: Knowns and unknowns. Int J Antimicrob Agents 48:583–591.

200. Kapoor G, Saigal S, Elongavan A. 2017. Action and resistance mechanisms of antibiotics: A guide for clinicians. J Anaesthesiol Clin Pharmacol 33:300–305.

Appendix I

This appendix shows the chemicals as well as their suppliers used in this thesis.

Chemicals used in this thesis and supplier information:

Cetrimide bromide (M7635, Sigma, USA)

Colistin sulfate (C2930-25G, TCI America, USA)

Benzalkonium chloride (12060-100G, Sigma, USA)

Chlorhexidine digluconate (AA41385AE, Fisher, USA)

Tobramycin (T2506, TCI America, USA)

Gentamicin sulfate (CA1000219-398, VWR)

Didodecyldimethylammonium bromide (382310-5G, Sigma, USA)

Cetylpyridinium chloride (H0078, TCI America, USA)

Cetyldimethylammonium bromide (D0721, TCI America,

Sytox™ blue (S11348, Fisher, USA)

Propidium iodide (P3566, Life technologies, USA)

Dimethyl sulfoxide (CABDH1115-1LP, VWR, Canada)

Glycerol (BP229-4, Fisher, USA)

Ampicillin (CA97061-442, VWR, Canada)

EZ-10 Spin Column Plasmid DNA Minipreps Kit (BS614-250, Biobasic, Canada)

Eco*RI* ANZA restriction enzyme (IVGN0116, Thermo-Fisher, USA)

Xba*I* ANZA restriction enzyme (IVGN0126, Thermo-Fisher, USA)

Gel extraction kit (9K-006-007, Biobasic Inc., Canada)

Black walled 96-well microplates (265301, Thermo Scientific, USA)

96-well microplates (167008, Thermo Scientific, USA)

Appendix II

This appendix offers a list of the strains and isolates, where they were obtained from, a brief description of the strains and isolates, and antimicrobial concentrations needed for selection.

Table of strains/isolates used in this thesis:

Strain/Isolate	Abbreviation in thesis	Description	Selection	Obtained from
Escherichia coli K-12 BW25113	EC	Unadapted control		Yale Coli Genetic Stock Centre
Escherichia coli K-12 BW25113	ECBZKT	BZK-adapted EC	40 µg/mL BZK	(166)
Escherichia coli K-12 BW25113	ECCETT	CET-adapted EC	50 µg/mL CET	(166)
Escherichia coli K-12 BW25113	ECCHXT	CHX-adapted EC	2 µg/mL CHX	(166)
Escherichia coli K-12 BW25113	ECCOLR	COL-adapted EC	100 µg/mL COL	(166)
Escherichia coli K-12 BW25113+pMS119EH	ECP	Unadapted control with empty vector	100 µg/mL AMP	this thesis
Escherichia coli K-12 BW25113+pMCR1	MCR1	ECP transformed with *mcr-1*	100 µg/mL AMP	this thesis
Escherichia coli Clinical isolate 93	EC93	Tobramycin resistant clinical isolate		CADHAM Provincial lab
Escherichia coli Clinical isolate 96	EC96	Tobramycin resistant clinical isolate		CADHAM Provincial lab
Escherichia coli Clinical isolate 97	EC97	Gentamicin resistant clinical isolate		CADHAM Provincial lab
Escherichia coli Clinical isolate 102	EC102	Gentamicin resistant clinical isolate		CADHAM Provincial lab
Acinetobacter baumannii DSM 6974	AB	Intrinsically tolerant control		Leibniz Institute DSMZ-German Collection of Microorganisms and Cell Cultures

Pseudomonas aeruginosa PA01 DSM 22644	PA	Intrinsically tolerant control		Leibniz Institute DSMZ-German Collection of Microorganisms and Cell Cultures
Klebsiella pneumoniae DSM 6135	KP	Unadapted control		this thesis
Klebsiella pneumoniae DSM 6135	KPBZKT	BZK-adapted KP	28 µg/mL BZK	this thesis
Shigella sonnei DSM 5570	SS	Unadapted control		this thesis
Shigella sonnei DSM 5570	SSBZKT	BZK-adapted SS	10 µg/mL BZK	this thesis

AMP: Ampicillin; BZK: Benzalkonium chloride; CET: Cetrimide bromide; CHX: Chlorhexidine; COL: Colistin; GNT: Gentamicin; TOB: Tobramycin.